MEMBRANE-BASED CONCENTRATION AND RECOVERY OF VIRUSES FROM COMPLEX WATER MATRICES

By

Hang Shi

A DISSERTATION

Submitted to
Michigan State University
In partial fulfillment of the requirements
for the degree of

Environmental Engineering - Doctor of Philosophy

2017

ABSTRACT

MEMBRANE-BASED CONCENTRATION AND RECOVERY OF VIRUSES FROM COMPLEX WATER MATRICES

By

Hang Shi

Prevention of waterborne disease outbreaks relies on the efficient detection of pathogens in drinking and recreational water. Development of sample concentration technologies that ensure fast and high recovery of pathogens from aquatic samples is crucial for timely detection. The most effective approaches to sample concentration and virus recovery employ membrane filtration and rely on controlling physicochemical interactions between the virus and the filter. The two main goals of the present work were to understand the reasons for the poor efficiency (typically below 30%) of the current methods in recovering human adenovirus and to propose alternative strategies that facilitate concentration and recovery of this important human virus. The first part of the dissertation is devoted to the study on how common methods of virus propagation (broth-based and agar-based) and purification (polyethylene glycol precipitation, centrifugal diafiltration and CsCl density gradient centrifugation) affect physicochemical properties of virions. Experimental data for bacteriophage MS2 showed that results of virus size, charge, and hydrophobicity measurements depend strongly on the methods and protocols used to grow and purify the virus. The optimal sample preparation protocol was determined to consist of broth-based growth followed by purification via CsCl density gradient centrifugation. This method was then used to measure physicochemical properties of human adenovirus 40 (HAdV40) and employ these values to calculate the energy of virion-virion and virion-membrane interactions. The

second part of the dissertation describes an experimental study on the recovery of HAdV40 from three water matrices (spiked deionized water, tap water, and high organic content surface water) by crossflow ultrafiltration. Prior to ultrafiltration, membranes were either blocked by calf serum or coated with a polyelectrolyte multilayer to minimize virus adsorption on the membrane surface. The multilayer was designed to be antiadhesive with respect to HAdV 40 using the virus-membrane interaction energy calculations performed earlier. In the sample concentration tests, HAdV 40 was recovered from ultrapure water, tap water, and surface water with very high post-elution recoveries of ~99%, ~91%, and ~84%, respectively. The obtained recovery data were interpreted in terms of physicochemical interactions of HAdV40 virions with the membrane and how components of the eluent disrupt specific interactions between HAdV40 and the membrane to maximize HAdV40 recovery. Results on HAdV40 concentration indicate that the composition of the eluent is the most important factor for achieving high virus recovery and can be designed to efficiently recover viruses even from highly complex water matrices.

ACKNOWLEDGEMENTS

Pursuing a PhD has not all been smooth sailing. It is full of ups and downs. There are many people I would like to acknowledge for helping me complete this milestone.

To my advisor, Dr. Volodymyr Tarabara, thank you for your continued support, constant guidance, your effort to translate my fragmented thoughts when I had some new exciting data. You are always willing to help me improve not only my technical skills, but also my presentation skills and allow me the opportunity to expand my horizons from which I will benefit throughout my life. Your encouragement and advice will continue to be invaluable to me for my future career.

I would like to thank my committee members, Dr. Kristin Parent, Dr. Merlin Bruening, Dr. Wei Zhang and Dr. Irene Xagoraraki for their suggestions and critical comments. Especially for Dr. Parent, thank you for always being available for offering help which really expedites my research.

To the former and current lab members in our research group, working with all of you is a great experience in my life, which not only gives me a chance to be exposed to other topics in this interdisciplinary filed, but also helps myself improve important skills required to become a solid team player.

I would like to thank Lori Larner, research administrator in our department and Joseph Nguyen, lab technician in our department. Thank you for your administrative and technical support.

To my parents, without your unconditional love and support, I would never have had a chance to come to this country for graduate study. I always feel loved and I love you both very much.

I would also like to thank Yu and my naughty hyper dog Mei-Chou-Chou for their company and bring laughter into my life in these tough years.

Last, I would like to thank the source of funding, The National Science Foundation (NSF) Partnerships for International Research and Education (PIRE) program under Grant IIA-1243433 that makes my research financially possible.

TABLE OF CONTENTS

LIST OF TABLES

LIST OF FIGURES

CHAPTER ONE

Dissertation Overview

Pathogenic viruses are a major cause of waterborne diseases. To prevent disease outbreaks, rapid and reliable detection of viruses in water is essential. The detection process typically requires concentration of the source water sample to increase the virus titer. VIRADEL (VIRus ADsorption-ELution) and CFUF (crossflow ultrafiltration) are two methods that are commonly used for concentrating large volume environmental samples. Although fast concentration of all viruses in a sample is ideal, engineering challenges such as membrane fouling and irreversible adsorption of viruses to components of the filtration unit limit the concentration speed and percent recovery. Better understanding the fate of viruses throughout the sample concentration process and identifying reasons for virus loss can guide process design for improving virus recoveries. The material presented in this dissertation divided into Chapter where each Chapter is a manuscript either already published or in preparation for submission.

Chapter 2 is a comprehensive review of the literature on membrane-based methods of virus concentration from aqueous media. Published data on noroviruses, adenoviruses and bacteriophage MS2 are critically analyzed to establish how parameters of the concentration process impact virus recovery. The review highlights the importance of physicochemical interactions of virions during sample concentration and concludes by identifying research needs.

The work presented in Chapter 3 is based on the premise that physicochemical interactions between the virus and the filter govern virus recovery. Indeed, VIRADEL and CFUF are designed to harness these interactions to achieve higher and more reproducible recoveries. It is important therefore to quantify key physicochemical properties of a virus accurately. The Chapter focuses on the impact of different sample preparation methods on virus physicochemical characterization. Two virus propagation methods (broth-based and double agar overlay growth) and three purification methods (PEG precipitation, centrifugal diafiltration, CsCl density gradient centrifugation) were systematically evaluated with bacteriophages MS2 and P22.

Chapter 4 builds on the findings presented in Chapter 3. Using the optimal sample preparation method, the study offers the first comprehensive physicochemical characterization of human adenovirus 40 (HAdV 40), an important human pathogen. The data on HAdV 40 surface properties was used to calculate the energy of virion-virion and virion-membrane interactions. In a set of cross-flow filtration tests, HAdV 40 was recovered from ultrapure water (99%), tap water (~91%), and high-carbon-content surface water with post-elution recoveries of 99%, ~91%, and ~84%, respectively. The composition of the eluent was designed to disrupt specific interactions between HAdV40 and the membrane and maximize HAdV 40 recovery.

Finally, Chapter 5 presents overarching conclusions drawn based on the material described in Chapters 2, 3, and 4.

CHAPTER TWO

Membrane-based methods of virus concentration from water: A review of process parameters and their effects on virus recovery

Abstract

This review focuses on membrane-based methods of virus concentration from aqueous media. The discussion is centered on two most commonly used sample concentration techniques: virus adsorption and elution (VIRADEL) and crossflow ultrafiltration (CFUF). We summarize all published VIRADEL and CFUF studies on the concentration of two human viral pathogens that are difficult to recover and quantify: noroviruses (17 reports total) and adenoviruses (15 reports total). We also include in the discussion all studies published since 2001 on the concentration of MS2, a bacteriophage commonly used in fate and transport studies as a surrogate of human viruses. The reported recoveries are analyzed in the context of key concentration process parameters including virus and membrane properties, initial virus content in the sample, details of the filtration protocol, as well as composition of the water and the eluent used to collect viruses adsorbed on the membrane surface. We conclude by identifying knowledge gaps and outlining a possible research agenda for improving the science and practice of virus separation for detection.

2.1 Introduction

2.1.1 The need for timely detection of viral pathogens in water

Waterborne diseases are infections transmitted through contact with contaminated waters. The main etiological agents of waterborne disease outbreaks are viruses, bacteria, protozoa, fungi and helminths [1]. The reservoirs of concern are recreational waters as well as surface and ground waters used as sources of drinking water. Developments in environmental regulation and progress in drinking water treatment technologies since the beginning of the 20th century led to a decrease in the occurrence of waterborne disease outbreaks resulting from exposure to contaminated drinking water [2]. As a result, such outbreaks have become relatively uncommon in the U.S. and other developed countries [3]. An average of 30 disease outbreaks associated with drinking water were reported every year to the Center for Disease Control during the 2001-2012 period in the U.S. [4-9]. Actual outbreak occurrence might have been higher as it has been suggested that only 10% to 50% of outbreaks are actually reported [2]. Within this time span, the number of affected persons per year varied from the minimum of 431 (2011-2012) to the maximum of 4,128 (2007-2008) while the number of resulting deaths per year varied from 3 (2011-2012) to 14 (2007-2008) [4-9]. It is estimated that since 2001 from 6% to 16% of the outbreaks, for which the etiological agent was identified, have been caused by viruses [4-9]. In addition to underreporting, viruses are also typically more difficult to detect as an etiologic agent. The difficulty is caused by a combination of factors including the typically very low concentrations of viruses in water

[10]; an overlap in clinical symptoms leading to possible misinterpretation of viral etiology for that of bacterial or protozoan origin [11]; and complexity of working with noroviruses, a leading documented cause of water-borne disease of viral origin [12, 13].

Rapid detection of waterborne pathogens with high sensitivity and reproducibility is essential. Although modern water treatment technologies are efficient at removing pathogens, complete removal cannot be guaranteed [14] and the consequences of even one incident can be dramatic. Since 1940s and 1950s when first studies demonstrated that waterborne diseases can be of viral etiology [15], multiple events have highlighted the risks that such outbreaks entail. More recently, contaminated water supply system led to the 1991 outbreak of hepatitis E virus in Kanpur, India which affected approximately 79,091 persons [16], The 1999 outbreak of aseptic meningitis associated with multiple enterovirus subtypes in Romania affected approximately 6,000 persons [17]. During 2008–2014, a total of 133 cruise ship acute gastroenteritis outbreaks were reported in US and among outbreaks in which specimens available for testing, 97% were caused by norovirus [18]. As of May 2017, the latest norovirus outbreak on a cruise ship occurred in March 2017, in which 157 passengers (out of 2,016 total) and 25 crew members (out of 881 total) reported being ill [19]. The 2004 multiple pathogens outbreak associated with groundwater along the shoreline of South Bass Island off the coast of Lake Erie, Ohio, led to approximately 1,450 reported cases of gastroenteritis [20, 21]. A study published a year before the South Bass Island outbreak showed that infective viruses were present in 5% of groundwater samples taken in 35 different states [22]. As the susceptibility to

infections among the general population increases [3], future outbreaks can be expected to have only more devastating effects.

2.1.2 The challenge of virus detection in complex water matrices

Contrary to the trend observed for drinking water, occurrence of waterborne disease outbreaks caused by the exposure to contaminated recreational water in the U.S. is on the rise from an average of 68 outbreaks resulting in about 3,215 illnesses per year for the 2001-2006 period to an average of 101 outbreaks resulting in about 5,693 illnesses per year for the 2007-2012 period [23-28]. Virus-associated outbreaks accounted for 1% to 10% of these incidents, with norovirus being the most prevalent viral etiological agent identified [23-28]. A recent review of published literature on waterborne disease outbreaks associated with recreational water also identified norovirus to be the largest cause of viral outbreaks followed by adenoviruses and echoviruses [29]. In swimming pools, where almost half (48%) of outbreaks occurred, 68% of those outbreaks were associated with inadequate disinfection. In lakes and ponds, the second largest affected recreational type of water, water quality surveillance is the most effective means of preventing outbreaks [29].

With direct and indirect water reuse gaining broader acceptance [30, 31], the potential for drinking water contamination increases and so does the need for monitoring the microbiological quality of water treated for reuse. The complex compositions of recreational water and treated wastewater complicate the detection of pathogens in

such matrices. Various dissolved and suspended species in water get concentrated along with target pathogens, foul the filters, slow down the concentration process, and interfere with assays performed on the concentrates.

2.1.3 Sample concentration as a key step in the detection process

Reliable virus preconcentration and recovery from water remains one of the most significant challenges in virus detection [32]. Typical virus concentrations are 10^1 to 10^4 particles/L in surface water [33, 34] and 10^5 or more particles/L in primary and secondary treated sewage effluent [35]; in drinking water, virus concentrations <1 particle per 100 L represent a significant risk of illness [36]. Thus, to reliably detect viruses in treated waters, large volumes (10 to 1,000 L) of source water must be concentrated to volumes amenable to rapid assays [37, 38]. Although fast concentration of all viruses in a sample is ideal, engineering challenges such as membrane fouling and irreversible adsorption of viruses to components of the filtration unit increase time required for concentration and limit recovery. The variability and complexity of water may result in virus recoveries that are unacceptably low, poorly reproducible or both. These problems often prohibit definitive association of waterborne viruses with specific disease outbreaks.

Primary concentration techniques employed currently include VIRADEL (VIRus ADsorption-ELution), which is the EPA-approved method of virus concentration (Tables 1, 3, and 5; see APPENDIX), crossflow ultrafiltration (CFUF; Tables 2, 4, and 6), ultracentrifugation [39, 40], centrifugal ultrafiltration [41], membrane-based electro-separation

[42], microfluidic evaporation [43] and flocculation/re-dissolution/ultrafiltration [44]. Only the first two methods are practical for concentrating large volume environmental samples and it is one of these two methods that is usually used for primary concentration. At the secondary concentration step the sample volume is reduced further to enable analyses such as quantitative polymerase chain reaction (qPCR). The primary concentration step is the bottleneck because of both its longer duration and the typically larger loss (i.e. lower recovery) of target pathogens.

Both VIRADEL and CFUF techniques perform well only with a limited range of viruses. The most difficult challenge that VIRADEL and UF-based methods share is poor reproducibility of elution [45], which is subject to multiple interferences [46-55]. Changes in pH [46, 47], concentration [54-56] and type [55, 56] of salts present in the sample, as well as the composition and loading of dissolved organics [46-48, 51, 52] lead to significant variations in virus recovery.

2.1.4 The scope and structure of this review

The scope of the paper includes VIRADEL and CFUF as the two main membrane-based methods of sample concentration for virus recovery. The review builds on and complements the recent reviews by Ikner et al. [57], Cashdollar and Wymer [15] and Gibson and Borchardt [58] by focusing on how various parameters of the concentration process affect virus recovery. The discussion distinguishes the primary and the secondary concentration stages and centers on the former as the bottleneck in the overall sample

concentration sequence. Virus recoveries reported in the literature are analyzed in the context of concentration process parameters with a special attention to the reproducibility of the recovery data. We summarize, in a tabulated format, all published VIRADEL and CFUF studies on the concentration of noroviruses (13 VIRADEL studies with 77 different concentration conditions and 4 CFUF studies with 8 different concentration conditions) and adenoviruses (10 VIRADEL studies with 42 different concentration conditions and 5 CFUF studies with 15 different concentration conditions), both important human pathogens with relatively low recoveries [15]. In support of the discussion, we also summarize all recent (published since 2001) VIRADEL and CFUF studies on the concentration of MS2 (6 VIRADEL studies with 35 different concentration conditions and 11 CFUF studies with 47 different concentration conditions), perhaps the most studied bacteriophage and a human virus surrogate commonly used in virus fate and transport studies.

The structure of this paper is as follows. The following section (Section 2) describes the VIRADEL and CFUF as applied to virus concentration from large water samples. Principles underpinning the two processes as well as their advantages and limitations are discussed in detail. Section 3 outlines the various parameters affecting the performance of VIRADEL and CFUF. Here we describe main physicochemical interactions that determine the efficiency of virus recovery and propose possible approaches to improving the sample concentration process. Section 4 identifies knowledge gaps and outlines a possible research agenda for improving the science and practice of virus separation for detection.

2.2 Currently practiced methods of primary concentration: Principles, advantages, limitations.

2.2.1 VIRus ADsorption and ELution

The VIRADEL method includes two steps: (1) adsorption of viruses by passing the sample (up to 1,000 L for drinking water) through a microfilter, which can be either electropositive [59-68] or electronegative [56, 60, 64, 67, 69, 70]; and (2) elution of viruses from the filter using a pH adjusted (usually basic) solution, the eluent. While the intended mechanism for virus removal at the first stage of the VIRADEL process is adsorption, straining by smaller pores of the microfilter can contribute to the overall removal. We also note that although the terms “electropositive” and “electronegative” have been broadly used to describe the charge on the filters used to concentrate viruses, the usage is unfortunate for two reasons. First, the charge is generally pH dependent. Second, the term electronegativity has an established and distinctly different meaning (the ability of an atom to attract electrons) in the chemistry literature.

In 1960, Metcalf used a membrane filter to perform a VIRADEL-like separation to concentrate influenza virus from bacterial mixtures. In these tests, instead of eluting viruses from the membrane, the membrane was crushed to pulp and resuspended for virus detection by hemagglutination tests and infectivity titrations [71]; the author noted that “on several occasions, …, essentially comparable recoveries could be achieved simply by washing the membrane surface.” The first application of the VIRADEL dates

back to 1967 when Wallis and Melnick concentrated poliovirus from saline-diluted crude harvest using an electronegative filter and a variety of eluents [72].

Commonly used electronegative filters include MF-Millipore™ Membrane Filters made of a mixture of cellulose nitrate and cellulose acetate [55, 61, 67, 73-76] and Filterite filters made of glass fiber bound by an epoxy resin [54, 60, 77, 78]. Due to the negative charge of most viruses at pH values typical for environmental water samples, the use of electronegative filters requires sample preconditioning either by acidification of the sample or by addition of multivalent cation salts to facilitate virus adsorption to the filter [56, 64] (see section 3.2). Sample preconditioning is often time-consuming and can limit the sample volume, especially if field-collected samples need to be sent to a remote laboratory. It may also be difficult to determine the dosage of acid and salts needed to pre-condition a complex environmental sample. Furthermore, sample acidification might affect virus integrity and infectivity [61, 79, 80] and confound accurate assessment of microbiological quality of the water.

A significant advantage of electropositive filters is that sample preconditioning can be avoided. Zeta Plus 1MDS microfilter (formerly marketed as Zeta Plus Virosorb 1MDS) made of charge-modified glass and cellulose was the only electropositive filter that the U.S. EPA originally recommended for the VIRADEL process [81]. Because of the filter's high cost ($200 to $300 [15]) and vulnerability with respect to fouling by colloids, several research groups have evaluated other electropositive filters as alternatives [59-62, 68, 82]. NanoCeram (a thermally bonded blend of microglass fibers and cellulose infused with

nanoalumina fibers in a non-woven matrix) is another positively charged filter used in virus concentration [68, 74, 83-85]; relatively inexpensive ($40 [15]), NanoCeram was found to be as efficient as Virosorb [68]. In 2010, U.S. EPA added NanoCeram to the list of recommended VIRADEL filters while pointing out that the NanoCeram is more susceptible to clogging than the 1MDS [86]. Other electropositive filters used in the VIRADEL process include Zeta Plus S series depth filters (surface-modified cellulose and filter aid mixtures) [60, 77, 87], lifeASSURE 045SP filter (Nylon 6,6 based; formerly marketed as Zetapor 045SP) [88], MK filter (molded waste fibers coated with melamine resin) [62], oiled sodocalcic glass wool filter [85, 89] and electronegative filters pretreated by a solution of multivalent cations [67, 76, 90] or a cationic polymer [61]. Zeta Plus 50S filter appeared to be as efficient as Virosorb in recovering viruses from various types of water [60]; Rose et al. obtained higher recoveries from primary effluent with Zeta Plus 50 S than with 1MDS and Zeta Plus 30 S, but saw no significant differences among these filters in virus recovery from a secondary effluent. MK filter was found to give recoveries that were both lower and more variable [62]. Diatomaceous earth filters treated with a cationic polymer (e.g. Nalco 7111) showed improved coliphage recovery from trickling filter effluent samples [61] when compared with Virosorb filters; however, unless a drop-by-drop elution (see section 3.5.1) was performed the coliphage recovery from sewage was still below 50% (data not available for tap water samples).

Tables 1 and 3 summarize recoveries reported for norovirus and adenovirus along with the experimental conditions used in the concentration tests. VIRADEL recoveries of MS2, the microorganism most commonly employed in virus concentration studies, are

provided in Table 5. The data clearly indicate that virus recovery by VIRADEL can be low and poorly reproducible [91]. Recoveries reported for adenovirus (e. g. 0.02% from a mixture of DI and tap water [66]) and certain other viruses such as astrovirus (0.5% from tap water [55]) are especially low. Borrego et al. observed that less than 35% of the indigenous *E. coli* phages present in tap water spiked with sewage were adsorbed on the Virosorb 1-MDS filter and less than 12% of those were recovered by elution [61] yielding the overall recovery of $\lesssim$ 4 %. Concentrating human adenovirus 41 by a NanoCeram filter, Gibbons et al. reported high retention (> 99%) by the filter but very low efficiency of elution (< 3%) with 3% beef extract solution used as the eluent [83]. Low elution recoveries were also observed by Abdelzaher et al. who showed 35% recovery of the coliphage spiked in seawater and adsorbed on a negatively charged cellulose membrane [79]. Although no study has definitively identified mechanisms behind the low elution efficiency of certain viruses by VIRADEL, it was hypothesized that virion capsid structure may play a role in virus entrapment by a filter matrix resulting in hindered elution [83, 84, 92].

2.2.2 Crossflow ultrafiltration

CFUF (also known as tangential ultrafiltration) has emerged as a promising alternative to VIRADEL [66, 93-99]. During CFUF, viruses are maintained in the recirculated retentate by an ultrafilter with a nominal pore size significantly smaller than the virus. In 1933, Clark et al. used a cotton membrane to concentrate poliomyelitis virus suspension from the growth medium by a factor of up to 165 [100]. It appears that the first tests on

concentrating water samples spiked with viruses were performed almost 40 years later. In 1971, Sweet et al. used an osmotic ultrafiltration system to concentrate poliovirus with an asymmetric cellulose acetate membrane and either $MgSO_4$ or sucrose providing osmotic driving force [101]. Then Morrow employed pressure-driven CFUF to concentrate the inactivated virus of foot-and-mouth disease; the method was proposed for possible applications in “vaccine production as a preliminary step in purification” [102]. In 1974, Belfort et al. employed cellulose acetate hollow fiber as an ultrafilter to concentrate poliovirus from water also using applied transmembrane pressure as the driving force [93].

CFUF has several advantages over VIRADEL. First, low molecular weight solutes, which can potentially inhibit the downstream detection by molecular methods and cell culture infectivity assays, pass through the membrane and are not concentrated together with pathogens [45]. Second, crossflow minimizes membrane fouling and virus deposition onto the membrane, and thus could increase virus recovery. Third, CFUF can simultaneously concentrate multiple pathogen types [103-109]. Fourth, the potential for virus inactivation due to pH changes in VIRADEL (e.g. pre-acidification of the sample and elution with high or low pH) is minimized. While some viruses are acid-tolerant and some are base-tolerant, many can be inactivated when exposed to low pH [110-112] or high pH [111, 113, 114]. Even for the same virus, different serotypes could have different response to low or high pH [115]. The loss of infectivity is caused by an irreversible change in the virus capsid; mechanisms hypothesized to be responsible for such changes include proteolytic cleavage [115], dissociation of capsid [111] and a decrease in its stability [110].

Including secondary concentration in their analysis, Hill et al. showed that CFUF gave significantly higher and more reproducible (58% ± 8% vs 33 ± 18%) total recoveries of echovirus 1 than VIRADEL [99]. Yet, virus deposition onto membranes was still observed in CFUF [95, 103, 106, 116]. To further recover the viruses adsorbed on the filters, elution may be performed after filtration using the approach similar to that of VIRADEL [66, 103-106, 116-121]. The molecular weight cutoff (MWCO) of membranes used to concentrate viruses by CFUF is typically in the 10 kDa to 100 kDa range ensuring virus retention of 2 log or higher. The membranes are made of polysulfone [104-107], polyethersulfone [116, 117, 121-123], polyacrylonitrile [103], or cellulose triacetate [124], all of which are polymers commonly used to make porous membranes. In practice, hollow fiber membranes assembled in large modules have been the most commonly used configuration [93, 94, 99, 103, 106, 125, 126]. These modules have the advantage of a high membrane packing density allowing for a fast filtration of large volumes of water. Such filtration systems are suitable for field applications and can be reused to make sample concentration more cost-effective.

2.3 Parameters influencing the performance of membrane-based methods of virus concentration

As discussed in section 2, VIRADEL is a two-stage process that necessarily includes filtration and elution steps. While essential in VIRADEL, elution is optional in CFUF and can be employed if preelution recovery by CFUF is insufficiently high. In a number of studies on CFUF-based sample concentration elution was not performed [95, 107, 123, 127]. During the elution step, both VIRADEL and CFUF aim at disrupting virus-membrane

interactions to recover attached viruses. During the filtration step, however, the two methods rely on opposite strategies: VIRADEL is designed to maximize virus adsorption onto the filter while CFUF employs anti-adhesive membranes to concentrate viruses in the recirculating retentate stream. Thus, conditions that increase virus recovery by VIRADEL may have an opposite effect during CFUF. In this section, the effects of various parameters on the virus recovery are discussed by contrasting their impact on VIRADEL and CFUF. We overview published data and, when possible, suggest reasons for study-to-study discrepancies and possible hypotheses that might be helpful to test.

2.3.1 Virus properties

Virus-surface interactions depend on physicochemical properties of viruses, including size, surface charge, isoelectric point (pI), surface energy and morphology. Because VIRADEL and CFUF rely on different principles for virus recovery, the same virus property may have an opposite effect on the recovery by these two methods. Analogously, one filter may yield different recoveries for different viruses.

In VIRADEL, strongly charged viruses should adsorb to the oppositely charged filter during the filtration step but may be difficult to “strip off” the filter during elution; Polaczyk et al. illustrated this with MS2 (pI = 3.9) and ΦX174 (pI = 6.6) bacteriophages in experiments conducted with 1MDS filter at pH ranging from 6.5 to 7 where MS2 carries a more negative surface charge [128]. When using an electronegative filter, adjusting pH to render viruses positively charged will also lower the negative charge on

the filter and possibly reverse the filter's charge to positive. The window of pH values where the virus and the filter have electrical charges of opposite signs depends on pI values of the virus and the filter and can be quite narrow. The closer the pI values are, the narrower this pH range is.

CFUF employs membranes that resist virus adhesion. In the case of non-enveloped viruses, for instance, membranes that exhibit low protein binding should show lower adhesion of viruses. Generally, membranes that present a highly hydrophilic surface are more fouling resistant and, therefore, preferable for CFUF [129-131]. At pH values typical for environmental samples most viruses are negatively charged and by choosing an electronegative membrane one can rely on electrostatic repulsion to reduce virus loss to the membrane. However, more apolar viruses could still be adsorbed onto membranes due to hydrophobic attraction hence the need for a hydrophilic membrane surface. Hydrophobicity can be operationally defined in terms of the water contact angle on a virus lawn [116, 121, 132] or virus partitioning coefficient in hydrophobic interaction chromatography [133]; these relatively simple metrics give an aggregate assessment of virus hydrophobicity, but the insight they provide is limited. Some of the contradictions reported in the literature can be due to the simplistic interpretation of, and lack of quantitative data on virus hydrophobicity. Determining individual surface energy components [116, 121, 132] for both viruses and membranes may help understand why surfaces of similar water contact angle and charge show different adsorption behavior.

Virus morphology is another factor that can affect recovery by both VIRADEL and CFUF. For example, fibers associated with each penton base of the adenovirus capsid could facilitate virion entrapment in the filter matrix making adenovirus difficult to elute [83, 84, 92]. Indeed, low elution efficiencies of adenoviruses were observed in several VIRADEL studies though virus retention by filters was high [83, 84]. Fiber or spike structures on the capsid surface can also sterically hinder virus adsorption to a membrane surface [134, 135]. However, in the presence of macroscopic repulsion between the virus and the membrane, the protrusions on the capsid may extend beyond the Debye layer leading to microscopic attraction [121]. An important question that needs to be answered is whether aggregate measures of the charge and surface energy of a virus (i.e. its zeta potential and hydrophobicity) can adequately describe virus adhesion. A general hypothesis that could be tested is that the local distribution of these properties along the virus surface affects virus adhesion.

2.3.2 Membrane properties

Due to the negative net charge of most viruses at the pH typical for tap and natural water samples (pH 6 to 8), electropositive filters are favored and have been extensively used in VIRADEL-type concentrations. With electronegative filters, either in-situ charge modification of filters or preconditioning of samples is possible with the former often being a more practicable approach, especially for large volume samples. Modifying negatively charged surfaces with positively charged amines [136] or multivalent cations (e. g. Mg^{2+} [90], Fe^{3+} [90], Al^{3+} [67, 70, 90]) enhances virus adsorption at pH above its pI. The

specific type of the VIRADEL filter may also affect recovery. In experiments on norovirus concentration by electropositive NanoCeram and 1MDS filters (exp. 18-21, Table 1) [68], higher recoveries were obtained with NanoCeram for both tap water (3.6% ± 0.6% vs 1.2% ± 1.4%) and river water (12.2% ± 16.3% vs 0.4% ± 1.8%).

In the case of CFUF, covering or "blocking" the membrane surface with a layer of protein (e.g. using solutions of beef extract [95, 137], calf serum [105, 116] or bovine serum albumin [137]), glycine [95] or sodium polyphosphate [104, 106] minimizes virus adhesion. The concept was first proposed in 1965 by Cliver who pretreated microfiltration membranes with serum and gelatin solution to minimize adsorption of two enteroviruses (poliovirus type 1 and Coxsackievirus B-2) to membrane surface [138]. The method was later used for poliovirus recovery by CFUF in a study by Berman et al. where the membrane was pre-treated with either 1% glycine or 3% flocculated beef extract [95]. The term "blocking" refers to the blockage of potential virus adsorption sites on the membrane surface and not to the membrane pore blockage. Pore blockage is undesirable as it leads to a decline in permeate flux and prolongs sample concentration. Ideally, the pore size of the membrane should be small enough to ensure no virus loss to the membrane pore space or the permeate and yet sufficiently large so that the blockage of adsorption sites by the blocking agent does not lead to a significant loss in permeate flux. Molecular blocking agents such as sodium polyphosphate (NaPP) (e. g. 600 Da [104, 106]) and glycine (75 Da) with molecular weights smaller than the MWCO of the membranes present an attractive choice: such molecules adsorb onto walls of ultrafiltration membrane pores but do not plug them.

The most common choices of blocking agents have been solutions of calf serum, bovine serum albumin and beef extract. Membrane pretreatment with 3% beef extract helped increase murine norovirus recovery by a polysulfone ultrafilter more than ten-fold (exp. 2-5, Table 2) [107] and MS2 bacteriophage recovery almost two-fold (see APPENDIX; exp. 23 and 24, Table 6) [107]. Only two papers, to our knowledge, reported that blocking a membrane with proteins had no effect on (see APPENDIX; exp. 31-36, Table 6) [118] or decreased [126] virus recovery. A possible reason for the discrepancy is that blocking agents are selected without regard to type of surface they modify. A useful hypothesis to explore is that the blocking efficiency is governed by membrane-blocking agent interaction; the more energetically preferable such interaction is in comparison to the interaction between blocking molecules, the better “blockage” is likely to be.

Protein-blocked membrane may not be practical for field sampling because of a possible contamination of the membrane by bacteria during storage and transport [104, 106]. Furthermore, because blocking is time-consuming (usually done overnight), the process is not optimal for rapid detection. Hill et al. showed that 15-min blocking of an UF membrane (MWCO 15 to 20 kDa) with NaPP solution resulted in the microbial recovery similar to that obtained in the control experiments with calf serum as the blocking agent (see APPENDIX; exp. 6-14, Table 6) [104]. While membrane blocking has been assumed to minimize virus adsorption to the membrane, all evidence for such an effect appears to be indirect and based on the observed higher values of virus recovery by blocked filters. For example, it was suggested that NaPP increases electrostatic

repulsion between the membrane and microorganisms [104] but surface charge data were not provided to support the statement. We suggest testing the hypothesis that the mechanism responsible for blocking is a combination of electrostatic and acid-base repulsive interactions between the virus and the blocked membrane.

Layer-by-layer coating by polyelectrolytes has been proposed as an alternative to the blocking process [116, 121]. Coating a membrane by a polyelectrolyte multilayer (PEM) film can produce surfaces with a broad range of properties, where variability is achieved by choosing various polyelectrolyte combinations and deposition condition (pH and ionic strength of deposition solutions, number of polyelectrolyte layers). This is in contrast to blocking by proteins, which can be viewed as intentional, but poorly controlled, fouling of the filter. Membranes coated with PEMs were shown to yield higher recoveries of bacteriophage P22 [116] and human adenovirus 40 [121] from DI water compared with the traditional blocking by beef extract (control). An analysis of virus-membrane interaction energy pointed to the membrane's higher negative charge and hydrophilicity as the reasons for higher recovery by PEM-coated membranes.

2.3.3 Design of the filtration process: Hydrodynamic conditions

Sample concentration is one of the most time-consuming steps in the overall detection process. Concentration times depend on many factors such as, for example, feed water turbidity and NOM content, both of which contribute to membrane fouling and, therefore, affect the rate of concentration. For example, concentrating 100 L of tap water to 400

mL by CFUF using a hollow fiber cartridge takes 2 h, and further volume reduction to a few mL for qPCR analysis requires another 1 to 3 h [106]. Because virus concentrations of less than one genomic copy per 100 L of water represents a significant risk of illness [36], virus monitoring in drinking water often requires testing up to 1,000 L [64]. One approach to minimizing virus adsorption in CFUF is to increase the crossflow rate. However, the shear stress on the virus can potentially disrupt its infectivity. Indeed, a decrease in infective virus titer in the retentate of a crossflow filtration unit has been reported [126, 139-141] although in at least one study such a trend was not observed [142]. In two studies, virus aggregation was initially considered but eventually ruled out as the reason for the observed loss of infectivity [140, 141]. Belfort et al. noticed no significant difference in poliovirus recovery by filtration through a non-blocked cellulose acetate membrane when tripling the crossflow rate; this observation, however, was based on only one filtration test performed at the low crossflow rate [93]. Polaczyk et al. observed no statistical difference in recoveries of MS2 and echovirus 1 when operating a membrane pretreated with NaPP at two different permeate flow rates [106] although the ratio of corresponding fluxes, J_x/J_p, remained within a narrow range from 5,800 to 6,500. Pasco et al. [116] evaluated a large range of operational conditions by varying J_x/J_p from 2,000 to 12,000 to concentrate P22 bacteriophage; pre-elution recovery with PEM-coated membranes significantly improved from 32% to 85% with an increase in J_x/J_p while no statistically significant change in recovery over the same range of hydrodynamic conditions was observed with membranes blocked by calf serum. Rhodes et al. concentrated MS2 and poliovirus from tap water with hollow fiber ultrafilters [127] and observed increased recoveries at lower permeate fluxes: an increase

from 64.7% ± 4.9% to 98.7% ± 5.3% for MS2 and an increase from 62.9% ± 4.7% to 104.5% ± 20.7% for poliovirus (see APPENDIX; exp. 29-30, Table 6).

The effect of permeate flux on the virus recovery by VIRADEL was also evaluated and, as with CFUF, results varied. In VIRADEL, lower flow rate at the filtration stage increases virus residence time within the filter and decreases permeate drag; theoretically, this should translate into more effective virus capture. Sobsey and Glass reported that poliovirus adsorption to Zeta Plus 50 filter from tap increased significantly ($p = 0.006$) from 62% to 86% when the permeate flux decreased 10 times from 15 to 1.5 mL/(min·cm^2) [77]. Jin et al. used Al(OH)$_3$-based electropositive granule media packed into a filter cartridge to concentrate poliovirus from tap water and obtained recoveries of 71% and <50% at flow rates of 300 and 500 mL/min, respectively (filtration fluxes of ~6.0 mL/(min·cm^2) and ~9.9 mL/(min·cm^2) based on the cartridge diameter reported by the authors) [143]. However, two other studies on poliovirus recovery from tap water showed no significant correlation between virus adsorption and permeate flux [62, 68].

Operating the concentration unit at a higher permeate flux would hasten the process; however, the larger permeate flux may decrease virus retention by the membrane (due to increased drag) and elution efficiency (due to virus entrapment on or within the membrane or the fouling layer). Moreover, a larger permeate flux typically translates into more membrane fouling, which can eventually offset the gains in the concentration rate. Adjusting hydrodynamics conditions inside the membrane channel can help optimize the process to achieve faster filtration without affecting virus recovery. To

better understand how recovery depends on the crossflow and permeate fluxes and understand the reasons behind the often contradictory findings cited above, one needs to comprehensively assess adsorption kinetics in a filter as a function of hydrodynamic drag and surface forces.

2.3.4 Composition of the water sample

2.3.4.1 Effect of water composition on VIRADEL

Spiking samples with humic or fulvic acids decreased virus recoveries by VIRADEL with both electropositive and electronegative filters [144, 145]. Complex water matrices were also shown to give lower virus recoveries by VIRADEL than simpler water types did. For example, Haramoto et al. achieved higher recoveries of human norovirus from MilliQ water, tap water, and bottled water than from river and pond water (exp. 29-33, Table 1) [67]. Noroviruses were recovered with higher efficiency from bore hole water than from other water types such as open well, river, food processing, and rain waters (exp. 68-77; Table 1) [146]. Karim et al. concentrated poliovirus with two electropositive filters (1MDS and NanoCeram) and observed higher recovery from tap water in comparison with river samples for both filters [68]. In a study by Dan et al., infectious recovery and genome recovery of adenovirus were higher from RO water samples compared with those from sea water and treated sewage (exp. 17-25, Table 3) [75]. Abd-Elmaksoud et al. seeded multiple pathogens into tap water with different added amounts of soil and found that recoveries of different viruses were significantly different only in the water matrix with low turbidity [147]. However, opposite trends were also

reported in several studies. Victoris et al. concentrated norovirus and astrovirus from multiple water matrices and obtained higher recoveries from mineral and river water than from tap water (exp. 6-17, Table 1) [55]. Hata et al. showed that virus recoveries from tap and river were comparable to or even higher than those from Milli-Q water [76]. Similarly, the recovery of murine norovirus from ground water was higher than that from surface water but the lowest recovery was obtained from ultrapure DI water (exp. 62-65, Table 1) [148]. Notably, in most studies the comparisons were drawn between tests with different feed waters but not against a certain control such as DI water.

Not all water constituents decrease virus recovery. Amending water samples with certain chemicals has been explored as a means to improve the process. For example, norovirus recovery from tap and river water was highest from samples with 5 mM $MgCl_2$ added to the water. For mineral and sea water, the highest recovery of norovirus was obtained from samples amended with 25 mM $MgCl_2$ and 50 mM $MgCl_2$, respectively (exp. 6-17, Table 1) [55]. The pH of the water sample was shown to have a significant influence on adenovirus recovery, which increased from <5% at pH 4.5 to 55% ± 19% at pH 3.5 (exp. 17-25, Table 3) [149]. Further, effects of the water matrix on virus recovery may vary for different types of filters used. Increasing concentration of salt in feed water increased virus adsorption on negatively charged nitrocellulose filter, but decreased adsorption on positively charged 1MDS (control: salt-free sample) [54]. However, virus adsorption onto another commonly used positively charged filter, NanoCeram, was not affected by high salt content in the samples [74].

2.3.4.2 Effect of water composition on CFUF

Many studies showed that increasing water complexity can also affect virus recovery by CFUF. This is to be expected as surface properties, permeability, and selectivity of the membrane affected by dissolved and suspended components and various salts in the feed water. Belfort et al. showed that poliovirus recovery by a polysulfone hollow fiber membrane decreased from 77% in DI water to 52% in tap water [94]. Shi et al. reported higher pre-elution recoveries of human adenovirus 40 from DI water (~75%) than from tap (~39%) and lake water (~21%) [121]. Kahler et al. showed that virus recovery decreased as water turbidity increased up to 26 NTU [119]. In at least one study, however, water complexity did not affect virus recovery as there was no significant difference between drinking and surface waters in recovery values for infective MS2 and PRD1 [124]; this result, however, may not be directly compared with those studies where qPCR was used to quantify viruses as infective recovery should not be expected to follow same trends as total recovery (see section 4.2 on recommendations for improving study-to-study comparability). Addition of 0.1% NaPP as a sample amendment was associated with significantly higher recovery of MS2 when filters were blocked with fetal bovine serum (see APPENDIX; exp. 2-5, Table 6; control: no amendment added) [104].

Ionic strength was found to correlate with the loss of virus infectivity in tap water [140, 141], although the correlation between sample conductivity and loss of infectivity was not observed in more complex water matrices [126]. This can be attributed to masking of the ions' effect by the complex chemistry of background solution. In addition to crossflow-

induced shear stress, virus morphology and presence of hydrophobic surfaces in the concentration unit have also been suggested as factors contributing to the loss of viral infectivity [139, 140]. Another factor that might influence infectivity assays, and thus recovery of infective viruses by crossflow filtration is the presence of natural organic matter or cations which have been shown to affect virus aggregation [150].

Effects of the water matrix on virus recovery also depend on the virus type. This is not unexpected as different viruses should interact with dissolved species in the water differently. Rhodes et al. examined multiple virus recoveries with hollow fiber ultrafiltration from river and tap water and found that recoveries for adenovirus (exp. 4 and 5, Table 4), poliovirus and bacteriophage ΦX174 were higher from tap water than those from river water while opposite trends were observed for enterovirus 70, echovirus 7 and coxsackievirus B4 [120]. Even for the same type of water, variations in membrane operation conditions and in water composition can greatly affect virus recovery [125, 126]. T1 phage recovery from surface water from 6 different locations varied from 34% to 75% [125], and PP7 recoveries from storm water from 21 different locations varied from 10% to 98 % (when assessed by qPCR), and from 25% to 90% (when assessed by cell culture infectivity assays) [126]. Water samples from the same site, but collected in different seasons, virus recoveries using the same ultrafiltration membrane may vary due to differences in the ionic makeup and TOC content (exp. 6-11, exp. 13-14, Table 4) [121]. Again, unless specified otherwise, recoveries were compared between tests with waters of different compositions but not against a common control. Since standard deviations of recoveries were not provided in some of the cited studies it is

unclear if the variations were due to differences in the water composition or to an inherent irreproducibility of the combination of the recovery and detection methods (see section 4.2). When determining virus recovery from drinking water from 8 different locations, Hill et al. [105] did perform replicate measurements and found no statistically significant correlations between the 7 parameters tested (pH, turbidity, alkalinity, conductivity, iron concentration, TOC, and DOC) and recoveries of MS2 or ΦX174 phages. A likely reason for the absence of correlations is that the parameters tested (x_i) are either not independent variables or do not form the complete variable set or both so that the recovery, r, cannot be described as $r = \sum_{i=1}^{7} x_i$.

Common to all studies summarized in the section is the dependence of virus recovery on the complexity of water matrix. Because of the lack of controls that can make inter-study comparisons possible, more specific generalizable conclusions cannot be drawn. Yet the very variability of the data points to a general hypothesis that the recovery is governed by interactions between water components and depend on the virus and membrane properties only inasmuch as their interactions with the water constituencies is concerned. Indeed, dissolved and suspended species in the feed water can alter the surface properties of both the membrane and the virus [151]. In addition, these various constituents in the sample can be concentrated simultaneously with viruses and can affect the downstream detection method [152], especially for samples with high total organic carbon (TOC) content.

2.3.5 Eluent composition and elution protocol

2.3.5.1 Elution in VIRADEL

Elution is an essential step in virus concentration by VIRADEL. Low virus recovery reported in multiple VIRADEL studies stemmed from low elution efficacy [79, 83, 84]. For electropositive filters, a commonly used eluent is beef extract solution (1.5%-3%) in the pH range from 7.5 to 9.5 [61, 62, 67, 68, 74, 85, 88, 90, 149], sometimes buffered with glycine [62, 68, 74, 85]. It has been suggested that beef extract improves virus elution by disrupting hydrophobic interactions between the virus and the membrane and facilitates bioflocculation during the following secondary concentration [70, 149]; this interpretation is consistent with the use of beef extract as a blocking agent (see section 3.2). The alkaline pH increases the net negative charge of both the filter surface and viruses thereby enhancing the electrostatic repulsion and promoting virus desorption [77, 87, 153]. Addition of 0.1% NaPP to the beef extract-based eluent helped increase recoveries for MS2 (see APPENDIX; exp. 5 and 7, Table 5) [128]. Unfortunately, organic components of the beef extract solution inhibit qPCR analysis [55, 70, 76, 154, 155]; yet, beef extract is still commonly used as an eluent. Farrah and Bitton determined that 4 M urea buffered with 0.05 M lysine at pH 9 was an efficient eluent for an electropositive filter [156] when recovering viruses from sludge [157] and treated wastewater [87]. Similar to beef extract, urea likely interferes with hydrophobic interactions between the virus and the filter while lysine is used to buffer the solution at a pH at which both the filter and virus have net negative charges [87]. Another eluent considered was 0.05 M glycine at pH 11.5, but the

corresponding elution efficacy was poor compared with that of 3% beef extract at pH 9.5 for both coliphages [60] and animal viruses [59, 60]. The lower recovery with the 0.05 M glycine-only eluent could be attributed to virus inactivation at the higher pH [158, 159]. Compared with beef extract-only eluent, solution of NaPP (1.0%) and glycine (0.05 M) in phosphate buffer (3.8 mM Na_2HPO_4, 6.5 mM KH_2PO_4; pH 7.5) was very effective in recovering MS2 (see APPENDIX; exp. 21-30, Table 5) [84]. Although the eluents have been mostly designed by a trial-end-error method, the common trend appears to be that eluent components are selected to target specific types of virus-filter interactions.

For electronegative filters, samples are usually acidified to induce a positive charge on the virus. Divalent cations are also often added to the sample, instead of or in addition to lowering its pH. Alkaline beef extract or glycine solution have been applied to elute virus adsorbed to electronegative filters as well [60, 79, 149]. These filters remain negatively charged in such eluent, but the charge sign of adsorbed virions is reversed to negative allowing for an efficient elution. In the study by Katayama et al. as well as in several more recent studies with electronegative filters, 1 mM NaOH (pH 10.5 to 10.8) was used as the eluent [55, 67, 70, 74, 76, 160]; in these tests, pretreatment was first performed either by soaking the filters in solution with multivalent cations (Mg^{2+}, Al^{3+}) or by adding those cations to the water. Cations can enhance virus adsorption to membranes by acting as bridges between the virus and the membrane [161]. After filtration, membranes were rinsed with 0.5 mM H_2SO_4 prior to elution with 1 mM NaOH. During the acid rinse, cations were removed while viruses attained a positive charge and directly adsorbed to electronegative filter. During the elution the virus charge reverses back to negative and

the viruses detach from the electronegative filter [70]. However, including the acid rinse step may inactivated viruses [88] (also see section 2.2).

The optimal choice of the eluent appears to be filter-specific even for membranes of like charges (e. g. NanoCeram and 1MDS, which are both electropositive). Lee et al. evaluated several elution buffers (1.5% beef extract, 0.05 M glycine, both with and without 0.01% Tween 80) to determine the recoveries of human norovirus (exp. 45-48; Table 1) [162]. Without 0.01% Tween 80, the recoveries were higher with 1MDS than with NanoCeram. At the same time, when 0.01% Tween 80 was added to the eluent, the recoveries from NanoCeram were significantly higher than those from 1MDS

In addition to the eluent type, the elution protocol itself may influence VIRADEL recovery. The standard elution procedure involves immersing the membrane in the eluent and then filtering the eluent through the membrane. The membrane-eluent contact time varies from study to study and ranges from 10 s to multiple hours (e.g. overnight exposure) [55, 61, 62, 68, 85, 87, 90, 149]. Working with bacteriophages in a trickling filter effluent, Borrego et al. reported that the slow (0.5 mL/min) drop-by-drop elution yielded slightly higher recovery in comparison to the elution performed at larger flowrates (~ 1 mL/s) [61]. To our knowledge, the work by Borrego et al. is the only one where the effect of elution flow rate was explored. Further studies are warranted to better understand the nature of the likely kinetics or mass transfer limitations on recovery (also see discussion in section 3.5.2).

Successive elutions, rather than a single elution, were performed in several studies to maximize recoveries [68, 74, 85]. Karim et al. tested poliovirus recoveries from tap water with NanoCeram by varying eluent-filter contact time and obtained the highest recovery (~77%) using a two-step elution with 1 min and 15 min immersion times during the first and the second elution, respectively [68]. Gibbons et al. achieved significantly higher recovery of norovirus (~99%) by recirculating the eluent than by passing it only once through the membrane (only 0.1%) (exp. 38 and 39, Table 1) [83]. Yet, in the same study, eluent recirculation had no statistically significant effect on adenovirus recovery (exp. 8-11, Table 3) [83]. Sun et al. tested three elution methods when concentrating adenovirus from seawater: (1) direct filtration of 1 mM NaOH; (2) shaking membrane in 1 mM NaOH on a vortex mixer and (3) magnetically stirring a 1 mM NaOH solution with suspended membrane coupons; stirring yielded the highest recovery of ~80% (exp. 40-42, Table 3) [160]. We recommend a systematic evaluation of virus desorption behavior, including both kinetics and equilibrium (isotherms) tests, to understand how the desorption (elution) protocol can be optimized. We suggest testing common eluents first to take advantage of the wealth of ad-hoc data already available in the literature.

2.3.5.2 Elution in CFUF

During CFUF, viruses are concentrated and recovered in the retentate stream. Size exclusion and electrostatic repulsion are main mechanisms of virus rejection while hydrophilicity of the membrane surface helps minimize virus adhesion to the membrane surface. However, significant virus deposition on the membrane was observed in many

studies prompting the use of elution [95, 103, 106, 116] either as backflush [104, 106, 163] or as crossflow rinse in the absence of a transmembrane pressure [103, 105, 106, 116-118, 120-122]. Pei et al. recovered 31 ± 8 % of MS2 from 10 L tap water using CFUF followed by elution with pure water [122]. Other researchers eluted ultrafilters with eluents commonly used in VIRADEL. Sylvain et al. eluted MS2 (73% to 84%) and ΦX174 (62% to 80%) using 1% beef extract buffered with 0.4% glycine at pH 9.5 [117]. Morales-Morales et al. eluted bacteriophages T1 and PP7 using 0.05 M glycine in the retentate [103]. Albinana-Gimenez et al. used 1 mM NaOH as the elutent and reported low recoveries for adenovirus (3% to 6%) and norovirus (<1%) [66]. A small amount (typically 0.01%) of NaPP coupled with 0.01% Tween 80 has been used to elute bacteriophages (MS2 [105, 106], ΦX174 [105, 120] and P22 [116]) and human viruses (poliovirus [120], coxsackievirus [120], adenovirus [120], echovirus [106, 120] and enterovirus [120]) from ultrafilters. It was suggested that NaPP likely increases the electrostatic repulsion between viruses and the membrane [104]. In contrast, Tween 80 as a non-ionic surfactant can disrupt hydrophobic attraction between virus and membrane [84, 104]. In our previous study on human adenovirus 40 recovery by CFUF, we showed that virus elution using aqueous solution of 0.01% NaPP and 0.01% Tween 80 as the eluent produced nearly 100% recoveries from both DI water and tap water [121]. However, the same eluent only gave <65% post-elution recovery of the virus from a surface water. Ethylenediaminetetraacetic acid (EDTA) in the eluent gave a significantly higher post-elution recovery (84.3% ± 4.5%) of adenovirus from high TOC water (exp. 12 and 15, Table 4) [121]. It was hypothesized that EDTA improved elution by eliminating cation bridging [161] between viruses and natural organic matter in water or deposited on the membrane. As with other parameters, the

mostly heuristic search for an optimal eluent and elution protocol yielded large amount of data that is often contradictory and difficult to generalize. To design the elution process deliberately one should consider specific interactions that resist virus desorption and aim at disrupting them by chemical or hydrodynamic means. Including appropriate controls (e.g. eluents without one of a constituents) will be needed. Unfortunately, most referenced studies compared recoveries obtained with different eluents in a pair-wise fashion without manipulating the composition of one eluent or adjusting the elution procedure to obtain baselines.

2.3.6 Initial virus content in the water sample

When evaluating a concentration method with respect to a particular water type, viruses are normally spiked into water to give an a priori known virus load in the sample. This is done to factor out the initial concentration of the virus, known to affect removal values [164]. Indeed, in most VIRADEL studies virus recovery from samples with higher virus content was found to be higher. Li et al. demonstrated this for both electropositive (NanoCeram) and electronegative (Millipore) microfilters when recovering infectious adenovirus 5 seeded at 10^2 PFU/L and 10^3 PFU/L levels in sea water, RO-treated sea water, and treated sewage (exp. 17-23; Table 3) [75]. Polaczyk et al. also found that mean recovery of MS2 decreased from 92% to 44% when reducing the feed concentration from 10^6 PFU/L to 10^3 PFU/L (see APPENDIX; exp. 6-8, Table 5); at the same time, the decrease in ΦX174 recovery observed in this study was not statistically significant [128]. At least two studies, however, showed an opposite trend. A lower

influent MS2 seed titer (10^4 versus 10^8 PFU) resulted in a higher recovery when using the optimal eluent (1.0% NaPP, phosphate buffer (3.8 mM Na_2HPO_4, 6.5 mM KH_2PO_4; pH 7.5)), 0.05 M Gly, pH 9.3) (see APPENDIX; exp. 20 and 21, Table 5) [84]. Working with murine norovirus, Cashdollar et al. found the lower titer in the feed to give a higher recovery (exp. 64 and 65; Table 1) [148]. The effect of the feed concentration on virus recovery was also evaluated in CFUF. Liu et al showed higher recoveries of MS2 and ΦX174 for higher seeding levels in 100 L reclaimed water samples [118]. However, in another study on the concentration of multiple virus types tap water (also 100 L samples), Polaczyk et al. did not observe a statistically significant effect of the seeding level on recovery [106].

2.4 Research needs and recommendations for future work

Two overarching conclusions can be drawn based on the already very large and growing number of studies on concentrating virus-containing water samples. First, physicochemical interactions between the virus and the filter govern virus recovery. Indeed, the primary concentration methods are designed to harness these interactions to achieve higher and more reproducible recoveries. Second, the effects of various parameters of the concentration process are complex and, in many cases, appear to be interrelated. Understanding virus-filter interactions and the effects - individual and combined - of various parameters is important for the design of an effective membrane-based concentration process. In this section, we identify knowledge gaps and offer several recommendations for future research.

2.4.1 Method development: Standard procedures

Interlaboratory and interstudy comparisons of virus recovery data are challenging. The difficulties in comparing results with different water matrices and target viruses are further confounded by a large variability in the methods of concentration and in operational parameters of each method. Filters, blocking agents and procedures, flow rates, concentration ratios, eluents, and other process parameters vary broadly from one laboratory to another and often between different studies within one lab. The variability reflects the largely heuristic nature of the work. Consequently, despite the large number of published studies it is difficult to generalize findings, identify trends and establish guidelines. In their recent review, Cashdollar and Wymer chose to limit their statistical analysis to mean recoveries because "the majority of the studies were concerned only with performance of a single filter type and do not afford direct comparison of tap water versus environmental samples, electropositive versus electronegative filters, nor sample volume" [15].

Establishing a standard protocol for evaluating concentration methods would make comparisons easier, save effort and resources. For example, a panel of virus surrogates (e. g. bacteriophages) can be selected to comprehensively cover the range of virus properties (size, charge, morphology) to generate better datasets for regulated and emerging human viruses. Similarly, standard aqueous solutions can be designed to represent important water types such as tap water, groundwater, surface water, sea water and treated wastewater effluent. The variability in the water composition – both

temporal and between water types and sources – would remain an uncertainty but experimenting with standards can provide guidelines and help with selecting optimal concentration procedures.

2.4.2 Data reporting and analysis

A more unified approach to the data reporting is also recommended. Many publications on virus concentration by CFUF only include total recovery and leave out the virus loss to the filter at the preelution stage. Similarly, few publications on VIRADEL indicate the amount of viruses not retained by the filter at the filtration stage. To better understand the fate of viruses throughout the sample concentration process and identify reasons for virus loss, it is recommended that both preelution recovery (or virus retention in VIRADEL) and post-elution recovery are measured and reported. The same recommendation was also made by Cashdollar and Wymer [15]. Given the large sample-to-sample variability in recovery values measured for most environmental samples, the data should be accompanied by a statistical analysis to give an estimate of the reproducibility of the measurements and, preferably, provide sufficient basis for risk assessment [165]. For human enteric viruses, we recommend that whenever possible culture assays are performed to report infectious virus recovery in addition to the total viral particle count. While molecular assays are fast and relatively accurate, their results account for non-infectious microorganisms that do not reflect the pathogenicity of microorganisms detected. Culture-based assays, although slow and prone to experimental error, would help ascertain the extent to which a concentration method

inactivates target viruses. Culture-based assays are performed routinely in studies with bacteriophages; when working with human viruses, however, many researchers have only used qPCR for quantifying concentrations and recoveries.

2.4.3 Multi-method testing and controls

Virus concentration is a complicated process that could be affected by many parameters. In some studies, rigorous controls were employed. For example, virus concentration with unmodified membrane was used as a control when effect of membrane coating was evaluated [95, 107, 118]. To test the effects of humic acid and fulvic acid on recovery, experiments performed without these macromolecules could be considered as appropriate controls [144, 145]. In most of the studies, however, the comparison of recoveries was performed on a test-to-test basis with one or more variable differing between the tests; the differences have often being in a complex aggregate variable (e.g. composition of a multicomponent eluent solution, feed water type [67, 68, 75, 120]) and not between samples and a control. A number of studies with multiple parameters were structured to optimize parameters sequentially. For example, the elution protocol [68] and hydrodynamic conditions [116] were optimized in tests on recovery from DI water and then were employed when concentrating pathogens from more complex matrices such as tap water [68] and MBR effluent [116]. While serving a purpose, this approach is not designed to gain mechanistic, generalizable insights that might be possible in the presence of rigorous controls.

From the point of view of establishing appropriate controls, the dependence of virus recovery on the virus load in the source water is of special concern because the virus load is the endpoint of the detection process and generally not known until after the samples are concentrated and analyzed. The dependence complicates the interpretation of results and calls for additional procedures that can help converge on an accurate estimate of the virus content in the sample. Additional tests may involve single or multiple dilutions of the source water sample, preparatory tests with a specific water type seeded with a virus at different concentrations, or application of an alternative concentration method to help verify and validate the initial estimate. Recovery control tests should be performed to confirm the efficiency of the concentration method and to verify if the sample inhibits downstream detection. A discussion of recovery control options can be found in the review by Gibson and Borchardt [58]. When additional experiments are not practical, an "educated guess" might be possible and warranted. Once the analysis is performed and an estimate of the virus load in the initial sample is available, one can consider how vulnerable the concentration method is with respect to the virus loss and make a qualitative allowance for the lower recovery. Typically, although not always [84, 106, 148], virus losses are higher for samples with a lower virus load (see section 3.6).

2.4.4 Virus interactions with components of a concentrated water sample

Dissolved and suspended constituents of the sample water matrix have been reported to affect virus recovery by both VIRADEL [67, 68, 75, 144, 145, 147] and CFUF [94, 116, 119-121]. During CFUF, the target virus is concentrated along with other components of the feed magnifying their effect on virus recovery. To assess potential virus losses during filtration, virus adsorption and aggregation behavior in such concentrated solutions needs to be understood.

Virus loss to the fouling layer in CFUF should be mitigated at higher crossflow-to-permeate flow ratios [116]. Because lower permeate fluxes mean longer concentration times, an increase in the crossflow rate is the preferred option. While it helps to decrease membrane fouling and virus adhesion, the larger crossflow shear rate may also affect virus infectivity. How susceptible various types of viruses are to the shear stress (see section 3.3) is a question that should be explored.

The issue of membrane fouling is important for both CFUF and VIRADEL because of their reliance on membrane-virus interactions (attractive in VIRADEL and repulsive in CFUF). For complex water matrices and with the exception of the very early stages of filtration, the filter surface is coated by foulants making the original surface properties of the filter irrelevant in terms of further virus capture and permeate flux decline. It is the properties of the components of water matrix and of the fouling layer they form on the filter surface that largely determine virus recovery. To optimize virus concentration by

VIRADEL and CFUF, one needs to consider virus interaction not only with the membrane surface, but also with the potential foulants. Because viruses adsorbed early in the filtration process are the most difficult to elute, there is still a benefit in designing the surface of the pristine filter to adsorb viruses reversibly.

2.4.5 Elution and sacrificial coatings as strategies for highly fouling water matrices

Elution is an essential step in VIRADEL. It is also typically performed in CFUF as preelution recoveries are often unacceptably low. Elution aims to disrupt favorable virus-membrane and virus-foulant interactions to release the virus to the bulk solution (permeate in VIRADEL and retentate in CFUF). Components of the eluent should not inactivate virus or interfere with the further analysis by qPCR and cell culture infectivity assay. For example, given that beef extract inhibits qPCR (see section 3.5), one should explore other eluents as alternatives to the beef extract solution. The choice of the eluent depends on the context. In the case of a specific virus in a high purity aqueous solution, the eluent composition can be tailored to the virus-filter combination at hand. Detecting a specific viral threat in drinking water (e. g. a virus surrogate used to test integrity of a water treatment system) is an example of the corresponding application. In contrast, screening for multiple unknown viruses in a complex water matrix calls for a non-specific eluent capable of disrupting fouling layers and releasing viruses from organics-rich aggregates. Filter backflush with an eluent or a sacrificial membrane coating that can be disassembled to remove the fouling layer with adsorbed or embedded viruses can possibly be used to maximize post-elution and total recoveries.

APPENDIX

APPENDIX

Table 1. Norovirus recovery by VIRADEL as a function of water matrix and VIRADEL process parameters.

Exp. #	Virus[A]	Water type[B]	Sample amendment	Virus concentration[C]	Sample volume, L	Filter (+/-)[D] /Treatment[E]	Eluent[F]	Primary recovery[G], %	Secondary concentration[H]	Total recovery[G], %	Ref.
1	HNoV (GI)	ground I	none	1.1×10^7 GC/L	20	glass wool (+) / none	3% BE 0.5 M Gly pH 9.5[Δ]	not reported	PEG precipitation	45	89
2		ground II								33	
3	HNoV (GII)	tap		1.3×10^3 GC/L						30	
4		ground I		$(1.9 \text{ to } 50)\times10^6$ GC/L						16	
5		ground II			10 to 20					32	
6	HNoV (GII)	tap	5 mM $MgCl_2$	4×10^5 GC/L	2	cellulose esters(-) / none	0.5 mM H_2SO_4 → 1 mM NaOH[⊥]	not reported	centrifugal UF	3 ± 1	55
7		sea		1.8×10^5 GC/L						1 ± 1	
8		river		3.3×10^6 GC/L						18 ± 9	
9		bottled		2.2×10^6 GC/L						17 ± 7	
10		tap	25 mM $MgCl_2$	4×10^5 GC/L						2 ± 3	

Table 1 (cont'd).

Exp. #	Virus[A]	Water type[B]	Sample amendment	Virus concentration[C]	Sample volume, L	Filter (+/-)[D] /Treatment[E]	Eluent[F]	Primary recovery[G], %	Secondary concentration[H]	Total recovery[G], %	Ref.
11	HNoV (GII)	sea	25 mM $MgCl_2$	1.3×10^6 GC/L	2	cellulose esters(-) / none	0.5 mM H_2SO_4 → 1 mM NaOH[±]	not reported	centrifugal UF	5 ± 7	55
12		river		1.4×10^6 GC/L						9 ± 1	
13		bottled		4.6×10^6 GC/L						23 ± 17	
14		tap	50 mM $MgCl_2$	3.5×10^5 GC/L						2 ± 2	
15		sea		1.6×10^6 GC/L						6	
16		bottled		4.1×10^5 GC/L						6 ± 5	
17		river		3.5×10^5 GC/L						4 ± 3	
18	HNoV	tap	none	1.2×10^6 GC/L	10 or 100	NanoCeram (+) / none	1.5% BE 0.05 M Gly pH 9.0[Δ]	not reported	Celite adsorption-elution	4 ± 1	68
19						1MDS (+) / none				1 ± 1	
20		river				NanoCeram (+) / none				12 ± 16	
21						1MDS (+) / none				0 ± 2	
22	HNoV (GII)	DI	none	$(2.9 \text{ to } 6.2)\times10^5$ GC/L	0.5	1MDS (+) / none	3% BE pH 9	77 to 107	not performed	same as primary recovery	67
23		tap		$(2.2 \text{ to } 5.8)\times10^5$ GC/L				14 to 46			

Table 1 (cont'd).

Exp. #	Virus[A]	Water type[B]	Sample amendment	Virus concentration[C]	Sample volume, L	Filter (+/-)[D] /Treatment[E]	Eluent[F]	Primary recovery[G], %	Secondary concentration[H]	Total recovery[G], %	Ref.
24	HNoV (GII)	river	none	$(7.9 \text{ to } 13)\times10^5$ GC/L	0.25	1MDS (+) / none	3% BE pH 9	13 to 24	not performed	same as primary recovery	67
25		DI		$(6.5 \text{ to } 57)\times10^5$ GC/L	0.5	cellulose esters (-) / $AlCl_3$	0.5 mM H_2SO_4 → 1 mM NaOH	54 to 154			
26		bottled		$(3.8 \text{ to } 6.7)\times10^5$ GC/L				25 to 95			
27		tap		$(5.8 \text{ to } 6.2)\times10^5$ GC/L				36 to 63			
28		river		$(1.7 \text{ to } 11)\times10^5$ GC/L	0.25			24 to 45			
29		DI	25 mM $MgCl_2$	$(5.3 \text{ to } 19)\times10^6$ GC/L	0.5	cellulose esters (-) / none		172 to 200			
30		bottled		$(4.3 \text{ to } 4.5)\times10^5$ GC/L				138 to195			
31		tap		7.9×10^5 to 6.0×10^7 GC/L				55 to 104			
32		river		$(2.7 \text{ to } 5.5)\times10^5$ GC/L	0.25			11 to 18			
33		pond		$(4.5 \text{ to } 6.9)\times10^5$ GC/L				38 to 39			
34	HNoV (GII)	DI + tap	pH 3.5	1.2×10^3 GC/L	10	glass wool (+) / none	3% BE 0.05 M Gly pH 9.5	not reported	3% BE flocculation	0 to 19	66
35			none							<1	

Table 1 (cont'd).

Exp. #	Virus[A]	Water type[B]	Sample amendment	Virus concentration[C]	Sample volume, L	Filter (+/-)[D] /Treatment[E]	Eluent[F]	Primary recovery[G], %	Secondary concentration[H]	Total recovery[G], %	Ref.
36	HNoV (GII)	DI + tap	none	2.4×10^2 GC/L	50	glass wool (+) / none	3% BE 0.05 M Gly pH 9.5	not reported	3% BE flocculation	<1	66
37						MK (+) / none	1% BE 0.25 M Gly pH 9.5			<1	
38	HNoV (GII)	sea	none	8.8×10^4 GC/L	40	NanoCeram (+) / none	3% BE 0.1 M Gly pH 9.5[Δ]	<0.1	not performed	same as primary recovery	83
39							3% BE 0.1 M Gly pH 9.5[†]	111 ± 28			
40							3% BE 0.1 M Gly 0.01% TW 80 pH 9.5[†]	88 ± 24			
41							3% BE 0.1 M Gly 0.1% TW 80 pH 9.5[†]	119 ± 26			
42	HNoV (GII)	DI	none	9.7×10^4 GC/L	10	NanoCeram (+) / none	1.5% BE pH 9.8	not reported	1.5% BE, 0.1% $FeCl_3$, flocculation	42 ± 8	166
43		tap								29 ± 15	

Table 1 (cont'd).

Exp. #	Virus[A]	Water type[B]	Sample amendment	Virus concentration[C]	Sample volume, L	Filter (+/-)[D] /Treatment[E]	Eluent[F]	Primary recovery[G], %	Secondary concentration[H]	Total recovery[G], %	Ref.
44	HNoV (GII)	river	none	9.7×10^4 GC/L	10	NanoCeram (+) / none	1.5% BE pH 9.8	not reported	1.5% BE, 0.1% $FeCl_3$, flocculation	18 ± 3	166
45	HNoV (GII)	DI	none	1.0×10^5 GC/L	1	1MDS (+) / none	1.5% BE, 0.05 M Gly, pH 9.5[Δ]	61 ± 11	not performed	same as primary recovery	162
46							1.5% BE, 0.05 M Gly, 0.01% TW 80 pH 9.5[Δ]	68 ± 40			
47						NanoCeram (+) / none	1.5% BE, 0.05 M Gly, pH 9.5[Δ]	27 ± 13			
48							1.5% BE, 0.05 M Gly, 0.01% TW 80 pH 9.5[Δ]	86 ± 26			
49	HNoV (GII)	lake	pH 6.5 to 7.0	$(4.6\pm8.1)\times10^3$ GC/L	10	Glasswool (+) / none	3% BE 0.5 M Gly pH 9.5	not reported	PEG precipitation	2	167
50	HNoV (GI)	irrigation	5 mM $AlCl_3$ pH 3.5	5×10^4 GC/L	10	Filterite (-) / none	10% TPB, 0.05 M Gly, pH 10	not reported	PEG precipitation	42 ± 7	168
51				5×10^5 GC/L						26 ± 5	
52				5×10^6 GC/L						43 ± 1	

Table 1 (cont'd).

Exp. #	Virus[A]	Water type[B]	Sample amendment	Virus concentration[C]	Sample volume, L	Filter (+/-)[D] /Treatment[E]	Eluent[F]	Primary recovery[G], %	Secondary concentration[H]	Total recovery[G], %	Ref.
53	HNoV (GI)	irrigation	5 mM $AlCl_3$ pH 3.5	5×10^4 GC/L	10	Filterite (-) / none	10% TPB, 0.05 M Gly, pH 10	not reported	organic flocculation	14 ± 1	168
54				5×10^5 GC/L						13 ± 0	
55				5×10^6 GC/L						16 ± 1	
56	HNoV (GII)			5×10^4 GC/L					PEG precipitation	38 ± 1	
57				5×10^5 GC/L						22 ± 7	
58				5×10^6 GC/L						38 ± 1	
59				5×10^4 GC/L					organic flocculation	15 ± 1	
60				5×10^5 GC/L						15 ± 0	
61				5×10^6 GC/L						16 ± 1	

Table 1 (cont'd).

Exp. #	Virus[A]	Water type[B]	Sample amendment	Virus concentration[C]	Sample volume, L	Filter (+/-)[D] /Treatment[E]	Eluent[F]	Primary recovery[G], %	Secondary concentration[H]	Total recovery[G], %	Ref.
62	MNoV	ground	none	5×10^5 PFU/L	10	NanoCeram (+) / none	1.5% BE, 0.05 M Gly, pH 9[Δ]	not reported	1.5% BE flocculation ⇨ centrifugal UF	30	148
63		surface								6	
64		DI		100 PFU/L						< 1	
65				30 PFU/L						2 to 16	
66	MNoV (S7)	DI	none	2.6×10^7 GC/L	5	cellulose ester (-) /$AlCl_3$	0.5 mM H_2SO_4 → 1 mM NaOH	45	not performed	same as primary recovery	76
67		tap		2.2×10^7 GC/L				31			
68	HNoV (GI)	bore hole	5mM $MgCl_2$ pH 3.5	10^6 GC/L	5	cellulose esters (-) / none	0.5 mM H_2SO_4 → Tr alk buffer[Δ]	not reported	PEG precipitation	16 to 30	146
69		rain			5					11 to 15	

Table 1 (cont'd).

Exp. #	Virus[A]	Water type[B]	Sample amendment	Virus concentration[C]	Sample volume, L	Filter (+/-)[D] /Treatment[E]	Eluent[F]	Primary recovery[G], %	Secondary concentration[H]	Total recovery[G], %	Ref.
70	HNoV (GI)	open well	5mM $MgCl_2$ pH 3.5	10^6 GC/L	2	cellulose esters (-) / none	0.5 mM H_2SO_4 → Tr alk buffer[Δ]	not reported	PEG precipitation	4 to 5	146
71		river			5					6 to 10	
72		food processing			1					4 to 12	
73	HNoV (GII)	bore hole		10^7 GC/L	5					23 to 32	
74		rain			5					17 to 25	
75		open well			2					10 to 11	
76		river			5					13 to 15	
77		food processing			1					14 to 24	

Table 1 (cont'd).

Notes for Table 1:

[A] HNoV (GI): human norovirus genogroup I; HNoV (GII): human norovirus genogroup II; MNoV: murine norovirus.

[B] DI: deionized water; DI+tap: mixture of equal volumes of DI water and tap water.

[C] GC/L: genome copies per liter; PFU/L: plaque forming units per liter.

[D] (+): electropositive filter; (-): electronegative filter.

[E] Filter pretreatment, if any.

[F] BE: beef extract; Gly: glycine; TW 80: Tween 80; TPB: tryptose phosphate broth; Tr alk buffer: 0.05 M KH_2PO_4, 1 M NaCl, 0.1% (v/v) Triton X-100, pH 9.2. The arrow (→) indicates sequential application of eluents. In most studies, the elution was performed by filtering the eluent. Additional features of the elution protocol include:

[Δ] Filters were soaked in the eluent prior to elution. See each study for specific contact time.

[†] Eluent is recirculated.

[⊥] Filter was placed feed side down in a Petri dish containing NaOH and shaken for 10 min.

[G] Recoveries were rounded to the nearest integer.

[H] The arrow (⇨) indicates the sequence of secondary concentration steps.

Table 2. Norovirus recovery by crossflow ultrafiltration as a function of water matrix and ultrafiltration process parameters.

Exp. #	Virus[A]	Water type[B]	Sample amendment[C]	Virus concentration[D]	Sample volume, L	Filter / MWCO[E] /Treatment[F]	Eluent[G]	Primary recovery[8], %	Secondary concentra-tion	Total recovery[H], %	Ref.
1	HNoV (GII)	DI + tap	none	1.2×10^3 GC/L	10	Infilco Degremont filter / (NA) / 0.1% BSA	1 mM NaOH[⊥]	not reported	centrifugal UF	<1	66
2	MNoV-1	DI	none	2×10^8 GC/L	5	PS / 15 - 20 kDa / none	none	5 ± 6	not performed	same as primary recovery	107
3						PS / 15 - 20 kDa / 3% BE		63 ± 30			
4		DI + 0.05 M Gly 0.14 M NaCl				PS / 15 - 20 kDa / none		6 ± 5			
5						PS / 15 - 20 kDa / 3% BE		53 ± 74			
6	MNoV-1	tap	0.01% NaPP	"High seeding level"	100	CTA / 70 kDa / 0.1% NaPP	0.01% NaPP 0.1% TW 80 0.001% antifoam A[†]	not reported	centrifugal UF	42	124
7		surface		10 to 100 PFU/L						74	

Table 2 (cont'd).

Exp. #	Virus[A]	Water type[B]	Sample amendment[C]	Virus concentration[D]	Sample volume, L	Filter / MWCO[E] /Treatment[F]	Eluent[G]	Primary recovery[8], %	Secondary concentra-tion	Total recovery[H], %	Ref.
8	HNoV (GII)	lake	none	$(4.6\pm8.1)\times10^3$ GC/L	10	REXEED-25S (29 kDa) / none	0.01% TW 80†	not reported	PEG precipitation	2	[167]

Notes for Table 2:

[A] HNoV (GII): human norovirus genogroup II; MNoV-1: murine norovirus-1

[B] DI: deionized water; DI+tap: mixture of equal volume of DI and tap; Gly: glycine

[C] NaPP: sodium polyphosphate

[D] GC/L: genome copy per liter; PFU/L: plaque forming unit per liter

[E] PS: polysulfone; CTA: cellulose triacetate. The value in parentheses is the molecular weight cutoff (MWCO) of the membrane filter; NA: not available; kDa: kilodalton

[F] Filter pretreatment, if any; BSA: bovine serum albumin; BE: beef extract; NaPP: sodium polyphosphate

[G] TW 80: Tween 80, NaPP: sodium polyphosphate. Additional features of the elution protocol:

± shaking 30 min

† crossflow

[H] Recoveries were rounded to nearest integer

Table 3. Adenovirus recovery by VIRADEL as a function of water matrix and VIRADEL process parameters.

Exp. #	Virus[A]	Water type[B]	Sample amendment	Virus concentration [C]	Sample volume, L	Filter (+/-)[D] /Treatment[E]	Eluent[F]	Primary recovery[G], %	Secondary concentration[H]	Total recovery[G], %	Ref.
1	HAdV 41	tap	none	8.5 to 1700 GC/L	10 to 1500	glass wool (+) / none	3% BE 0.5 M Gly pH 9.5[Δ]	not reported	PEG precipitation	28	89
2		ground I		(8 to 16)×10^2 GC/L	20					22	
3		ground II								8	
4	HAdV 2	DI+tap	pH 3.5	2.6×10^6 GC/L	10	glass wool (+) / none	3% BE 0.05 M Gly pH 9.5	not reported	3% BE flocculation	2 to 7	66
5			none							~1	
6				5.3×10^5 GC/L	50					1 to 2	
7						MK (+) / none	1% BE 0.25 M Gly pH 9.5			0.01 to 0.02	
8	HAdV 41	sea	none	1.6×10^7 GC/L	40	NanoCeram (+) / none	3% BE 0.1 M Gly pH 9.5[Δ]	1	not performed	same as primary recovery	83
9							3% BE 0.1 M Gly pH 9.5[†]	5 ± 3			
10							3% BE 0.1 M Gly 0.1% TW 80 pH 9.5[†]	1 ± 0			

Table 3 (cont'd).

Exp. #	Virus[A]	Water type[B]	Sample amendment	Virus concentration[C]	Sample volume, L	Filter (+/-)[D] /Treatment[E]	Eluent[F]	Primary recovery[G], %	Secondary concentration[H]	Total recovery[G], %	Ref.
11	HAdV 41	sea	none	1.6×10^7 GC/L	40	NanoCeram (+) / none	3% BE 0.1 M Gly 0.01% TW 80 pH 9.5†	1 ± 1	not performed	same as primary recovery	83
12				4.5×10^5 GC/L			soy-based eluent pH 7.0†	0.2 ± 0.1			
13							soy-based eluent 0.01% TW 80 pH 7.0†	1 ± 1			
14				2.5×10^7 GC/L			3% BE 0.1 M Gly pH 9.5†	3 ± 2			
15		surface						2 ± 1			
16		treated-surface						1 ± 1			
17	HAdV 5	sea	none	10^3 PFU/L	1	nanoalumina fiber (+) / none	3% BE pH 6.0Δ	not reported	centrifugal UF	82 ± 11	75
18				10^2 PFU/L						37 ± 5	
19		RO treated sea		10^3 PFU/L						91 ± 12	
20				10^2 PFU/L						64 ± 8	
21		sewage effluent		10^3 PFU/L						86 ± 8	

Table 3 (cont'd).

Exp. #	Virus[A]	Water type[B]	Sample amendment	Virus concentration [C]	Sample volume, L	Filter (+/-)[D] /Treatment[E]	Eluent[F]	Primary recovery[G], %	Secondary concentration[H]	Total recovery[G], %	Ref.
22		sewage effluent	none	10^2 PFU/L		nanoalumina fiber (+)	3% BE pH 6.0[Δ]			44 ± 6	
23		sea	pH 3.5		1					66 ±10	
24		RO treated sea	5 mM $AlCl_3$, pH 3.5	10^3 PFU/L		cellulose esters (-) / none	0.5 mM H_2SO_4 → 1 mM NaOH[±]	not reported	centrifugal UF	90 ± 8	75
25		sewage effluent			0.2					60 ± 8	
26	HAdV 41	source water	pH 3.5	2.5×10^6 GC/L	1	cellulose esters (-) / none	1.5% BE 0.75% glycerol pH 9.0[±]	55 ± 19	evaporation or centrifugal UF	not reported	149
27			pH 4.5					<5		not reported	
28	HAdV 2	tap	none	5×10^6 $TCID_{50}$/L	20	NanoCeram (+) / none	1.0% NaPP PB 0.05M Gly pH 9.3[Ł]	39 ± 13	centrifugal UF	14 ± 4	84
29	HAdV 41	DI	none	10^2 IU/L	10	NanoCeram (+) / none	1.5% BE pH 9.8	not reported	1.5% BE, 0.1% $FeCl_3$, flocculation	19 ± 2	166
30		tap								21 ± 3	
31		river								19 ± 3	
32	HAdV 41	lake	pH 6.5 to 7.0	$(5.9\pm3.4)\times10^4$ GC/L	10	glass wool (+) / none	3% BE 0.5 M Gly pH 9.5	not reported	PEG precipitation	5	167

Table 3 (cont'd).

Exp. #	Virus[A]	Water type[B]	Sample amendment	Virus concentration [C]	Sample volume, L	Filter (+/-)[D] /Treatment[E]	Eluent[F]		Primary recovery[G], %	Secondary concentration[H]	Total recovery[G], %	Ref.
33	HAdV 41	lake	none	$(5.9\pm3.4)\times10^4$ GC/L	10	NanoCeram (+) / none	1.5% BE 0.05 M Gly pH 9		not reported	Celite adsorption-elution ⇨ PEG precipitation	0.02	167
34	HAdV 40	tap	none	10^7 to10^8 GC/L	0.1	1MSD (+) / none	1.5% BE 0.05 M Gly pH 7.5		not reported	Celite adsorption-elution	24 ± 8	92
35							1.5% BE 0.05 M Gly pH 10				52 ± 22	
36			pH 5								14 ± 7	
37	HAdV 41		none				1.5% BE 0.05 M Gly pH 7.5				9 ± 3	
38							1.5% BE 0.05 M Gly pH 10				64 ± 4	
39			pH 5								13 ± 4	
40	HAdV 7	sea	25 mM $AlCl_3$	10^5 PFU/L	1	cellulose esters (-) / none	0.5 mM H_2SO_4 → 1 mM NaOH	stirring[#] 30 min	79 ± 5	not performed	same as primary recovery	160
41								shaking[⊥] 30 min	54			

Table 3 (cont'd).

Exp. #	Virus[A]	Water type[B]	Sample amendment	Virus concentration [C]	Sample volume, L	Filter (+/-)[D] /Treatment[E]	Eluent[F]		Primary recovery[G], %	Secondary concentration[H]	Total recovery[G], %	Ref.
42	HAdV 7	sea	25 mM $AlCl_3$	10^5 PFU/L	1	cellulose esters (-) / none	0.5 mM H_2SO_4 → 1 mM NaOH	stirring[#] 45 min	52	not performed	same as primary recovery	160

Notes for Table 3:

[A] HAdV: human adenovirus.

[B] DI: deionized water; DI+tap: mixture of equal volumes of DI water and tap water; source water: water collected from Water and Sewer Authority.

[C] GC/L: genome copies per liter; PFU: plaque forming unit per liter; $TCID_{50}$/L: 50% tissue culture infective dose per liter; IU/L: infectious unit per liter.

[D] (+): electropositive filter; (-): electronegative filter.

[E] Filter pretreatment, if any.

[F] BE: beef extract; Gly: glycine; TW 80: Tween 80; PB: phosphate buffer (3.8 mM Na_2HPO_4, 6.5 mM KH_2PO_4); The arrow (→) indicates sequential application of eluents.

In most studies, the elution was performed by filtering the eluent. Additional features of the elution protocol:

[Δ] Filters were soaked in eluent first prior to filtration of eluent. See each study for specific contact time.

[†] Eluent is recirculated.

[‡] Filter was placed into a tube containing NaOH and vortexed. See each study for specific vortex times.

Table 3 (cont'd).

Notes for Table 3:

[L] Filter was immersed in the eluent. Filtration housing unit was inverted 10 times followed by 15 min of hold time. The procedure was performed 3 times prior to elution.

[#] Filter was soaked in the flask containing NaOH and stirred with a magnetic bar.

[G] Recoveries were rounded to the nearest integer (except when recoveries are below 1%).

[H] The arrow (⇨) indicates the sequence of secondary concentration steps.

Table 4. Adenovirus recovery by crossflow ultrafiltration as a function of water matrix and ultrafiltration process parameters.

Exp. #	Virus[A]	Water type[B]	Sample amendment[C]	Virus concentration, GC/L[D]	Sample volume, L	Filter (+/-)[E] / MWCO / Treatment[F]	Eluent[G]	Primary recovery[H], %	Secondary concentration	Total recovery[H], %	Ref.
1	HAdV 2	DI + tap	none	2.6×10^{6}	10	Infilco Degremont filter / NA / 0.1% BSA	1 mM NaOH[±]	not reported	centrifugal UF	3 to 6	66
2	HAdV 41	lake	none	$(5.9 \pm 3.4)\times10^{4}$	10	REXEED-25S / 29 kD / none	0.01% TW 80[†]	not reported	PEG precipitation	1	167
3	HAdV 5	cell culture	none	$>10^{12}$	0.45	PES / 750 kDa / none	none	~75	not performed	same as primary recovery	123
4	HAdV 41	tap	0.01% NaPP	$(2.5 \pm 0.5)\times10^{3}$	100	REXEED-25S / 30 kDa / none	0.01%NaPP 0.01% TW 80 0.001% antifoam A[†]	69 ± 12	Celite adsorption-elution	68 ± 14	120
5		river		$(2.6 \pm 0.3)\times10^{3}$	50			56 ± 8		30 ± 19	
6	HAdV 40	DI	none	~10^{9}	1	PES / 30 kDa) / 5% CS	0.01% NaPP 0.01% TW 80[†]	pre: 54 ± 6 post: 99 ± 8	not performed	same as primary recovery	121
7		tap						pre: 38 ± 9 post: ~90			
8		DI				PES (30 kDa) / PEM		pre: 75 ± 10 post:100 ± 7			
9		tap						pre: 41 ± 10 post: ~ 90			

Table 4 (cont'd).

Exp. #	Virus[A]	Water type[B]	Sample amendment [C]	Virus concentration, GC/L[D]	Sample volume, L	Filter (+/-)[E] / MWCO / Treatment[F]	Eluent[G]	Primary recovery[H], %	Secondary concentra-tion	Total recovery[H], %	Ref.
10	HAdV 40	lake I	none	~10^9	1	PES / 30 kDa / 5% CS	0.01% NaPP 0.01% TW 80†	pre: ~40 post: 61 ± 3	not performed	same as primary recovery	121
11		lake II						pre: ~20 post: 35 ± 10			
12		lake II					0.01% NaPP 0.01% TW 80 0.01% EDTA†	pre: ~20 post: ~84			
13		lake I				PES / 30 kDa / PEM	0.01% NaPP 0.01% TW 80†	pre: ~40 post: 62 ± 2			
14		lake II						pre: ~20 post: 42 ± 2			
15		lake II					0.01% NaPP 0.01% TW 80 0.01% EDTA†	pre: ~20 post: ~84			

Notes for Table 4:

[A] HAdV : human adenovirus

[B] DI: deionized water; DI+tap: mixture of equal volume of DI and tap;

[C] NaPP: sodium polyphosphate

[D] GC/L: genome copy per liter

Table 4 (cont'd).

Notes for Table 4:

[E] PES: polyethersulfone; The value in parentheses is the molecular weight cutoff (MWCO) of the membrane filter; NA: not available; kDa: kilodalton

[F] Filter pretreatment, if any; BSA: bovine serum albumin; CS: calf serum; PEM: polyelectrolyte multilayer

[G] TW 80: Tween 80, NaPP: sodium polyphosphate; EDTA: Ethylenediaminetetraacetic acid. Additional features of the elution protocol:

[⊥] shaking for 30 min

[†] crossflow

[H] Recoveries were rounded to the nearest integer; pre: pre-elution recovery; post: post-elution recovery

Table 5. Primary recovery of bacteriophage MS2 by VIRADEL as a function of water matrix and VIRADEL process parameters.

Exp. #	Water type[A]	Sample amendment	Virus concentration, PFU/L[B]	Sample volume, L	Filter (+/-)[C] /Treatment[D]	Eluent[E]	Primary recovery[F],	Ref.
1	tap	pH 3.5	not reported	10	filterite (-) / none	5% BE 0.1% TW 80 pH 7	67±11	56
2		0.1 M $MnCl_2$, pH 3.5	not reported				79±14	
3	tap	pH 6.5 to 7	10^6	1	1-MDS (+) / none	1.5% BE 0.05M Gly pH 8[Δ]	31 ± 12	128
4						1.5% BE 0.05M Gly pH 9[Δ]	24 ± 5	
5						1.5% BE 0.05 M Gly 0.01% TW 80 pH 8[Δ]	31 ± 4	
6						1.5% BE 0.05 M Gly 0.01% TW 80 0.1% NaPP pH 8[Ŧ]	92 ± 10	
7						1.5% BE 0.05 M Gly 0.01% TW 80 0.1% NaPP pH 8[Δ]	89 ± 10	

Table 5 (cont'd).

Exp. #	Water type[A]	Sample amendment	Virus concentration, PFU/L[B]	Sample volume, L	Filter (+/-)[C] /Treatment[D]	Eluent[E]	Primary recovery[F],	Ref.
8	tap	pH 6.5 to 7	10^3	1	1-MDS (+) / none	1.5% BE 0.05 M Gly 0.01% TW 80 0.1% NaPP pH 8[Δ]	44 ± 9	128
9			5×10^4	20		1.5% BE 0.05 M Gly 0.01% TW 80 0.1% NaPP pH 8[▼]	32 ± 13	
10	sea[G]	none	(1.5 to 4.6)×10^5	0.1	cellulose ester (-) / none	1.5% BE pH 9*	35	79
11						0.5 mM H_2SO_4 → 1.5% BE pH 9*	20	
12						1mM NaOH*	16	
13						0.5 mM H_2SO_4 → 1.5% BE pH 9	9	
14						1mM NaOH	6	
15						0.5mM H_2SO_4 → 1mM NaOH	2	

Table 5 (cont'd).

Exp. #	Water type[A]	Sample amendment	Virus concentration, PFU/L[B]	Sample volume, L	Filter (+/-)[C] /Treatment[D]	Eluent[E]	Primary recovery[F],	Ref.
16	DI	none	5×10^4	20	NanoCeram (+) / none	1.5% BE 0.05M Gly 0.01% TW 80 pH 9.5[Δ]	65 ± 23	74
17					1-MDS (+) / none		30 ± 10	
18	sea				NanoCeram (+) / none		63 ± 13	
19		0.1M $MgCl_2$			nitrocellulose ester(-) / none	0.5mM H_2SO_4 → 1mM NaOH	15 ± 5	
20	tap	none	~5×10^2	20	NanoCeram (+) / none	1.0% NaPP PB 0.05 M Gly pH 9.3[Ł]	86 ± 9	84
21			~5×10^6				57 ± 3	
22						1.0% NaPP PB 0.05 M Gly pH 7.5[Ł]	26 ± 4	
23						3% BE pH 9.3[Ł]	34 ± 18	
24						0.05 M Gly pH 9.3[Ł]	0.4 ± 0.5	
25						3% BE 0.05 M Gly pH 9.3[Ł]	12 ± 1	

Table 5 (cont'd).

Exp. #	Water type[A]	Sample amendment	Virus concentration, PFU/L[B]	Sample volume, L	Filter (+/-)[C] /Treatment[D]	Eluent[E]	Primary recovery[F],	Ref.
26	tap	none	~5×10^6	20	NanoCeram (+) / none	PB 0.05 M Gly pH 9.3[ŀ]	26 ± 5	84
27						PB 0.05 M Gly pH 7.5[ŀ]	24 ± 7	
28						PB 0.05 M Gly 0.3% TW 80 pH 9.3[ŀ]	37 ± 2	
29						0.1% NaPP PB 0.05 M Gly pH 9.3[ŀ]	40 ± 7	
30						0.6 M NaI PB 0.05 M Gly pH 9.3[ŀ]	3 ± 2	
31	river+DI	0.05 M $MgCl_2$	10^7	0.1	cellulose ester (-) / none	3% BE 0.5 M NaCl pH 9[⊥]	52 ± 6	169
32		0.05 M $MgCl_2$ pH 3.5				0.5 mM H_2SO_4 →0.05 M KH_2PO_4 0.1 M NaCl 0.1% TritonX-100 pH 9.2[⊥]	16 ± 3	

Table 5 (cont'd).

Exp. #	Water type[A]	Sample amendment	Virus concentration, PFU/L[B]	Sample volume, L	Filter (+/-)[C] /Treatment[D]	Eluent[E]	Primary recovery[F],	Ref.
33	river+DI	none	10^7	0.1	Zeta Plus 60S (+) / none	2.9% TPB 6%Gly pH 9$^{\overline{\top}}$	1 ± 0	169
34						PB 1% NaPP 0.05 M Gly pH 9.3$^{\overline{\top}}$	2 ± 0	
35		pH 5.5 to 6				0.05 M arginine 1% BE	0.04 ± 0.05	

Notes on Table 5:

[A] DI: deionized water; river+DI: river water diluted with sterile water

[B] PFU/L: plaque forming units per liter

[C] (+): electropositive filter; (-): electronegative filter

[D] Filter pretreatment, if any

[E] BE: beef extract; TW 80: Tween 80; Gly: glycine; NaPP: sodium polyphosphate; PB: phosphate buffer (3.8 mM Na_2HPO_4, 6.5 mM KH_2PO_4); TPB: tryptose phosphate buffer; The arrow (→) indicates sequential application of eluents. In most studies, elution was performed by filtering the eluent, but the elution protocol could include additional features. These features are marked as follows:

- [Δ] Filters were soaked in eluent first prior to filtration of eluent. See each study for specific contact time
- [$\overline{\top}$] Eluent heated to 37˚C
- [▼] Eluent was pumped in the direction opposite to that of the water sample flow, then filter was soaked for 10 min in the eluent prior to eluent collection

Table 5 (cont'd).

Notes on table 5:

* Sample prefiltered through PVDF membrane and drop-by-drop elution was performed

[L] Filter was immersed in the eluent. Filtration housing unit was inverted 10 times followed by 15 min hold time. Such procedure was performed 3 times prior to filtering the eluent

[⊥] Filter was placed feed side down in a Petri dish containing eluent

[F] Recoveries were rounded to the nearest integer (except for recoveries < 1%)

[G] This work was performed with an indigenous coliphage (and not MS2 specifically). The study is included in the Table as illustrative of the effect of the eluent on coliphage recovery.

Table 6. Primary recovery of bacteriophage MS2 by crossflow ultrafiltration as a function of water matrix and ultrafiltration process parameters.

Exp. #	Water type[A]	Sample amendment[B]	Virus concentration, PFU/L[C]	Sample volume, L	Filter (MWCO/size)[D] /Treatment[E]	Eluent[F]	Primary recovery[G],	Ref.
1	tap	none	~10^5	10	PS (15 to 20 kDa)/ none	none	44 ± 30	104
2					PS (15 to 20 kDa) / 5% FBS (overnight)		51 ± 19	
3					PS (15 to 20 kDa) / 5% FBS (1 hour)		50 ± 14	
4		0.1% NaPP			PS (15 to 20 kDa) / 5% FBS (overnight)		108 ± 16	
5					PS (15 to 20 kDa) / 5% FBS (1 hour)		71 ± 11	
6					PS (15 to 20 kDa) / 5% CS	0.1% NaPP‡	pre: 84 ± 13 post: 89 ± 15	
7					PS (15 to 20 kDa) / 0.1% NaPP		pre: 71 ± 25 post: 82 ± 25	
8		0.01% NaPP			PS (15 to 20 kDa) / 0.01% NaPP	0.01% NaPP‡	pre: 86 ± 20 post: 96 ± 21	

Table 6 (cont'd).

Exp. #	Water type[A]	Sample amendment[B]	Virus concentration, PFU/L[C]	Sample volume, L	Filter (MWCO/size)[D] /Treatment[E]	Eluent[F]	Primary recovery[G],	Ref.
9	tap	0.01% TW 80	~10^5	10	PS (15 to 20 kDa) / 0.01% NaPP	0.01% NaPP‡	pre: 105 ± 23 post:106 ±	104
10		0.002% TW 80					pre: 70 post: 73	
11		none			PS (15 to 20 kDa) / none	tap‡	34±28	
12		0.01% NaPP			PS (15 to 20 kDa) / 0.01% NaPP	0.01% NaPP‡	59 ± 10	
13						0.01% NaPP 0.01% TW 80 0.01% TW 20 0.001% antifoam A‡	65 ± 35	
14						0.01% NaPP 0.5% to 1% Tween 80 0.001% antifoam A ‡	91 ± 33	
15	tap	0.01% NaPP	720 ± 240	100	PS (30 kDa) / 5% CS	0.01% NaPP 0.01% TW 80 0.001% antifoam Y-30†	120 ± 22	105
16	tap	none	~10^4	100	PS (30 kDa) / 0.1% NaPP	0.01% NaPP 0.5% TW 80 0.001%	52 ± 34	106*

Table 6 (cont'd).

Exp. #	Water type[A]	Sample amendment[B]	Virus concentration, PFU/L[C]	Sample volume, L	Filter (MWCO/size)[D] /Treatment[E]	Eluent[F]	Primary recovery[G],	Ref.
17	tap	0.01% NaPP	~10^4	100	PS (30 kDa) / 0.1% NaPP		84 ± 12	106*
18						0.01% NaPP 0.1% TW 80 0.001% antifoam A‡	94 ± 11	
19						0.01% NaPP 0.1% TW 80 0.001% antifoam A†	53 ± 13	
20	tap	none	10^4	100	PS & CTA (20 to 70 kDa) /0.5% CS	0.001% TW 80‡	64 ± 48	163
21	river	none	5×10^4	20	PES (30 kDa) / none	1%BE, 0.4% Gly pH 9.5†	73 to 84	117
22						MilliQ water (1#)† → 1%BE 0.4% Gly pH 9.5 (2#)†	42 to 64	
23	DI	none	2×10^9	5	PS (15 to 20 kDa) / none	none	30 ± 7	107
24					PS (15 to 20 kDa) / 3% BE		54 ± 24	

Table 6 (cont'd).

Exp. #	Water type[A]	Sample amendment[B]	Virus concentration, PFU/L[C]	Sample volume, L	Filter (MWCO/size)[D] /Treatment[E]	Eluent[F]	Primary recovery[G],	Ref.
25	DI + 0.05 M Gly 0.14 M NaCl	none	2×10^9	5	PS (15 to 20 kDa) / none	none	34 ± 16	107
26					PS (15 to 20 kDa) / 3% BE		33 ± 19	
27	DI+ 100 mM Tris-HCl				PS (15 to 20 kDa) / none		18 ± 10	
28					PS (15 to 20 kDa) / 3% BE		29 ± 7	
29	tap	0.01% NaPP	$(4.9\pm1.4)\times10^2$	100	REXEED-25S (30 kDa) / none	none	65 ± 5[a]	127
30			$(7.4\pm6.8)\times10^2$				99 ± 5[b]	
31	treated wastewater	none	630±340	10	PS (30 kDa) / 5% CS	none	84 ± 2	118
32					PS (30 kDa) / none		79 ± 18	
33					PS (65 kDa) / 5% CS		80 ± 6	

Table 6 (cont'd).

Exp. #	Water type[A]	Sample amendment[B]	Virus concentration, PFU/L[C]	Sample volume, L	Filter (MWCO/size)[D] /Treatment[E]	Eluent[F]	Primary recovery[G],	Ref.
34	treated wastewater	none	630±340	10	PS (65 kDa) / none	none	42 ± 12	118
35					CTA (70 kDa) / 5% CS		87 ± 10	
36					CTA (70 kDa) / none		88 ± 15	
37					PS (30 kDa) / none	none	110 ± 18	
38					PS (30 kDa) / none	0.01% NaPP, 0.01% TW 80, 0.001% antifoam Y-30†	120 ± 20	
39					CTA (70 kDa) / none	none	80 ± 14	
40					CTA (70 kDa) / none	0.01% NaPP, 0.01% TW 80, 0.001% antifoam Y-30†	130 ± 10	
41	tap	none	9×10^3 to 2×10^7	10	PES (20 nm) / none	water†	31 ± 8	122
42	lake	none	$(4.6\pm3.1)\times10^4$	10	REXEED-25S (29 kDa) / none	0.01% TW 80†	68	167

Table 6 (cont'd).

Exp. #	Water type[A]	Sample amendment[B]	Virus concentration, PFU/L[C]	Sample volume, L	Filter (MWCO/size)[D] /Treatment[E]	Eluent[F]	Primary recovery[G],	Ref.
43	river	0.01% NaPP	$(1.2\pm0.5)\times10^2$	50	PS (30 kDa) / 5% CS	0.01% NaPP 0.01% TW 80 0.001% antifoam Y-30†	91 ± 38	119
44	lake I						65 ± 33	
45	lake II						53 ± 19	
46	ground I						85 ± 23	
47	ground II						77 ± 8	

Notes on Table 6:

[A] DI: deionized water; Gly: glycine

[B] NaPP: sodium polyphosphate; TW 80: Tween 80

[C] PFU/L: plaque forming units per liter

[D] PS: polysulfone; CTA: cellulose triacetate; PS & CTA: recovery averaged with polysulfone membrane and cellulose triacetate membrane; PES: polyethersulfone; The value in parentheses is the molecular weight cutoff (MWCO) or pore size of the membrane filter

[E] Filter pretreatment, if any; FBS: fetal bovine serum; CS: calf serum; NaPP: sodium polyphosphate; BE: beef extract

Table 6 (cont'd).

Notes on table 6:

[F] NaPP: sodium polyphosphate; TW 80: Tween 80; TW 20: Tween 20; BE: beef extract; Gly: glycine; The arrow (→) indicates sequential application of eluents. Additional features of the elution protocol are marked as follows:

[†] crossflow

[‡] backflush

[#] Number of rinses (1[#]: rinsed once; 2[#]: rinsed twice)

[G] Recoveries were rounded to the nearest integer; pre: pre-elution recovery; post: post-elution recovery

[a] recovery at a high filtration rate (2500 mL/min)

[b] recovery at a low filtration rate (1750 mL/min)

[*] In this paper, Polaczyk et al. performed secondary concentration as well and reported only one recovery value: "ultrafiltration recovery efficiency". It is this value that is included herein

REFERENCES

REFERENCES

1. *Waterborne zoonoses: Identification, causes and control*, World Health Organization, Geneva, Switzerland, 2004.

2. H. Leclerc, L. Schwartzbrod and E. Dei-Cas, *Crit. Rev. Microbiol.*, 2002, **28**, 371-409.

3. J. Theron and T. E. Cloete, *Crit. Rev. Microbiol.*, 2002, **28**, 1-26.

4. *Surveillance for waterborne disease outbreaks associated with drinking water - United States, 2001-2002*, Morbidity and Mortality Weekly Report. Centers for Disease Control and Prevention, 2004.

5. *Surveillance for waterborne disease and outbreaks associated with drinking water and water not intended for drinking - United States, 2003-2004*, Morbidity and Mortality Weekly Report. Centers for Disease Control and Prevention, 2006.

6. *Surveillance for waterborne disease and outbreaks associated with drinking water and water not intended for drinking - United States, 2005–2006*, Morbidity and Mortality Weekly Report. Centers for Disease Control and Prevention, 2008.

7. *Surveillance for waterborne disease outbreaks associated with drinking water - United States, 2007-2008*, Morbidity and Mortality Weekly Report. Centers for Disease Control and Prevention, 2011.

8. *Surveillance for waterborne disease outbreaks associated with drinking water and other nonrecreational water - United States, 2009-2010*, Morbidity and Mortality Weekly Report. Centers for Disease Control and Prevention, 2013.

9. *Surveillance for waterborne disease outbreaks associated with drinking water - United States, 2011-2012*, Morbidity and Mortality Weekly Report. Centers for Disease Control and Prevention, 2015.

10. N. I. o. Health, *Biological sciences curriculum study. NIH Curriculum Supplement Series. National Institutes of Health, Bethesda, MD*, 2007.

11. C. W. LeBaron, N. P. Furutan, J. F. Lew, J. R. Allen, V. Gouvea, C. Moe and S. S. Monroe, *MMWR. Recommendations and reports : Morbidity and mortality weekly report. Recommendations and reports*, 1990, **39**, 1-24.

12. S. M. Karst, *Viruses*, 2010, **2**, 748-781.

13. E. Papafragkou, J. Hewitt, G. W. Park, G. Greening and J. Vinje, *Plos One*, 2013, **8**, e63485.

14. S. E. Hrudey and E. J. Hrudey, *Safe drinking water: Lessons from recent outbreaks in affluent nations*, IWA Publishing, London, 2004.

15. J. L. Cashdollar and L. Wymer, *J. Appl. Microbiol.*, 2013, **115**, 1-11.

16. S. R. Naik, R. Aggarwal, P. N. Salunke and N. N. Mehrotra, *Bulletin of the World Health Organization*, 1992, **70**, 597-604.

17. *Outbreak of aseptic meningitis associated with multiple enterovirus subtypes-Romania, 1999*, Morbidity and Mortality Weekly Report. Centers for Disease Control and Prevention, 2000.

18. A. L. Freeland, G. H. Vaughan Jr. and S. N. Banerjee, *Acute Gastroenteritis on Cruise Ships - United States, 2008-2014*, Morbidity and Mortality Weekly Report. Centers for Disease Control and Prevention, 2016.

19. Investigation Update on the Coral Princess (https://www.cdc.gov/nceh/vsp/surv/outbreak/2017/march18_coral_princess.html; accessed on May 5, 2017).

20. T. T. Fong, L. S. Mansfield, D. L. Wilson, D. J. Schwab, S. L. Molloy and J. B. Rose, *Environ. Health Perspect.*, 2007, **115**, 856-864.

21. C. E. O'Reilly, A. B. Bowen, N. E. Perez, J. P. Sarisky, C. A. Shepherd, M. D. Miller, B. C. Hubbard, M. Herring, S. D. Buchanan, C. C. Fitzgerald, V. Hill, M. J. Arrowood, L. X. Xiao, R. M. Hoekstra, E. D. Mintz and M. F. Lynch, *Clin. Infect. Dis.*, 2007, **44**, 506-512.

22. M. Abbaszadegan, M. LeChevallier and C. Gerba, *J. Am. Water Works Assn.*, 2003, **95**, 107-120.

23. *Surveillance for waterborne disease outbreaks associated with recreational water - United States, 2001-2002*, Morbidity and Mortality Weekly Report. Centers for Disease Control and Prevention, 2004.

24. *Surveillance for waterborne disease outbreaks associated with recreational water - United States, 2003-2004*, Morbidity and Mortality Weekly Report. Centers for Disease Control and Prevention, 2006.

25. *Surveillance for waterborne disease and outbreaks associated with recreational water use and other aquatic facility-associated health events - United States, 2005–2006* Morbidity and Mortality Weekly Report. Centers for Disease Control and Prevention, 2008.

26. *Surveillance for waterborne disease outbreaks and other health events associated with recreational water - United States, 2007-2008*, Morbidity and Mortality Weekly Report. Centers for Disease Control and Prevention, 2011.

27. *Recreational water associated disease outbreaks-United States, 2009–2010*, Morbidity and Mortality Weekly Report. Centers for Disease Control and Prevention, 2014.

28. *Outbreaks of illness associated with recreational water - United States, 2011-2012*, Morbidity and Mortality Weekly Report. Centers for Disease Control and Prevention, 2015.

29. R. G. Sinclair, E. L. Jones and C. P. Gerba, *J. Appl. Microbiol.*, 2009, **107**, 1769-1780.

30. M. H. Nellor, R. B. Baird and J. R. Smyth, *J. Am. Water Works Assn.*, 1985, **77**, 88-96.

31. *Issues in potable reuse: The viability of augmenting drinking water supplies with reclaimed water* National Research Council, Washington, DC, 1998.

32. A. P. Wyn-Jones and J. Sellwood, *J. Appl. Microbiol.*, 2001, **91**, 945-962.

33. S. Choi and S. C. Jiang, *Appl. Environ. Microbiol.*, 2005, **71**, 7426-7433.

34. I. Xagoraraki, D. H. Kuo, K. Wong, M. Wong and J. B. Rose, *Appl. Environ. Microbiol.*, 2007, **73**, 7874-7881.

35. J. W. He and S. Jiang, *Appl. Environ. Microbiol.*, 2005, **71**, 2250-2255.

36. C. P. Gerba, J. B. Rose, C. N. Haas and K. D. Crabtree, *Water Res.*, 1996, **30**, 2929-2940.

37. M. D. Sobsey, in *Strategies for Drinking Water Contaminants*, Commission on Geosciences, Environment and Resources, National Academy Press, Washington, DC, 1999, pp. 173-205.

38. K. E. Gibson, K. J. Schwab, S. K. Spencer and M. A. Borchardt, *Water Res.*, 2012, **46**, 4281-4291.

39. S. Di Pasquale, M. Paniconi, B. Auricchio, L. Orefice, A. C. Schultz and D. De Medici, *J. Virol. Methods*, 2010, **165**, 57-63.

40. T. M. Fumian, J. P. G. Leite, A. A. Castello, A. Gaggero, M. S. L. de Caillou and M. P. Miagostovich, *J. Virol. Methods*, 2010, **170**, 42-46.

41. U. L. Tsai, M. D. Sobsey, L. R. Sangermano and C. J. Palmer, *Appl. Environ. Microbiol.*, 1993, **59**, 3488-3491.

42. W. Kang and J. L. Cannon, *PLOS ONE*, 2015, **10**.

43. J. Zhang, M. Mahalanabis, L. Liu, J. Chang, N. Pollock and C. Klapperich, *Diagnostics*, 2013, **3**, 155.

44. J. Y. Liu, Q. P. Wu and X. X. Kou, *J. Microbiol.*, 2007, **45**, 48-52.

45. T. M. Straub and D. P. Chandler, *J. Microbiol. Methods*, 2003, **53**, 185-197.

46. S. R. Farrah, S. M. Goyal, C. P. Gerba, C. Wailis and P. T. B. Shaffer, *Water Res.* , 1976, **10**, 897-901.

47. S. R. Farrah, C. Wallis, P. T. B. Shaffer and J. L. Melnick, *Appl. Microbiol.*, 1976, **32**, 654-658.

48. M. D. Sobsey, C. Wallis, M. Henderson and J. L. Melnick, *Appl. Microbiol.* , 1978, **26**, 529-534.

49. C. P. Gerba, *Adv. Appl. Microbiol.*, 1984, **30**, 133-168.

50. J. L. Melnick, R. Safferman, V. C. Rao, S. Goyal, G. Berg, D. R. Dahling, B. A. Wright, E. Akin, R. Stetler, C. Sorber, B. Moore, M. D. Sobsey, R. Moore, A. L. Lewis and F. M. Wellings, *Appl. Environ. Microbiol.*, 1984, **47**, 144-150.

51. M. D. Sobsey and J. S. Glass, *Appl. Environ. Microbiol.*, 1984, **47**, 956-960.

52. N. Guttmanbass and J. Catalanosherman, *Appl. Environ. Microbiol.*, 1985, **49**, 1260-1264.

53. M. D. Sobsey, T. Cromeans, A. R. Hickey and J. S. Glass, *Water Sci. Technol.*, 1985, **17**, 665-679.

54. J. Lukasik, T. M. Scott, D. Andryshak and S. R. Farrah, *Appl. Environ. Microbiol.*, 2000, **66**, 2914-2920.

55. M. Victoria, F. Guimaraes, T. Fumian, F. Ferreira, C. Vieira, J. P. Leite and M. Miagostovich, *J. Virol. Methods*, 2009, **156**, 73-76.

56. T. M. Scott, J. Lukasik and S. R. Farrah, *Can. J. Microbiol.*, 2002, **48**, 305-310.

57. L. A. Ikner, C. P. Gerba and K. R. Bright, *Food Environ. Virol.*, 2012, **4**, 41-67.

58. K. E. Gibson and M. A. Borchardt, in *Viruses in Foods*, eds. S. M. Goyal and J. L. Cannon, Springer, 2016, pp. 277-301.

59. M. D. Sobsey and B. L. Jones, *Appl. Environ. Microbiol.*, 1979, **37**, 588-595.

60. J. B. Rose, S. N. Singh, C. P. Gerba and L. M. Kelley, *Appl. Environ. Microbiol.*, 1984, **47**, 989-992.

61. J. J. Borrego, R. Cornax, D. R. Preston, S. R. Farrah, B. McElhaney and G. Bitton, *Appl. Environ. Microbiol.*, 1991, **57**, 1218-1222.

62. J. F. Ma, J. Naranjo and C. P. Gerba, *Appl. Environ. Microbiol.*, 1994, **60**, 1974-1977.

63. D. C. Roepke, D. A. Halvorson, S. M. Goyal and C. J. Kelleher, *Avian Diseases*, 1989, **33**, 649-653.

64. *Manual of Methods for Virology. U.S. Environmental Protection Agency*, Report 600/4-84/013, Washington D.C., 2001.

65. J. Brassard, K. Seyer, A. Houde, C. Simard and Y. L. Trottier, *J. Virol. Methods*, 2005, **123**, 163-169.

66. N. Albinana-Gimenez, P. Clemente-Casares, B. Calgua, J. M. Huguet, S. Courtois and R. Girones, *J. Virol. Methods*, 2009, **158**, 104-109.

67. E. Haramoto, H. Katayama, E. Utagawa and S. Ohgaki, *J. Virol. Methods*, 2009, **160**, 206-209.

68. M. R. Karim, E. R. Rhodes, N. Brinkman, L. Wymer and G. S. Fout, *Appl. Environ. Microbiol.*, 2009, **75**, 2393-2399.

69. S. M. Goyal and C. P. Gerba, *J. Virol. Methods*, 1983, **7**, 279-285.

70. H. Katayama, A. Shimasaki and S. Ohgaki, *Appl. Environ. Microbiol.*, 2002, **68**, 1033-1039.

71. T. G. Metcalf, *Appl. Microbiol.*, 1961, **9**, 376-379.

72. C. Wallis and J. L. Melnick, *J. Virol.*, 1967, **1**, 472-477.

73. W. Jakubowski, W. F. Hill and N. A. Clarke, *Appl. Microbiol.*, 1975, **30**, 58-65.

74. H. B. Bennett, H. D. O'Dell, G. Norton, G. Shin, F. C. Hsu and J. S. Meschke, *Water Sci. Technol.*, 2010, **61**, 317-322.

75. D. Li, H. C. Shi and S. C. Jiang, *J. Microbiol. Methods*, 2010, **81**, 33-38.

76. A. Hata, K. Matsumori, M. Kitajima and H. Katayama, *Food Environ. Virol.*, 2015, **7**, 7-13.

77. M. D. Sobsey and J. S. Glass, *Appl. Environ. Microbiol.*, 1980, **40**, 201-210.

78. S. R. Farrah, C. P. Gerba, C. Wallis and J. L. Melnick, *Appl. Environ. Microbiol.*, 1976, **31**, 221-226.

79. A. M. Abdelzaher, H. M. Solo-Gabriele, M. E. Wright and C. J. Palmer, *J. Environ. Qual.*, 2008, **37**, 1648-1655.

80. C. M. Sabatino and S. Maier, *Can. J. Microbiol.*, 1980, **26**, 1403-1407.

81. *Manual of Methods for Virology. U.S. Environmental Protection Agency*, Report EPA/600/4-84/013 (originally published in 1984), Washington, DC., 2001.

82. D. R. Preston, T. V. Vasudevan, G. Bitton, S. R. Farrah and J. L. Morel, *Appl. Environ. Microbiol.*, 1988, **54**, 1325-1329.

83. C. D. Gibbons, R. A. Rodriguez, L. Tallon and M. D. Sobsey, *J. Appl. Microbiol.*, 2010, **109**, 635-641.

84. L. A. Ikner, M. Soto-Beltran and K. R. Bright, *Appl. Environ. Microbiol.*, 2011, **77**, 3500-3506.

85. N. Deboosere, S. V. Horm, A. Pinon, J. Gachet, C. Coldefy, P. Buchy and M. Vialette, *Appl. Environ. Microbiol.*, 2011, **77**, 3802-3808.

86. G. S. Fout, N. E. Brinkman, J. L. Cashdollar, S. M. Griffin, B. R. McMinn, E. R. Rhodes, E. A. Varughese, M. R. Karim, A. C. Grimm, S. K. Spencer and M. A. Borchardt, *Method 1615. Measurement of Enterovirus and Norovirus Occurrence in Water by Culture and RT-qPCR. U. S. Environmental Protection Agency*, Report EPA/600/R-10/18, 2010.

87. L. T. Chang, S. R. Farrah and G. Bitton, *Appl. Environ. Microbiol.*, 1981, **42**, 921-924.

88. E. Haramoto and H. Katayama, *Food Environ. Virol.*, 2013, **5**, 77-80.

89. E. Lambertini, S. K. Spencer, P. D. Bertz, F. J. Loge, B. A. Kieke and M. A. Borchardt, *Appl. Environ. Microbiol.*, 2008, **74**, 2990-2996.

90. S. R. Farrah, D. R. Preston, G. A. Toranzos, M. Girard, G. A. Erdos and V. Vasuhdivan, *Appl. Environ. Microbiol.*, 1991, **57**, 2502-2506.

91. P. Schaudies and D. A. Robinson, *Literature review of molecular methods for simulateneous detection of pathogens in water. U.S. Environmental Protection Agency.*, Report 600/R-07/128 Washington D.C., 2007.

92. B. R. McMinn, *J. Virol. Methods*, 2013, **193**, 284-290.

93. G. Belfort, Y. Rotem and E. Katzenelson, *Water Res.*, 1975, **9**, 79-85.

94. G. Belfort, Y. Rotem and E. Katzenelson, *Water Res.*, 1976, **10**, 279-284.

95. D. Berman, M. E. Rohr and R. S. Safferman, *Appl. Environ. Microbiol.*, 1980, **40**, 426- 428.

96. D. M. Dziewulski and G. Belfort, *Water Sci. Technol.*, 1983, **15**, 75-89.

97. H. V. Adikane, S. N. Nene, S. S. Kulkarni, P. U. Baxi, D. S. Khatpe and P. A. Aphale, *J. Membr. Sci.*, 1997, **132**, 91-96.

98. C. Chamorro, J. C. Espinoza, K. Soto and J. Kuznar, *Archivos De Medicina Veterinaria*, 2006, **38**, 77-82.

99. V. R. Hill, A. L. Polaczyk, A. M. Kahler, T. L. Cromeans, D. Hahn and J. E. Amburgey, *J. Environ. Qual.*, 2009, **38**, 822-825.

100. P. F. Clark, R. C. Ainsworth and L. G. Kindschi, *Exp. Biol. Med.*, 1933, **31**, 255-259.

101. B. H. Sweet, J. S. McHale, K. J. Hardy, F. Morton, J. K. Smith and E. Klein, *Water Res.*, 1971, **5**, 823-&.

102. A. W. Morrow, *J. Appl. Chem. Biotechnol.*, 1972, **22**, 501-505.

103. H. A. Morales-Morales, G. Vidal, J. Olszewski, C. M. Rock, D. Dasgupta, K. H. Oshima and G. B. Smith, *Appl. Environ. Microbiol.*, 2003, **69**, 4098-4102.

104. V. R. Hill, A. L. Polaczyk, D. Hahn, J. Narayanan, T. L. Cromeans, J. M. Roberts and J. E. Amburgey, *Appl. Environ. Microbiol.*, 2005, **71**, 6878-6884.

105. V. R. Hill, A. M. Kahler, N. Jothikumar, T. B. Johnson, D. Hahn and T. L. Cromeans, *Appl. Environ. Microbiol.*, 2007, **73**, 4218-4225.

106. A. L. Polaczyk, J. Narayanan, T. L. Cromeans, D. Hahn, J. M. Roberts, J. E. Amburgey and V. R. Hill, *J. Microbiol. Methods*, 2008, **73**, 92-99.

107. H. Kim, H. Park and G. Ko, *J. Food Protect.*, 2009, **72**, 2547-2552.

108. K. E. Gibson and K. J. Schwab, *Appl. Environ. Microbiol.*, 2011, **77**, 355-362.

109. P. S. K. Knappett, A. Layton, L. D. McKay, D. Williams, B. J. Mailloux, M. R. Huq, M. J. Alam, K. M. Ahmed, Y. Akita, M. L. Serre, G. S. Sayler and A. van Geen, *Groundwater*, 2011, **49**, 53-65.

110. J. Rexroad, R. K. Evans and C. R. Middaugh, *Journal of pharmaceutical sciences*, 2006, **95**, 237-247.

111. Y. Y. Feng, S. L. Ong, J. Y. Hu, X. L. Tan and W. J. Ng, *Journal of industrial microbiology & biotechnology*, 2003, **30**, 549-552.

112. I. Samandoulgou, R. Hammami, R. M. Rayas, I. Fliss and J. Jean, *Applied and Environmental Microbiology*, 2015, **81**, 7680-7686.

113. J. J. Hansen, P. S. Warden and A. B. Margolin, *International journal of environmental research and public health*, 2007, **4**, 61-67.

114. R. Nims and M. Plavsic, *Pharmaceuticals (Basel, Switzerland)*, 2013, **6**, 358-392.

115. A. L. Favier, W. P. Burmeister and J. Chroboczek, *Virology*, 2004, **322**, 93-104.

116. E. V. Pasco, H. Shi, I. Xagoraraki, S. A. Hashsham, K. N. Parent, M. L. Bruening and V. V. Tarabara, *J. Membr. Sci.*, 2014, **469**, 140-150.

117. S. Skraber, C. Gantzer, K. Helmi, L. Hoffmann and H. M. Cauchie, *Food Environ. Virol.*, 2009, **1**, 66-76.

118. P. B. Liu, V. R. Hill, D. Hahn, T. B. Johnson, Y. Pan, N. Jothikumar and C. L. Moe, *J. Microbiol. Methods*, 2012, **88**, 155-161.

119. A. M. Kahler, T. B. Johnson, D. Hahn, J. Narayanan, G. Derado and V. R. Hill, *Water*, 2015, **7**, 1202-1216.

120. E. R. Rhodes, E. M. Huff, D. W. Hamilton and J. L. Jones, *J. Virol. Methods*, 2016, **228**, 31-38.

121. H. Shi, I. Xagoraraki, K. N. Parent, M. L. Bruening and V. V. Tarabara, *Appl. Environ. Microbiol.*, 2016, **82**, 4982-4993.

122. L. Pei, M. Rieger, S. Lengger, S. Ott, C. Zawadsky, N. M. Hartmann, H. C. Selinka, A. Tiehm, R. Niessner and M. Seidel, *Environ. Sci. Technol.*, 2012, **46**, 10073-10080.

123. P. Nestola, D. L. Martins, C. Peixoto, S. Roederstein, T. Schleuss, P. M. Alves, J. P. B. Mota and M. J. T. Carrondo, *PLOS ONE*, 2014, **9**.

124. K. E. Gibson and K. J. Schwab, *Appl. Environ. Microbiol.*, 2011, **77**, 385-391.

125. J. Olszewski, L. Winona and K. H. Oshima, *Can. J. Microbiol.*, 2005, **51**, 295-303.

126. V. B. Rajal, B. S. McSwain, D. E. Thompson, C. M. Leutenegger, B. J. Kildare and S. Wuertz, *Water Res.*, 2007, **41**, 1411-1422.

127. E. R. Rhodes, D. W. Hamilton, M. J. See and L. Wymer, *J. Virol. Methods*, 2011, **176**, 38-45.

128. A. L. Polaczyk, J. M. Roberts and V. R. Hill, *J. Microbiol. Methods*, 2007, **68**, 260-266.

129. D. B. Burns and A. L. Zydney, *Biotechnol. Bioeng.*, 1999, **64**, 27-37.

130. J. A. Koehler, M. Ulbricht and G. Belfort, *Langmuir*, 1997, **13**, 4162-4171.

131. J. F. Hester, P. Banerjee and A. M. Mayes, *Macromolecules*, 1999, **32**, 1643-1650.

132. R. Attinti, J. Wei, K. Kniel, J. T. Sims and Y. Jin, *Environ. Sci. Technol.*, 2010, **44**, 2426-2432.

133. P. A. Shields and S. R. Farrah, *Appl. Environ. Microbiol.*, 2002, **68**, 3965-3968.

134. L. Gutierrez, S. E. Mylon, B. Nash and T. H. Nguyen, *Environ. Sci. Technol.*, 2010, **44**, 4552-4557.

135. K. Wong, B. Mukherjee, A. M. Kahler, R. Zepp and M. Molina, *Environ. Sci. Technol.*, 2012, **46**, 11145-11153.

136. K. S. Zerda, C. P. Gerba, K. C. Hou and S. M. Goyal, *Appl. Environ. Microbiol.*, 1985, **49**, 91-95.

137. L. J. Winona, A. W. Ommani, J. Olszewski, J. B. Nuzzo and K. H. Oshima, *Can. J. Microbiol.* , 2001, **47**, 1033-1041.

138. D. O. Cliver, *Appl. Microbiol.*, 1965, **13**, 417-425.

139. C. A. Sorber, B. P. Sagik and J. F. Malina, *Water Res.*, 1972, **6**, 1377-1388.

140. A. Furiga, G. Pierre, M. Glories, P. Aimar, C. Roques, C. Causserand and M. Berge, *Appl. Environ. Microbiol.*, 2011, **77**, 229-236.

141. G. l. Pierre, A. l. Furiga, M. Berge, C. Roques, P. Aimar and C. Causserand, *J. Membr. Sci.*, 2011, **381**, 41-49.

142. R. Michalsky, P. H. Pfromm, P. Czermak, C. M. Sorensen and A. L. Passarelli, *J. Virol. Methods*, 2008, **153**, 90-96.

143. M. Jin, X. Guo, X. W. Wang, D. Yang, Z. Q. Shen, Z. G. Qiu, Z. L. Chen and J. W. Li, *Environ. Sci. Technol.*, 2014, **48**, 6947-6956.

144. M. D. Sobsey and A. R. Hickey, *Appl. Environ. Microbiol.*, 1985, **49**, 259-264.

145. N. Guttmanbass and J. Catalanosherman, *Appl. Environ. Microbiol.*, 1986, **52**, 556-561.

146. A. De Keuckelaere, L. Baert, A. Duarte, A. Stals and M. Uyttendaele, *J Virol. Methods*, 2013, **187**, 294-303.

147. S. Abd-Elmaksoud, S. K. Spencer, C. P. Gerba, A. H. Tamimi, W. E. Jokela and M. A. Borchardt, *Food Environ. Virol.*, 2014, **6**, 253-259.

148. J. L. Cashdollar, N. E. Brinkman, S. M. Griffin, B. R. McMinn, E. R. Rhodes, E. A. Varughese, A. C. Grimm, S. U. Parshionikar, L. Wymer and G. S. Fout, *Appl. Environ. Microbiol.*, 2013, **79**, 215-223.

149. J. Wu, R. A. Rodriguez, J. R. Stewart and M. D. Sobsey, *J. Appl. Microbiol.*, 2011, **110**, 1332-1340.

150. S. E. Mylon, C. I. Rinciog, N. Schmidt, L. Gutierrez, G. C. L. Wong and T. H. Nguyen, *Langmuir*, 2010, **26**, 1035-1042.

151. J. Heffron and B. K. Mayer, *Environ. Sci.: Water Res. Technol.*, 2016, **2**, 443-459.

152. R. A. Guy, P. Payment, U. J. Krull and P. A. Horgen, *Appl. Environ. Microbiol.*, 2003, **69**, 5178-5185.

153. M. Soto-Beltran, L. A. Ikner and K. R. Bright, *Food Environ. Virol.*, 2013, **5**, 91-96.

154. M. Abbaszadegan, M. S. Huber, C. P. Gerba and I. L. Pepper, *Appl. Environ. Microbiol.*, 1993, **59**, 1318-1324.

155. K. J. Schwab, R. Deleon and M. D. Sobsey, *Appl. Environ. Microbiol.*, 1995, **61**, 531-537.

156. S. R. Farrah and G. Bitton, *Can. J. Microbiol.*, 1979, **25**, 1045-1051.

157. S. R. Farrah, P. R. Scheuerman and G. Bitton, *Appl. Environ. Microbiol.*, 1981, **41**, 455-458.

158. M. D. Sobsey, J. S. Glass, R. J. Carrick, R. R. Jacobs and W. A. Rutala, *J. Am. Water Works Assn.*, 1980, **72**, 292-299.

159. M. D. Sobsey, J. S. Glass, R. R. Jacobs and W. A. Rutala, *J. Am. Water Works Assn.*, 1980, **72**, 350-355.

160. S. Sun, Y. L. Shi, H. I. Tong, W. Kang, Z. Wang, E. Allmann and Y. A. Lu, *J. Virol. Methods*, 2016, **229**, 78-85.

161. S. Yoon, C. Lee, K. Kim and A. G. Fane, *Water Res.*, 1998, **32**, 2180-2186.

162. H. Lee, M. Kim, S. Y. Paik, C. H. Lee, W. H. Jheong, J. Kim and G. Ko, *J. Water Health*, 2011, **9**, 27-36.

163. P. M. Holowecky, R. R. James, D. P. Lorch, S. E. Straka and H. D. A. Lindquist, *J. Appl. Microbiol.*, 2009, **106**, 738-747.

164. R. Lu, Q. Li, Z. Yin, I. Xagoraraki, V. V. Tarabara and T. H. Nguyen, *J. Membr. Sci.*, 2016, **497**, 120-127.

165. S. Petterson, R. Grøndahl-Rosado, V. Nilsen, M. Myrmel and L. J. Robertson, *Water Res.*, 2015, **87**, 79-86.

166. X. L. Pang, B. E. Lee, K. Pabbaraju, S. Gabos, S. Craik, P. Payment and N. Neumann, *J. Virol. Methods*, 2012, **184**, 77-83.

167. D. S. Francy, E. A. Stelzer, A. M. Brady, C. Huitger, R. N. Bushon, H. S. Ip, M. W. Ware, E. N. Villegas, V. Gallardo and H. D. Lindquist, *Appl. Environ. Microbiol.*, 2013, **79**, 1342-1352.

168. W. M. El-Senousy, M. I. Costafreda, R. M. Pinto and A. Bosch, *Int. J. Food Microbiol.*, 2013, **167**, 74-79.

169. T. H. Jones, V. Muehlhauser and G. Thériault, *J. Virol. Methods*, 2014, **206**, 5-11.

CHAPTER THREE

The choice of virus propagation and purification methods affects results of virus size and surface charge measurements

Abstract

Two virus propagation methods (in broth and double agar overlay) and three purification procedures (PEG precipitation, centrifugal diafiltration, CsCl density gradient centrifugation) were employed to grow and purify bacteriophages MS2 and P22. The prepared suspensions were characterized in terms of virus size, charge, and hydrophobicity using dynamic light scattering, phase analysis light scattering, and contact angle measurements, respectively. The results of physicochemical characterization of purified bacteriophages were found to depend on the choice of propagation and purification methods. Regardless of the purification method applied, virus propagation in broth showed advantage over that in double agar overlay, since the latter introduced difficult-to-remove impurities attributable to residual agar. Of the three purification methods evaluated with MS2 and P22 propagated in broth, CsCl density gradient centrifugation gave the highest quality bacteriophage suspensions with a narrow size distribution. The impurities remaining in the virus stock after PEG precipitation and centrifugal diafiltration broadened the size distribution and interfered with either charge measurements or hydrophobic characterization or both. Electrophoretic mobilities determined after centrifugal ultrafiltration were similar to those with CsCl density gradient centrifugation, but hydrophobicity characterization indicated

impurities. The isoelectric points of MS2 and P22 after PEG precipitation produced a shift; the shift can be attributed to the change of virus hydrodynamic permeability in the presence of residual PEG. Although time-consuming, propagation in broth combined with CsCl density gradient centrifugation gives highest quality virus suspensions.

3.1 Introduction

Viral contamination of the water supply is a common cause of waterborne diseases worldwide [1-3]. Combined and sanitary sewer overflow, illicit discharge to storm water systems and septic system failure can lead to a release of viruses into environment, posing a threat to public health [4, 5].

Mechanistic studies of virus adsorption on soils and aqueous colloids have been conducted by many researchers. In water and wastewater treatment, complete virus removal by filtration can be difficult due to their small size [6, 7]. In addition to virus removal, filtration was also widely used to concentrate virus from samples prior to detection. Low concentrations of viruses in natural waters and treatment systems highlight the importance of sample concentration for reliable virus detection [8]. Several research efforts have been made to study the factors governing the virus fate during filtration which can guide the design of virus removal [9-11] or concentration [8, 12, 13] processes for effective removal or recovery. Comprehensive studies of viruses' interaction with various environmental and engineered surfaces are essential to understanding mechanisms that control transport of viruses in different systems and

further prevent outbreak of viruses. Numerous studies on virus-surface interaction have demonstrated the significant role of surface properties of viruses. Scrupulous physicochemical characterization of viruses needs to be performed and thus, enables rigorous modeling to understand the energetics of interactions. However, viruses directly harvested from host bacteria or cell lines are stored in growth media containing a large fraction of impurities such as incomplete virions, cell debris, microbial product (protein, DNA, etc.). Experiments on virus physicochemical interaction and characterization require that virions be separated from those impurities as the essential step. Virus purification methods include density gradients centrifugation [8, 14-16], polyethylene glycol (PEG) precipitation [16-19], direct diafiltration [20, 21] or dialysis [22, 23], ultracentrifugation [24] and chromatography [25, 26].

Density gradient centrifugation can be of two general types: rate-zonal centrifugation and isopycnic centrifugation. Sucrose and CsCl are commonly-used to prepare density gradients in both methods. Rate-zonal centrifugation separates viruses primarily based on differences in size and mass, which result in different sedimentation rates. In rate-zonal separation, a virus sample is layered as a narrow zone on the top of continuous density gradient. In contrast, isopycnic centrifugation separates viruses based solely on differences in the buoyant density rather than size. In this method, a virus sample could be either overlaid on or placed under prepared density gradient (either continuous or discontinuous). Alternatively, to ease the sample handling, some gradient materials (e.g. CsCl, Cs_2SO_4, iodixanol) can be directly dissolved into virus sample and gradient can be self-generated during ultracentrifugation. Both rate-zonal and isopycnic

centrifugation methods could effectively separate viruses from other impurities by forming a band that contains only the target virus. Unfortunately, some viruses (e.g. herpesvirus [27], rotavirus [28], human respiratory syncytial virus [29]) may lose infectivity during density gradient centrifugation.

Virus precipitation using PEG relies on PEG acting as an “inert solvent sponge” that sterically excludes viruses from the solvent and causes viruses precipitate from the growth medium [30, 31]. Other growth medium components including metals [32], proteins [32] and DNA [33] can be co-precipitated. However, PEG removal by dialysis is not easy and could be time-consuming due to the low diffusivity of this relatively large (typically 6 to 8 kDa) molecule [34, 35].

Centrifugal diafiltration, similar to dialysis is a technique that uses ultrafiltration membranes to separates virions from other components in the growth medium based on their size. With pressure applied across a membrane, virus purification using diafiltration could be performed much faster than with dialysis, which is driven by a concentration gradient and requires frequent changes of the buffer solution. In addition, diafiltration concentrates and purifies viruses in one batch process minimizing virus loss whereas traditional dialysis involving multiple changes of the dialysis bag only purifies, but not concentrates virus. Two major drawbacks common to dialysis and diafiltration are potential virus aggregation [36] and retention of impurities with the molecular weight larger than the pore size of the dialysis or diafiltration membrane.

Chromatographic technique separates the target virus based on its interactions with chromatographic resin. The interactions depend on the choice of the resin and virus properties such as size, charge, hydrophobicity and ligand specificity, all of which determine separation efficiency. Drawbacks of the method include possible virus degradation due to harsh desorption condition and virus aggregation [8, 37, 38].

Differential ultracentrifugation involves the pelleting of viruses from growth medium followed by resuspension of virus pellets with desired buffer. However, cost of ultracentrifugation machine is high and ultracentrifugation is a time-consuming process, especially for small viruses. Impurities with small molecular weight present at the bottom in homogeneous sample could also cross-contaminate the virus pellets. Furthermore, differential pelleting of viruses could possibly damage and aggregate some viruses, leading to low recoveries. For example, bovine rotavirus recovery was significantly reduced with ultracentrifugation (7%) relative to that with PEG precipitation (64%).

The same virus, but purified with different methods could result in distinct adsorption behavior [39], aggregation dynamic [17, 36] and electrokinetics [36]. Armanious et al. observed that MS2 purified with PEG precipitation leads to less adsorption on poly-L-lysine surface in QCM-D study than that purified with diafiltration [39]. In a study by Dika et al., MS2 and MS2 like particle were prepared with three purification methods (dialysis, PEG precipitation and density gradient) and for both particles, size as function of pH and electrophoresis as function of ionic strength varied with different purification protocols [36]. Poorly purified virus stock may disrupt physicochemical characterization in two ways:

(1) measurement results were not only contributed by virions, but also adversely affected by impurities present in the solution, leading to measurement artifact; (2) impurities were adsorbed to viral capsid, masking the surface properties of virions [40]. These studies indicated that purity of virus stock is an important factor to consider when evaluating the physicochemical interactions of virus in aqueous environments. Dika et al. showed effects of virus purification on size and electrokinetics, but such effects remain unknown on other important physicochemical properties of the virus such as its isoelectric point (pI) and surface tension.

In this study, we purified viruses with three commonly used methods (CsCl density gradient, PEG precipitation and centrifugal diafiltration) and evaluated effects of those methods on determination of hydrodynamic size and electrophoresis as function of pH, IEP and surface tensions. Two bacteriophages were used in this study: one is MS2 with ssRNA and the other one is P22 with dsDNA. Both were typical surrogates for human enteric viruses [12, 41-43].

The premise of the present work is that the propagation and purification procedures should be selected together as an appropriate sample preparation method. While human viruses can only be grown in an established cell line that is maintained in culture vessel with growth medium, bacteriophages can be propagated using host bacteria either cultivated on agar plate or suspended in liquid broth. The choice of the growth medium determines which impurities can be introduced to the virus suspension during the growth stage and what purification method is best suited for removing these

contaminants while avoiding virus loss. The optimal growth-purification sequence should yield high titer purity virus stock while preserving virus infectivity. For this purpose, we also compared infectious recoveries by different purification methods tested.

3.2 Material and Methods

Table 7 summarizes the propagation and purification methods evaluated in this study. The double layer agar method was not studied for the P22 phage.

Table 7. The propagation and purification methods evaluated in this study.

Preparation	Phage	Propagation medium	Purification method
"MS2-agar-PEG"	MS2	Double layer agar	PEG precipitation
"MS2-agar-UF"			Centrifugal diafiltration
"MS2-agar-CsCl"			CsCl ρ-gradient centrifugation
"MS2-broth-PEG"		*E. coli* broth	PEG precipitation
"MS2-broth-UF"			Centrifugal diafiltration
"MS2-broth-CsCl"			CsCl ρ-gradient centrifugation
"P22-broth-PEG"	P22	Lysogeny broth	PEG precipitation
"P22-broth-UF"			Centrifugal diafiltration
"P22-broth-CsCl"			CsCl ρ-gradient centrifugation

3.2.1 Virus propagation

Bacteriophage MS2 was purchased from ATCC (ATCC 15597-B1) and propagated in both double agar overlay (recommended by ATCC) and liquid broth with Escherichia medium (ATCC medium 271) and *Escherichia coli* strain C3000 (ATCC 15597) as the host. Bacteriophage P22 and its host, *Salmonella enterica* subsp. *enterica* serovar Typhimurium strain LT2, were provided by Dr. Kristin Parent (Michigan State University). In contrast to MS2, P22 was propagated only in Lysogeny broth (LB). In this study, virus propagated in double agar overlay is referred to as agar-propagated virus, while virus propagated in suspended broth is referred to as broth-propagated virus.

3.2.1.1 Virus propagation in double agar overlay

For phage propagation in double layer agar, fresh colonies of host bacteria were first inoculated into broth and incubated at 37 ^{o}C for approximately 2 h to reach the log phase. Melted nutrient soft agar (8 mL, 0.5% w/v) was poured into each tube and kept at 48 ^{o}C. A suspension of host bacteria in log phase (300 µL) and diluted stock of phages, (200 µL, 5×10^{5} phage/mL) were then inoculated into soft agar sequentially. After inoculation, soft agar was immediately overlaid on a nutrient agar plate (1.5% w/v). Plates were incubated at 37 ^{o}C overnight. To harvest viruses, 5 mL of broth was added on each plate and plates were placed again in 37 ^{o}C for 3 h. Then, to separate virus from soft agar and host bacteria, soft agar was scraped off the surface of agar plates, placed into a centrifuge tube and centrifuged at 8,000 g and 4 ^{o}C; after 15 min of

centrifugation the supernatant was collected, filtered through 0.22 µm filter and stored at 4 ^{o}C until purification.

3.2.1.2 Virus propagation in broth

For phage propagation in broth, a fresh colony of host bacteria was inoculated to 10 mL broth one day prior to phage propagation and was incubated overnight. Next day, overnight culture was added into fresh broth and the bacterial culture was shaken at 200 rpm at 37 ^{o}C. When optical density at wavelength 600 nm (OD_{600}) reached 0.1, phage stock was inoculated into bacterial culture with multiplicity of infection (MOI) of 0.1. Bacterial culture was further incubated at 37 ^{o}C with shaking (at 200 rpm for P22 and at 100 rpm for MS2) for another 8 h. Prior to virus harvest, several drops of chloroform were added to culture. Culture was then rested for 10 to 15 min and transferred to a centrifuge tube. Bacteria debris were removed via centrifugation at 8,000 g for 10 min at 4 ^{o}C. The supernatant with the phage was filtered through a 0.22 µm filter and stored at 4 ^{o}C until purification.

3.2.2 Virus purification

Figure 1 showed schematic graph of purification methods. The detailed procedure for each purification method were discussed below.

3.2.2.1 Virus purification by CsCl density gradient centrifugation

Phages were pre-concentrated prior to purification due to volume limitation of ultracentrifuge tubes used. For P22, phages were pelleted from stock via centrifugation at 28,000 g for 90 min at 4 ^{o}C. After centrifugation, supernatant was discarded. Pellet was resuspended in 2 mL of the pH 7.6 buffer (10 mM Tris, 10 mM $MgCl_2$; later in the text the buffer is denoted Tris-$MgCl_2$) by overnight nutation at 4 ^{o}C. The small size of MS2 virions makes pelleting this phage difficult and MS2 stock was concentrated down to 2 mL using Amicon Ultra-4 centrifugal filters instead.

CsCl solutions with different densities were prepared for isopycnic centrifugation. Each CsCl solution was layer-by-layer loaded into a tube with the highest density layer at the bottom and the lowest density layer at the top. CsCl solutions were then capped with a 25% sucrose solution as a cushion. Density steps for MS2 were 1.50 g/cm^3 CsCl, 1.35 g/cm^3 CsCl, 25% sucrose cushion; For P22, density steps were 1.60 g/cm^3 CsCl, 1.40 g/cm^3 CsCl, 25% sucrose cushion.

Phage resuspension was applied onto sucrose cushion and a virus band was obtained via ultracentrifugation at 30,000 rpm at 18 ^{o}C for 3 h. The virus band was collected with a syringe by puncturing the tube. CsCl in purified virus stock was then removed via dialysis against 1 mM NaCl (pH 5.7, unadjusted) and the purified stock was stored at 4 ^{o}C.

3.2.2.2 Virus purification by PEG precipitation

PEG 6,000 was added into phage stock with gentle stirring to reach the final concentration of 10% (w/v), followed by addition of NaCl with the final concentration of 0.5 M. Upon addition of PEG and NaCl, virus stock became turbid. Virus stock was stored in the dark at 4 ^{o}C with gentle stirring overnight. The stock was then centrifuged at 10,000 g for 30 min at 4 ^{o}C. The supernatant was discarded and the pellet was resuspended via overnight nutation with 1 mM NaCl (pH 5.7, unadjusted) which was filtered through a 0.22 µm pore size membrane prior to use.

The solution with the resuspended virus was treated by adding chloroform (1:1 v/v) to remove remnant PEG. Upon addition of chloroform, resuspension was vigorously vortexed for 30 s and then centrifuged at 1,700 g for 30 min. The aqueous fraction above the white layer was carefully aspirated into tube as stock without disrupting the white layer. Finally, the virus stock was dialyzed against 1 mM NaCl (pH 5.7, unadjusted) and stored at 4 ^{o}C.

3.2.2.3 Virus purification by centrifugal diafitration

Amicon Ultra-4 centrifugal filters (MWCO 100 KDa) were used to purify viruses by centrifugal diafiltration. Phage stock was loaded into Amicon Ultra filter unit and centrifuged at 1,500 g to bring the concentrate volume to ~0.5 mL. Pre-filtered 1 mM NaCl solution (pH 5.7, unadjusted) was then added to the concentrate to fill up the

centrifuge tube and the suspension was centrifuged again at 1,500 g until 0.5 mL sample remained in the concentrate. This washing step was repeated at least 10 times to remove broth remnants and to complete storage solution exchange. Finally, the concentrate with was collected and used as the purified stock.

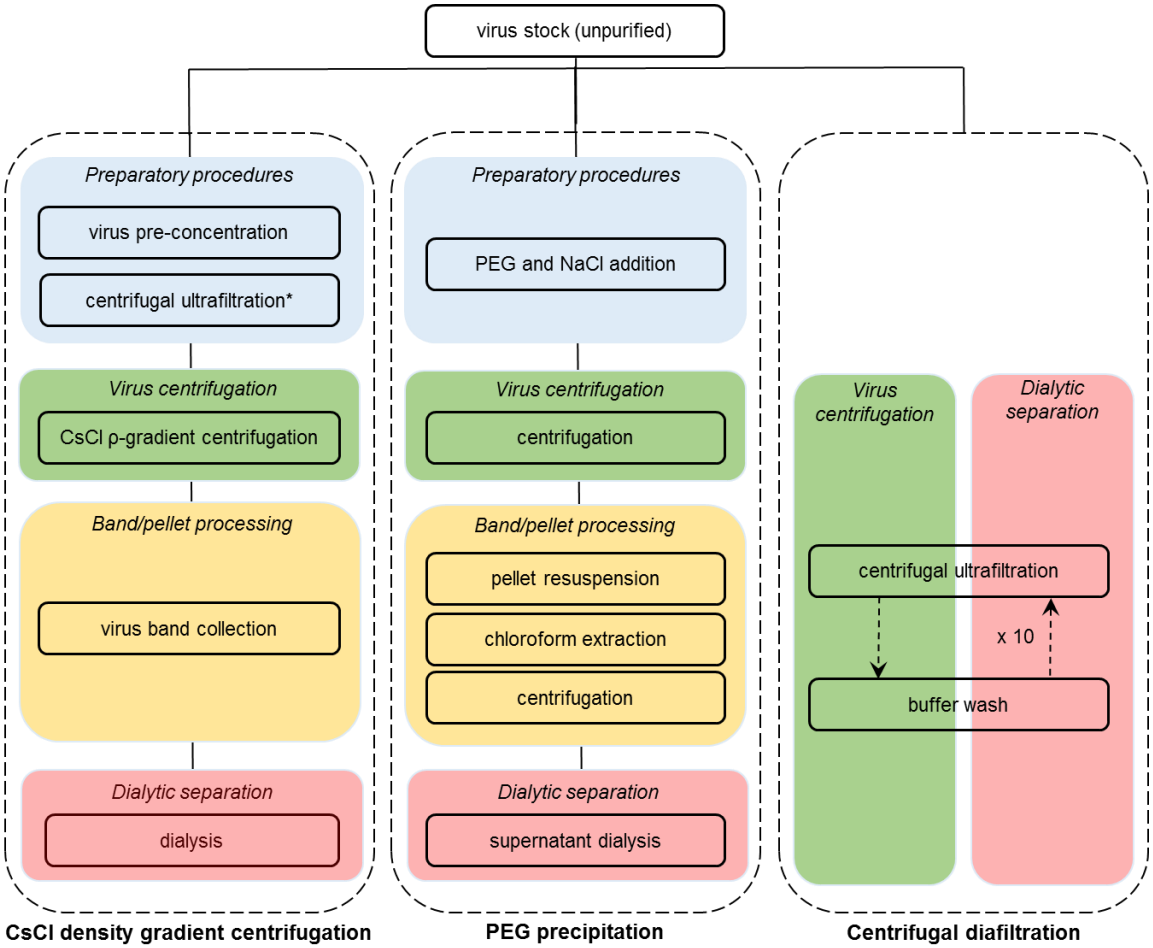

Figure 1. Schematic graph of purification with CsCl density gradient, polyethylene glycol precipitation and centrifugal diafiltration.

3.2.3 Hydrodynamic diameter and electrophoretic mobility measurements

Malvern Zetasizer Nano-ZS was used to measure both the hydrodynamic diameter and the electrophoretic mobility of virions. Hydrodynamic diameter was measured by dynamic light scattering while electrophoretic mobility was determined by phase analysis light scattering. Zeta potential was then calculated from electrophoretic mobilities. Prior to virus size and charge characterization, purified stocks were filtered using 0.22 µm filter for P22 and 0.1 µm filter for MS2 to remove any aggregates that could have formed after purification. Hydrodynamic diameter and electrophoretic mobility were measured as functions of pH. Purified virus stocks were diluted with background solutions with varied pH adjusted using NaOH and HCl. 1 mM NaCl solution was used as background electrolyte for all pH except pH 7.6. The pH of 1 mM NaCl solution could not be stabilized at pH 7.6 by adding NaOH or HCl only. Instead, Tris-$MgCl_2$ buffer was used as the background solution at this pH.

3.2.4 Surface tension and hydrophobicity determination

Surface tension of viruses purified by different methods was determined using the protocol described in our previous work [8, 12]. Briefly, to prepare a virus lawn, purified virus stock was filtered through a 30 KDa ultrafiltration membrane. The membrane coated with a multilayer cake of virus particles was dried at room temperature until the water contact angle on the membrane reached a plateau. Contact angles of three probe liquids (water, glycerol and diiodomethane) on the virus lawn were then measured using

sessile drop method. Surface tension components of each virus (γ_v^{LW}, γ_v^+, γ_v^-) were obtained by substituting measured contact angles and known surface tensions of probe liquids into the Young-Dupré equation:

$$(1+\cos\theta)\gamma_l^{TOT} = 2\left(\sqrt{\gamma_v^{LW}\gamma_l^{LW}} + \sqrt{\gamma_v^+\gamma_l^-} + \sqrt{\gamma_v^-\gamma_l^+}\right) \quad (3\text{-}1)$$

where θ is the contact angle of the probe liquid on the virus lawn, γ^{TOT} is the total surface energy, $\gamma^{LW}$is the LW component of surface energy, γ^+ is the electron-acceptor parameter of surface energy, and γ^- is the electron-donor parameter of surface energy. Subscripts l and v refer to probe liquid and virus respectively. The free energy of interfacial interaction between two virions immersed in water (ΔG_{vwv}) was calculated using equation (3-2):

$$\Delta G_{vwv} = -2\left(\sqrt{\gamma_v^{LW}} - \sqrt{\gamma_w^{LW}}\right)^2 - 4\left(\sqrt{\gamma_v^+\gamma_v^-} + \sqrt{\gamma_w^+\gamma_w^-} - \sqrt{\gamma_v^+\gamma_w^-} - \sqrt{\gamma_v^-\gamma_w^+}\right) \quad (3\text{-}2)$$

and used as a quantitative measure of hydrophobicity of the virus in question. A virus is hydrophobic when $\Delta G_{vwv} < 0$. The absolute value of ΔG_{vwv} indicates the degree of hydrophobicity (or hydrophilicity, when $\Delta G_{vwv} > 0$) of the virus.

3.3 Results and Discussion

3.3.1 Effects of the virus propagation method on the hydrodynamic size and surface charge of MS2 purified by three different procedures

3.3.1.1 Effect on MS2 hydrodynamic size

MS2 propagated either on agar or in *E. coli* culture broth was purified by one of the three methods: PEG precipitation, centrifugal diafiltration, and CsCl ρ-gradient centrifugation (Table 7). To evaluate the effect of the propagation protocol on virus physicochemical properties, we only compared results obtained with phages from stocks purified by the same method, but propagated differently. Figure 2 shows intensity-based size distribution in 1 mM NaCl, unadjusted pH 5.7 (storage solution for purified virus) for agar-propagated MS2 and broth-propagated MS2 with each purification applied. The average hydrodynamic diameter ($\overline{d}_h$) and polydispersitivity index in storage solution in each case were summarized in Table 8. $\overline{d}_h$ for MS2-broth-CsCl batch in the storage solution was 30.2 ± 0.3 nm, which was similar to the individual virion size (27 nm [44]) obtained by TEM. The single peak at 30 nm with a narrow half-width (PDI ~0.12) suggests minimal aggregation. The average hydrodynamic diameter, $\overline{d}_h$, was higher (37.8 ± 0.2 nm) in the MS2-agar-CsCl batch. An additional small peak (18.3% of the intensity) at ~400 to 500 nm was observed in this condition with high PDI (~0.32). Because the purification method was the same (CsCl density gradient), the broadening of the PSD is an effect of the propagation method.

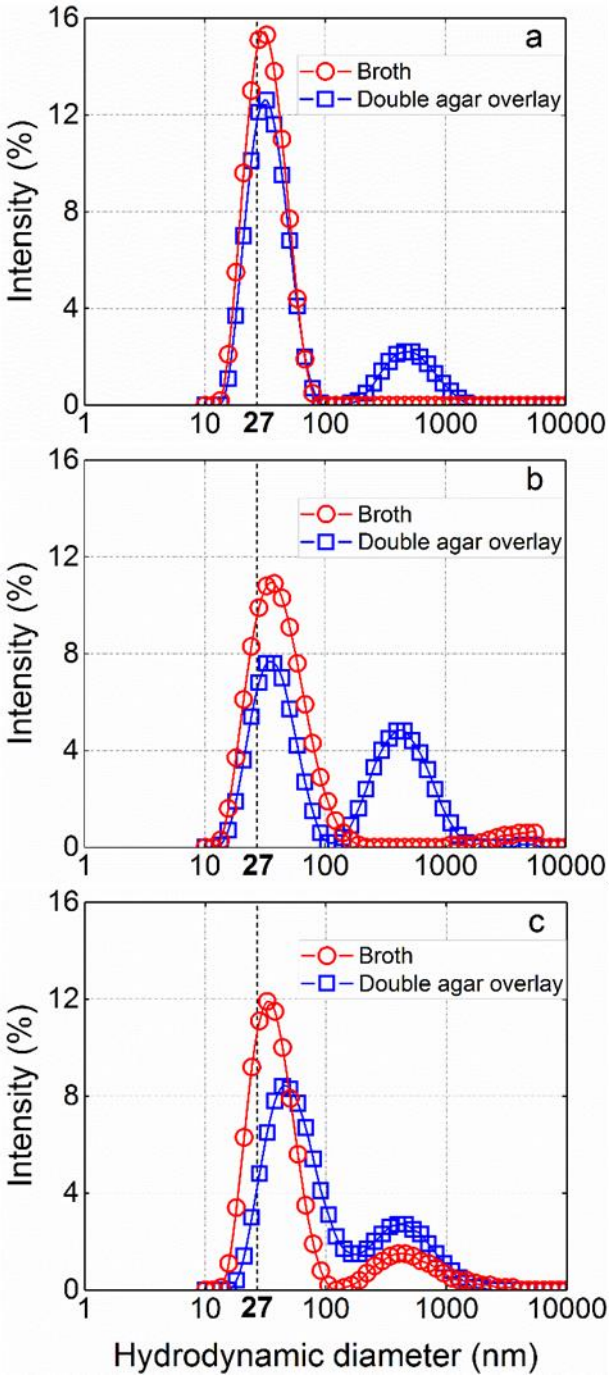

Figure 2. Size distribution of MS2 propagated by two different methods (in broth and on double layer agar overlay) and purified by CsCl density gradient centrifugation (a), PEG precipitation (b) and centrifugal ultrafiltration (c). Solution: 1mM NaCl, pH 5.7.

Average hydrodynamic diameter of MS2 in MS2-agar-PEG was 57 ± 2 nm, significantly larger than in the MS2-broth-PEG (38 ± 2 nm). Similar trends were observed when MS2 stock was purified by centrifugal diafiltration, which gave $\overline{d}_h$ of 61 ± 3 nm in MS2-agar-UF preparation and 39 ± 2 nm and in MS2-broth-UF preparation). For both purification methods, the PDI values for agar-propagated MS2 (PDI of ~0.44 and ~0.66 for MS2-agar-PEG and MS2-agar-UF) were higher than for broth-propagated MS2 (PDI of ~0.23 and ~0.29 for MS2-broth-PEG and MS2-broth-UF respectively). Regardless of the propagation method used, a bimodal size distribution was obtained.

Table 8. Summary of average hydrodynamic diameter and polydispersity index for MS2 in storage solution recorded for the six different preparations evaluated in this study.

Preparation	**Average size, $\overline{d}_h$** (nm)	**Polydispersity index, PDI**
"MS2-agar-PEG"	57 ± 2	0.66
"MS2-agar-UF"	61 ± 3	0.44
"MS2-agar-CsCl"	38 ± 0	0.32
"MS2-broth-PEG"	38 ± 2	0.23
"MS2-broth-UF"	39 ± 2	0.29
"MS2-broth-CsCl"	30 ± 0	0.12

Regardless of the purification method applied, higher $\overline{d}_h$, broadening of the main peak and an additional peak with higher intensity were measured for agar-propagated MS2 indicating MS2 aggregation. We tentatively attribute this behavior to heteroaggregation of MS2 virions with impurities introduced during MS2 propagation by the double agar overlay method.

If a bimodal size distribution was obtained, an additional size measurement was conducted with the same virus stock filtered again through a 0.1 μm pore size membrane. This additional filtration step eliminated the peak corresponding to large particles for all broth-propagated MS2 (regardless of the purification method) and for the MS2-agar-CsCl preparation. Surprisingly, in MS2-agar-UF and MS2-agar-PEG, the peak corresponding to large particles (~ 0.4 to 0.5 μm) remained even after multiple filtrations through the 0.1 μm filter. We attribute the peak to the components of the agar as agar is the only additional substance used in the double agar overlay procedure in comparison with the broth-based growth.

Although agar gel had been removed from the virus harvest by centrifugation and filtration (see Section 2.1.1), small agar molecules (MW range from <20 kDa to >150 kDa [45]) or aggregates could remain in the stock. Virus pellets produced in the MS2-agar-PEG process were gelatinous and gel aggregates were observed in the UF concentrate during MS2-agar-UF. The gel could be agar aggregates formed from smaller ($\lesssim$ 0.1 μm) agar molecules concentrated along with the virus during purification. Indeed it has been reported that agar molecules in filtrate can form double helix structures and re-aggregate [45]. We did observe an increase in the intensity of the size distribution peak in the 400 to 500 nm range for post-filtration samples.

$\overline{d}_h$ of MS2 as a function of pH for agar-propagated MS2 and broth-propagated MS2 with each purification method was shown in Figure S1. Regardless of the purification

method, very large aggregates of 3 to 7 μm were observed in broth-propagated MS2 samples at pH 3.5 and lower. For agar-propagated MS2, such severe aggregation was not observed when virus were purified with PEG precipitation or centrifugal diafiltration. In those cases, $\overline{d}_h$ only increased to ~70 to 80 nm with a decrease in pH to 2.5. In MS2-agar-CsCl samples, aggregates of ~3 μm were observed at pH 3.0.

3.3.1.2 Effect on MS2 charge

In a separate set of tests, the electrophoretic mobility, μ, of MS2 propagated and purified by six different protocols (Table 7) was measured. Eectrophoretic mobility and calculated zeta potential as a function of pH are shown in Figure 3. The mobility of MS2-agar-CsCl samples in the storage solution (pH 5.7, unadjusted) and 1 mM NaCl was -3.2 ± 0.2 μm cm·s^{-1}·V^{-1}. For any of purification methods applied, negative electrophoretic mobility for MS2 propagated in double agar overlay at pH 5.7 was always higher in magnitude than that propagated in broth. Depending on the purification method applied, the pI of broth-propagated MS2 was either ~ 3.1 (for CsCl density gradient purification and centrifugal diafiltration purification) or in the range between 2.2 and 2.5 (for PEG precipitation purification). In MS2-agar-PEG and MS2-agar-UF samples, was not observed for the phage was found to be negative charged over the entire pH range investigated (pH 2 to 10). This may explain the absence of large MS2 aggregates at low pH with these two purification methods as discussed earlier (see section 3.3.1.1). Agar-based impurities such as agaropectin could potentially coat the virus to impart a strong negative charge to it, even at very low pH. Agaropectin, a non-

gelling fraction of agar, is a highly negatively charged polysaccharide with acidic side-groups such as ester sulfate, D-glucuronic acid, and pyruvic acid [46]. Negative surface charge and steric hindrance on MS2 caused by adsorption of agaropectin could potentially explain the very moderate increase in $\overline{d}_h$ at low pH with these two preparation methods. pI was observed (between pH 2.5 and 2.7) for MS2-agar-CsCl samples; the value was lower than pH ~3.1 measured for the phage in MS2-broth-CsCl samples.

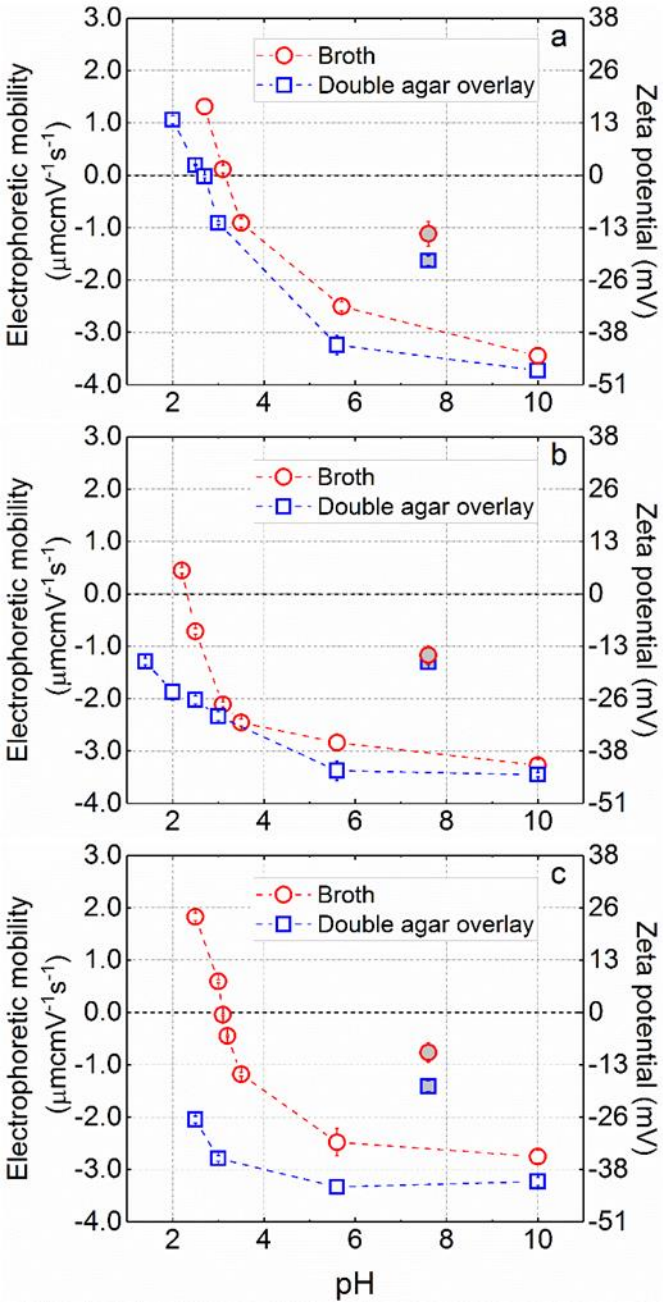

Figure 3. Electrophoretic mobility and zeta potential as function of pH for MS2 propagated by two different methods (in broth and on double layer agar overlay) and purified by CsCl density gradient centrifugation (a), PEG precipitation (b) and centrifugal ultrafiltration (c).

The presented data and analysis clearly indicate that broth-based propagation introduces less impurities that interfere with size and charge measurements of bacteriophages. Of the three purification methods tested, CsCl density gradient

centrifugation was the only technique that could remove agar-derived impurities introduced at the propagation stage. CsCl density gradient centrifugation, however, is a labor-intensive and time-consuming process. This conclusion prompted a closer inspection of the impact that each of the three purification methods has on results of the physicochemical characterization of the virus.

3.3.2 Effects of the virus purification method on virus size and charge measurements

To solely evaluate the effect of the purification method, P22 and MS2 were used as model viruses. Both phages were propagated in liquid broth to avoid the interference of impurities from agar (see section 3.3.1). Figure 4 shows the intensity based size distribution in storage solution and electrophoretic mobility as a function of pH for both MS2 and P22 with each purification method. Results for broth-propagated MS2 with each purification method having been shown in Figure 2 (size measurement) and Figure 3 (electrophoretic mobility measurement) were regenerated in Figure 4(a) and Figure 4(b) here to better evaluate. those for broth-propagated P22 were shown in Figure 4 (a) and Figure 4 (b).

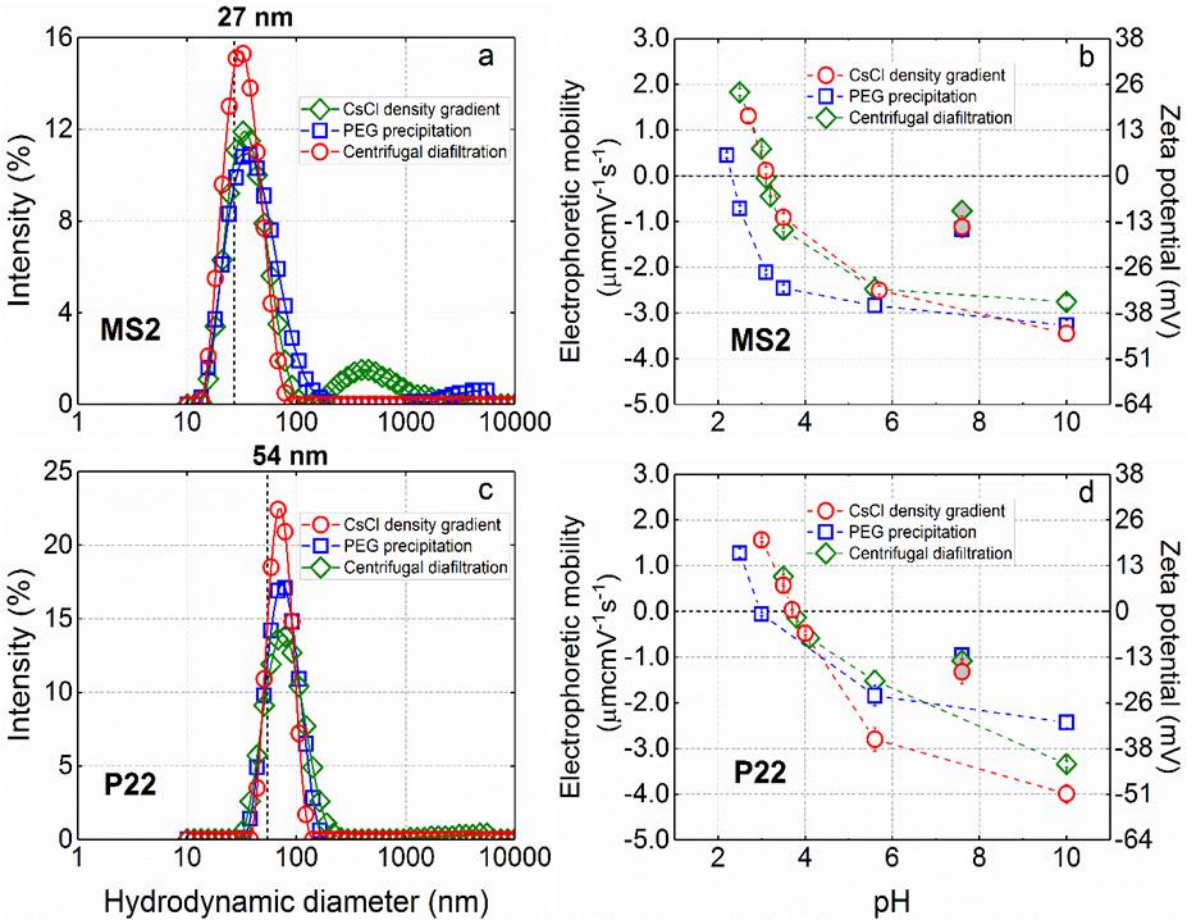

Figure 4. Size distribution (a, c) and electrophoretic mobility (b, d) of broth-propagated MS2 (a, b) and P22 (c, d) phages purified by CsCl density gradient centrifugation, PEG precipitation and centrifugal ultrafiltration. Solution used in size measurements: 1mM NaCl, pH 5.7. Data for MS2 overlaps with parts of Figures 2 and 3 and are shown here for easier comparisons.

As mentioned in Section 3.3.1, MS2 size in MS2-broth-CsCl samples in the storage solution was measured to be 30.2 ± 0.3 nm with low PDI (~0.12) indicating a stable suspension of monodisperse MS2 virions. In the MS2-broth-UF samples at the same pH, $\overline{d}_h$ was ~38 nm with a higher PDI (~0.29) and a bimodal size distribution (main peak at 32 nm and an additional lower band at ~400 nm) suggesting that aggregates form during diafiltration. Compared with diafiltration purified MS2, PEG precipitation purified MS2 gave similar $\overline{d}_h$ (~38 nm), but lower PDI (~0.23) with main peak at 32 nm and negligible aggregation ranging from 1 to 5 μm. $\overline{d}_h$ for PEG purified MS2 in this study was in agreement with those from other studies with the same purification method: 40 nm [17] and 40 to 60 nm [36]. Since in MS2-broth-PEG aggregation was negligible (~4% of the population), the higher $\overline{d}_h$ may have stemmed from PEG adsorbed to the viral capsid; such sorption would decrease particle diffusivity and increase the hydrodynamic size [36]. This assumption is consistent with the finding by Gao et al. who reported that conjugation of 5 kDa PEG to the adenovirus capsid (10% modification ratio) increased virion size from 113 to 122 nm [47].

Figure 4 (c) illustrates the effects of the three purification methods on the hydrodynamic diameter of bacteriophage P22. In the storage solution (1 mM NaCl, pH 5.7), the P22-broth-CsCl was characterized by $\overline{d}_h$ of 69.4 ± 1.2 nm and a single peak at 68 nm with the PDI of 0.04. The individual P22 virion size determined by TEM imaging was ~54 nm[12]. The difference could stem from the tail structure of P22, which impacts its diffusivity [12, 48]. As was the case with MS2, higher $\overline{d}_h$ (~72 nm) was measured for P22 in P22-broth-PEG than in P22-broth-CsCl corroborating the hypothesis of PEG adsorption

on the capsid surface. Centrifugal diafiltration method resulted in bimodal size distribution for P22, though 1 μm to 5 μm aggregates contributing to the secondary peak in the size distribution were very minor (together corresponding to 2.8% of population). $\overline{d}_h$ increased to 76 nm with PDI at 0.18 in this case.

For both MS2 and P22 in the storage solution, the narrowest siz distributions were always after purification by the CsCl density gradient. Comparing sizing data for MS2 and P22, one can see that each P22 suspension was more narrowly distributed than the corresponding MS2 suspension purified by the same method. $\overline{d}_h$ as a function of pH for both phages with each purification method were shown in Figure S2. As pH decreased, severe aggregation of MS2 was observed in all sample preparations (Figure S2 (a)). Larger aggregates (up to ~7 μm) were observed after PEG precipitation and diafiltration, while CsCl density gradient resulted in relatively small aggregates (< 3 μm). In comparison with MS2, the largest P22 aggregates were detected as pH decreased were ~600 nm with CsCl density gradient purification (Figure S2(b)). This suggests that, in comparison with MS2, P22 virions could be better separated from the components of the growth medium (broth) and are more stable in the 1 mM NaCl background solution. For measurements at pH 7.6 Tris-$MgCl_2$ buffer was used as the background solution. At this pH, the sis distribution of P22 had a single narrow peak at ~70 nm, close to the size measured in 1 mM NaCl at pH 5.7. In contrast, $\overline{d}_h$ for MS2 depended on the choice of the purification method. MS2-broth-CsCl preparations had $\overline{d}_h$ of 29 nm, which was very close to the size obtained in TEM. MS2-broth-UF and MS2-broth-PEG preparations, however, had $\overline{d}_h$ values of 45 nm and 59 nm, respectively. These larger averages

could possibly be explained by impurities that may aggregate in higher IS (~25 mM) of the Tris-$MgCl_2$ buffer. The difference further underscores the advantage for CsCl density gradient centrifugation as the purification method.

Figure 4 (c) and (d) presents electrophoretic mobility and corresponding zeta potential values as functions of pH. In the storage solution, MS2 has electrophoretic mobility of -2.5 ± 0.3 $\mu m \cdot s^{-1} \cdot V^{-1} \cdot cm$ when purified with diafiltration. Dika et al. [49, 50] and Langlet et al. [23] reported similar MS2 electrophoretic mobility in $NaNO_3$ and at the same pH of 5.6 for MS2 purified by dialysis, a method closely related to diafiltration. Regardless of the purification method, the smaller magnitude of electrophoretic mobility was observed in the Tris-$MgCl_2$ buffer (pH 7.6) relative to 1mM NaCl, which can be attributed to electric double layer compression at the higher ionic strength of buffer. The pI of MS2 ranges from 2.2 to 4.0 depending on the solution chemistry [40]. In our study, pI of MS2 was ~ 3.1 in both MS2-broth-UF and MS2-broth-CsCl preparations in 1 mM NaCl; this value is in agreement with the results by Langlet et al, who reported pI of 3.1 for dialysis-purified MS2 in 1 mM $NaNO_3$ [23]. No significant differences in electrophoretic mobility were observed for pH > 5.6 among the three purification methods. For pH <3.5, however. MS2 phages in MS2-broth-PEG samples showed lower value of electrophoretic mobility than MS2 purified with the other two methods. which lead to a decreased pI ranging from 2.2 to 2.5 for PEG precipitation method.

Regardless of the purification method, the electrophoretic mobility for P22 measured in Tris-$MgCl_2$ (pH 7.6) was smaller in magnitude than that in 1 mM NaCl, pH 5.7, same

trend as MS2. For P22-broth-UF and P22-broth-CsCl in 1 mM NaCl, the pI of P22 was ~3.7, similar to pI of 3.4 reported by Fidalgo de Cortalezzi et al. for diafiltration-purified P22 in 15 mM NaCl [51]. The theoretical pI of P22 calculated by ProtParam, an analysis software that calculates various physicochemical parameters for proteins was higher at ~5.0 [52]. The difference, also observed for other viruses could also reflect the effect of the viral genome on the pI.

Similar to MS2, pI shift (reduced to ~3) was also observed for P22 when it is purified by PEG precipitation method.

The pI shift for both phages may stem from interaction of PEG with virion though PEG is neural polymer. A virus could be regarded as a permeable soft particle[53], with the surface charge partly dependent on the inner structure of virus (genome or protein inside capsid). PEG-virion interaction could impact the electrophoretic mobility and pI in a manner that depends on the structure of a PEG layer on the virion surface. PEG can impact the electrokinetic properties of the virus also through its propensity to induce virion aggregation at lower pH (see Figure S2) wherein the aggregate structure affects both hydrodynamic and electrostatic properties of aggregated virions [53].

In our case, phage permeability may increase when aggregates occurred in presence of PEG. Such increase in virion permeability may highlight the effect of internal genome structure (RNA for MS2 with pI as low as ~2 [36]) on its electrophoretic mobility, thus lower the pI of phage as a whole particle. Moreover, as mentioned in introduction, PEG

precipitates both viruses and, potentially, impurities (e.g. DNA, proteins). The impurities co-precipitated with viruses may also be responsible for the pI shift observed for PEG-purified batches.

3.3.3 Effects of virus purification methods on surface tension parameters and hydrophobicity of bacteriophages

We also evaluated the effect of the purification method on the values of surface tension parameters calculated based on contact angle measurements. For P22 purified by CsCl density gradient centrifugation, surface tension parameters and the interfacial free energy had been reported in our previous work and were used here for comparison [12]. For all P22 preparations, apolar surface energy components (γ^{LW}) are between 42 and 44 mJ/m^2 (Table 9), which is a range typical for biological materials [54]. The purification procedure did have an effect on the polar surface energy components. For P22-broth-CsCl, the electron donor (γ^-) and electron acceptor (γ^+) parameters were 25.8 mJ/m^2 and 0.06 mJ/m^2, respectively, translating into the overall polar component, γ^{AB} of 2.4 mJ/m^2. For P22-broth-PEG and P22-broth-UF preparations, we could not calculate the appropriate virus surface tension components after substitution of the known probe liquids surface tension and corresponding contact angles into Young-Dupré equation (equation (3-1)).

Table 9. Measured contact angles, calculated surface energy parameters and free energy of interfacial interaction when immersed in water for broth-propagated P22 bacteriophage as a function of the purification method.

Purification method	Contact angle with probe liquid (^{0})			Surface energy parameters (mJ/m^2)					Free energy of interfacial interaction in water, ΔG_{vwv}(mJ/m^2)
	H_2O	Glycerol	DIM[#]	γ^{LW}	γ^{+}	γ^{-}	γ^{AB}	γ^{TOT}	
CsCl density gradient	55 ± 2	56 ± 6	34 ± 3	42.5	0.06	25.8	2.4	44.9	-6.3
PEG precipitation	44 ± 5	65± 4	34 ± 6	42.5	-	52.9	-	42.5	+38.1
Centrifugal diafiltraiton	49 ± 8	75 ± 6	30 ± 2	44.2	-	57.3	-	44.2	+43.0

[#] DIM = diiodomethane

Slightly negative values for $\sqrt{\gamma^+}$ were obtained (~-0.9 for P22-broth-PEG and ~-1.8 for P22-broth-UF). This may be explained by the presence of impurities that PEG precipitation and diafiltration failed to remove (e.g. DNA, protein, other cellular lysis debris and PEG). These impurities could be concentrated with the virus and non-uniformly distributed within the virus lawn. Each apparent contact angle on such surface only depends on local structures instead of overall surface, which can bring error to our measurements. This interpretation is consistent with the lower average water contact angle on P22 lawn formed from P22-broth-CsCl than from P22-broth-CsCl and P22-broth-CsCl preparations. Indeed, some of the potential impurities - DNA, RNA, and PEG - are hydrophilic substances but with a negligible γ^+ [54]. Based on the surface tension data reported in our previous work [8] and other studies [54], a very small value of γ^+ is also a common characteristic of non-enveloped viruses, which suggests that a small error in contact angle measurements could lead to $\sqrt{\gamma^+}$ <0.

We further calculated the interfacial free energy (ΔG_{vwv}) for each purification method using eqn (2). For PEG precipitation and diafitration methods, the calculation was made with the assumption that γ^+ was negligible (~0). For P22-broth-CsCl, P22 was found to be hydrophobic (ΔG_{vwv} <0) whereas for the other two methods ΔG_{vwv} was calculated to be positive indicating that P22 is hydrophilic. Our results indicated that purification methods could significantly impact the virus polarity characterization.

3.4 Summary

Two virus propagation methods (in broth and double agar overlay) and three purification procedures (PEG precipitation, centrifugal diafiltration, CsCl density gradient centrifugation) were employed to grow and purify bacteriophages MS2 and P22. The prepared suspensions were characterized in terms of virus size, charge, and hydrophobicity using dynamic light scattering, phase analysis light scattering, and contact angle measurements, respectively. The physicochemical properties of purified bacteriophages were found to depend on the choice of propagation and purification methods.

Hydrodynamic size and electrophoretic mobility data for MS2 indicated that double agar overlay growth introduces difficult-to-remove impurities that confound results of physicochemical characterization of the virus. Specifically, agar-propagated MS2 stock purified by PEG precipitation or centrifugal diafiltration included large (~ 0.4 to 0.5 μm) “unfilterable” aggregates detected after repeated post-filtration with a 0.1 μm nominal pore size membrane. Further, the isoelectric point of MS2 in this preparation could not be determined as the bacteriophage remained electronegative even at the pH as low as 1.4. CsCl density gradient centrifugation could remove most impurities but still gave a relatively broad MS2 size distribution. Such interferences were not observed for MS2 propagated in *E. coli* broth regardless of the purification method employed.
The degree of bacteriophage purity achievable with each of the three purification methods was compared based on the data for MS2 and P22 propagated in broth media.

The impacts of the virus purification protocol on size and charge characteristics of P22 and MS2 were similar. The highest purity was achieved with CsCl density gradient centrifugation, which consistently gave bacteriophage suspensions with a narrow size distribution. PEG precipitation method produced broader size distributions and ionic strength-dependent pI values. The dependency on ionic strength was interpreted to result from PEG adsorption on the virus capsid rendering a “soft” aggregate of PEG and one or more virions. Centrifugal diafiltration gave size and charge data of quality close to that obtained with CsCl density gradient centrifugation; however, contact angle measurements of probe liquids on lawns of diafiltration-purified viruses indicated impurities that could not be discerned in particle size data.

PEG precipitation may be suitable for applications where the remnant PEG is not a concern (e.g. due to its biological inertness) but should be avoided if impurity-free virions are needed.

3.5 Conclusions

The performance of virus purification procedures depends on the choice of the propagation method used to grow the virus. Agar-based propagation introduced impurities that neither of the three purification procedures could remove fully. For viruses propagated in broth media, the highest quality virus stock was obtained after purification by CsCl density gradient centrifugation. The other two purification methods are less costly and time-consuming and can be adequate choices for certain applications. In general, the choice of the optimal purification procedure is a matter of

tradeoff where the demands for product quantity and quality (e.g. virus concentration and infectivity, amount of residual impurities) should be weighed against issues of practicability such as the time and cost of virus purification.

APPENDIX

APPENDIX

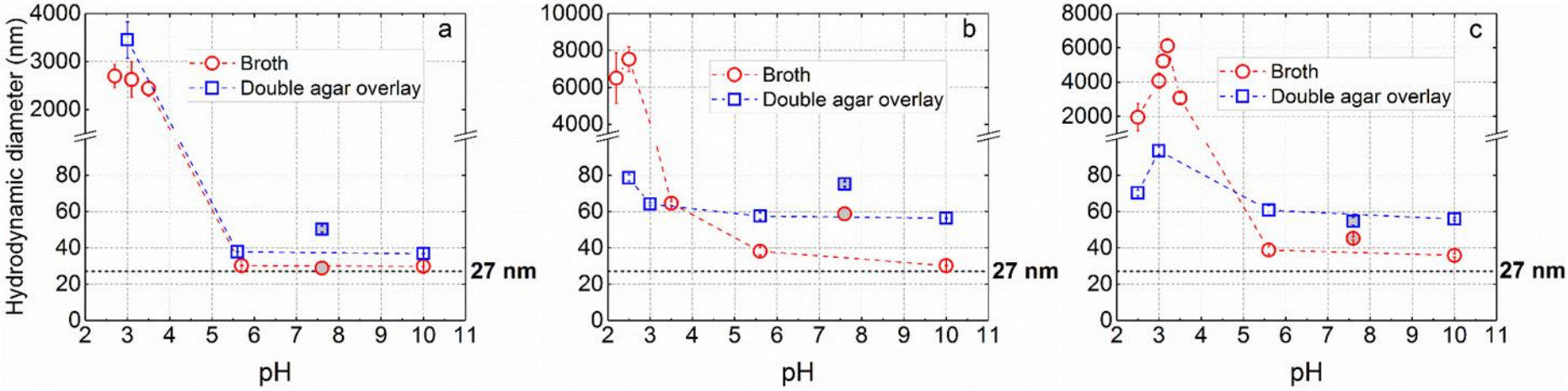

Figure 5. Average hydrodynamic diameter as function of pH for MS2 purified by CsCl density gradient (a), PEG precipitation (b) and centrifugal ultrafiltration (c).

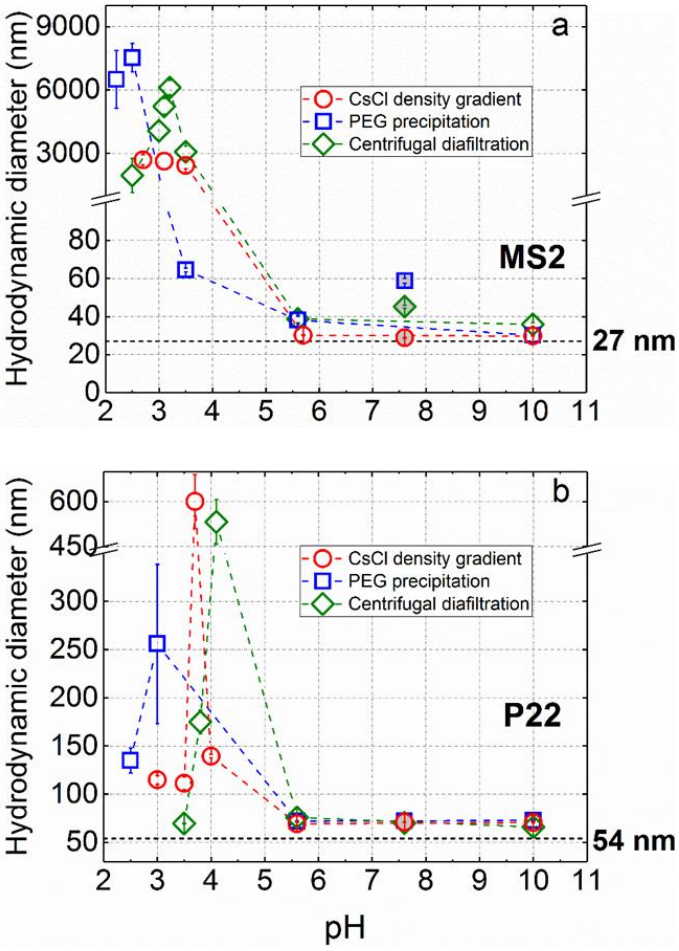

Figure 6. (a) Average hydrodynamic diameter as function of pH for MS2 purified by CsCl density gradient, PEG precipitation and centrifugal ultrafiltration.

REFERENCES

REFERENCES

1. T. T. Fong and E. K. Lipp, *Microbiology and molecular biology reviews : MMBR*, 2005, **69**, 357-371.

2. R. G. Sinclair, E. L. Jones and C. P. Gerba, *Journal of applied microbiology*, 2009, **107**, 1769-1780.

3. A. M. Gall, B. J. Marinas, Y. Lu and J. L. Shisler, *PLoS pathogens*, 2015, **11**, e1004867.

4. USEPA, *Journal*, 2001.

5. R. D. Arnone and J. P. Walling, *Journal of water and health*, 2007, **5**, 149-162.

6. Z. Altintas, M. Gittens, J. Pocock and I. E. Tothill, *Biochimie*, 2015, **115**, 144-154.

7. M. D. Sobsey, *Managing water in the home: accelerated health gains from improved water supply*, World Health Organization Geneva, 2002.

8. H. Shi, I. Xagoraraki, K. N. Parent, M. L. Bruening and V. V. Tarabara, *Appl. Environ. Microbiol.*, 2016, 4982-4993.

9. R. M. Chaudhry, R. W. Holloway, T. Y. Cath and K. L. Nelson, *Water research*, 2015, **84**, 144-152.

10. J. Langlet, L. Ogorzaly, J.-C. Schrotter, C. Machinal, F. Gaboriaud, J. F. L. Duval and C. Gantzer, *J. Membr. Sci.*, 2009, **326**, 111-116.

11. H. Huang, T. A. Young, K. J. Schwab and J. G. Jacangelo, *J. Membr. Sci.*, 2012, **409**, 1-8.

12. E. V. Pasco, H. Shi, I. Xagoraraki, S. A. Hashsham, K. N. Parent, M. L. Bruening and V. V. Tarabara, *J. Membr. Sci.*, 2014, **469**, 140-150.

13. A. L. Polaczyk, J. M. Roberts and V. R. Hill, *Journal of Microbiological Methods*, 2007, **68**, 260-266.

14. K. Wong, B. Mukherjee, A. M. Kahler, R. Zepp and M. Molina, *Environmental science & technology*, 2012, **46**, 11145-11153.

15. J. F. Torres-Salgado, M. Comas-Garcia, M. V. Villagrana-Escareno, A. L. Duran-Meza, J. Ruiz-Garcia and R. D. Cadena-Nava, *Journal of Physical Chemistry B*, 2016, **120**, 5864-5873.

16. T. L. Cromeans, A. M. Kahler and V. R. Hill, *Applied and Environmental Microbiology*, 2010, **76**, 1028-1033.

17. T. H. Nguyen, N. Easter, L. Gutierrez, L. Huyett, E. Defnet, S. E. Mylon, J. K. Ferri and N. A. Viet, *Soft Matter*, 2011, **7**, 10449-10456.

18. M. Tong, Y. Shen, H. Yang and H. Kim, *Colloids and surfaces. B, Biointerfaces*, 2012, **92**, 340-347.

19. C. T. Tanneru, J. D. Rimer and S. Chellam, *Environmental science & technology*, 2013, **47**, 4612-4618.

20. A. Armanious, M. Munch, T. Kohn and M. Sander, *Environmental science & technology*, 2016, **50**, 3597-3606.

21. L. Gutierrez, X. Li, J. Wang, G. Nangmenyi, J. Economy, T. B. Kuhlenschmidt, M. S. Kuhlenschmidt and T. H. Nguyen, *Water research*, 2009, **43**, 5198-5208.

22. B. Michen, F. Meder, A. Rust, J. Fritsch, C. Aneziris and T. Graule, *Environmental science & technology*, 2012, **46**, 1170-1177.

23. J. Langlet, F. Gaboriaud, J. F. Duval and C. Gantzer, *Water research*, 2008, **42**, 2769-2777.

24. R. Attinti, J. Wei, K. Kniel, J. T. Sims and Y. Jin, *Environmental science & technology*, 2010, **44**, 2426-2432.

25. R. Monjezi, B. T. Tey, C. C. Sieo and W. S. Tan, *Journal of Chromatography B*, 2010, **878**, 1855-1859.

26. K. Farkas, A. Varsani and L. P. Pang, *Food and Environmental Virology*, 2015, **7**, 261-268.

27. H. Pertoft, *Virology*, 1970, **41**, 368-372.

28. D. Y. Chen and R. F. Ramig, *Virology*, 1992, **186**, 228-237.

29. E. Gias, S. U. Nielsen, L. A. F. Morgan and G. L. Toms, *Journal of Virological Methods*, 2008, **147**, 328-332.

30. G. D. Lewis and T. G. Metcalf, *Appl. Environ. Microbiol.*, 1988, **54**, 1983-1988.

31. D. H. Atha and K. C. Ingham, *J. Biol. Chem.*, 1981, **256**, 12108-12117.

32. A. J. Prussin, L. C. Marr and K. J. Bibby, *FEMS Microbiol. Lett.*, 2014, **357**, 1-9.

33. N. Hammerschmidt, S. Hobiger and A. Jungbauer, *Proc. Biochem.*, 2016, **51**, 325-332.

34. C. R. Cantor and R. K. Scopes, *Protein Purification: Principles and Practice*, Springer, New York, 1994.

35. M. Kleiner, L. V. Hooper and B. A. Duerkop, *BMC Genomics*, 2015, **16**, 7.

36. C. Dika, C. Gantzer, A. Perrin and J. F. Duval, *Phys. Chem. Chem. Phys.*, 2013, **15**, 5691-5700.

37. K. S. Vijayaragavan, Doctor of Philosophy in Chemical Engineering Michigan Technological University, 2014.

38. V. Mautner, *Methods Mol. Med.*, 2007, **130**, 145-156.

39. A. Armanious, M. Aeppli, R. Jacak, D. Refardt, T. Sigstam, T. Kohn and M. Sander, *Environ. Sci. Technol.*, 2016, **50**, 732-743.

40. B. Michen and T. Graule, *J. Appl. Microbiol.*, 2010, **109**, 388-397.

41. J. Bae and K. J. Schwab, *Appl. Environ. Microbiol.*, 2008, **74**, 477-484.

42. D. J. Dawson, A. Paish, L. M. Staffell, I. J. Seymour and H. Appleton, *J. Appl. Microbiol.*, 2005, **98**, 203-209.

43. Y. Masago, T. Shibata and J. B. Rose, *Appl. Environ. Microbiol.*, 2008, **74**, 5838-5840.

44. J. H. Strauss, Jr. and R. L. Sinsheimer, *Journal of molecular biology*, 1963, **7**, 43-54.

45. R. Armisén and F. Gaiatas, in *Handbook of Hydrocolloids (Second edition)*, Woodhead Publishing, 2009, DOI: http://dx.doi.org/10.1533/9781845695873.82, pp. 82-107.

46. A. Nussinovitch, in *Hydrocolloid Applications: Gum technology in the food and other industries*, Springer US, Boston, MA, 1997, DOI: 10.1007/978-1-4615-6385-3_1, pp. 1-18.

47. J.-Q. Gao, Y. Eto, Y. Yoshioka, F. Sekiguchi, S. Kurachi, T. Morishige, X. Yao, H. Watanabe, R. Asavatanabodee, F. Sakurai, H. Mizuguchi, Y. Okada, Y. Mukai, Y. Tsutsumi, T. Mayumi, N. Okada and S. Nakagawa, *Journal of Controlled Release*, 2007, **122**, 102-110.

48. R. E. Baltus, A. R. Badireddy, A. Delavari and S. Chellam, *Environmental science & technology*, 2016, DOI: 10.1021/acs.est.6b05323.

49. C. Dika, J. F. Duval, H. M. Ly-Chatain, C. Merlin and C. Gantzer, *Appl Environ Microbiol*, 2011, **77**, 4939-4948.

50. C. Dika, M. H. Ly-Chatain, G. Francius, J. F. L. Duval and C. Gantzer, *Colloids and Surfaces A: Physicochemical and Engineering Aspects*, 2013, **435**, 178-187.

51. M. M. Fidalgo de Cortalezzi, M. V. Gallardo, F. Yrazu, G. J. Gentile, O. Opezzo, R. Pizarro, H. R. Poma and V. B. Rajal, *Journal of Environmental Chemical Engineering*, 2014, **2**, 1831-1840.

52. K. N. Parent, E. B. Gilcrease, S. R. Casjens and T. S. Baker, *Virology*, 2012, **427**, 177-188.

53. J. Langlet, F. Gaboriaud, C. Gantzer and J. F. Duval, *Biophysical journal*, 2008, **94**, 3293-3312.

54. C. J. Van Oss, *Interfacial forces in aqueous media*, Taylor & Francis, Boca Raton, Fla, 2006.

CHAPTER FOUR

Elution is a critical step for human adenovirus 40 recovery from tap and surface water by crossflow ultrafiltration

Abstract

This paper examines the recovery of enteric adenovirus HAdV 40 by crossflow ultrafiltration and interprets recovery values in terms of physicochemical interactions of virions during sample concentration. Prior to ultrafiltration, membranes were either blocked by calf serum (CS) or coated with a polyelectrolyte multilayer (PEM). HAdV 40 is a hydrophobic virus with a point of zero charge between pH 4.0 and pH 4.3. In accordance with prediction by the extended Derjaguin-Landau-Verwey-Overbeek theory, pre-elution recovery of HAdV, r_{pre}, from deionized water was higher with the PEM-coated membranes (r_{pre}^{PEM}= 74.8 ± 9.7%) than with CS-blocked membranes (r_{pre}^{CS} = 54.1 ± 6.2%). With either membrane type, the total virion recovery after elution, r_{post}, was high in both deionized water (r_{post}^{PEM} = 99.5 ± 6.6%; r_{post}^{CS} = 98.8 ± 7.7%) and tap water (r_{post}^{PEM} = 89 ± 15% and r_{post}^{CS} = 93.7 ± 6.9%). The nearly 100% recoveries suggest that the polyanion (sodium polyphosphate) and surfactant (Tween 80) in the eluent disrupt electrostatic and hydrophobic interactions between the virion and the membrane. Addition of ethylenediamine tetraacetic acid (EDTA) to the eluent greatly improved the elution efficacy (r_{post}^{CS} = 88.6 ± 4.3%; r_{post}^{PEM} = 87.0 ± 6.9%) from surface water even when organic carbon concentration in the water is high (9.4 ± 0.1 mg/L).

EDTA likely disrupts cation bridging between virions and particles in the feed water matrix or the fouling layer on the membrane surface. For complex water matrices, the eluent composition is the most important factor for achieving high virion recovery.

Importance

This study presents results of the first comprehensive physicochemical characterization of HAdV 40, an important human pathogen. The obtained data on HAdV 40 surface properties enabled rigorous modeling to understand energetics of virion-virion and virion-filter interactions. This is the first evaluation of crossflow filtration for concentration and recovery of HAdV 40 and the first study where HAdV 40 is recovered by crossflow filtration from practical water matrices. We demonstrate high HAdV 40 post-elution recoveries from ultrapure water (99%), tap water (~91%), and high carbon content surface water (~84%). These results are significant because of the very low adenovirus recoveries that have been reported to date for other methods. We interpret recovery data in terms of specific interactions and design the eluent composition accordingly to maximize HAdV 40 recovery.

4.1 Introduction

Pathogenic microorganisms cause many waterborne diseases, and the World Health Organization reports that water supply contamination leads to 842,000 deaths annually [1]. Along with caliciviruses (e.g. norovirus), enteroviruses (e.g. poliovirus,

coxsackievirus, echovirus), and Hepatitis A viruses, human adenovirus (HAdV) is one of the viral pathogens in EPA contaminant candidate lists 3 and 4 and is the second-leading cause of childhood gastroenteritis worldwide [2-4]. Most cases of adenovirus-associated gastroenteritis stem from HAdV serotypes 40 and 41 [5], which are relatively resistant to environmental stressors (e.g. they survive longer in the environment than poliovirus, Hepatitis A virus, and fecal indicator bacteria [6]) and treatment with UV irradiation [7]. Monitoring HAdV 40 and 41 levels is essential to better understand their fate in the environment and treatment systems, and eventually to prevent HAdV outbreaks. However, the low concentrations of HAdV in various natural waters,10^1 to 10^4 genome copies (GC) per liter in river and lake water [8-10] and 10^3 to 10^5 GC/L in wastewater treatment effluent [11, 12], make detection challenging and highlight the importance of sample concentration for rapid and reliable virus detection.

VIRADEL (virus adsorption-elution), the standard method for virus concentration, includes adsorption of virions on either electropositive or electronegative filters and subsequent elution of the adsorbed virions. Although recoveries by VIRADEL depend on the specific filter and eluent and vary greatly as a function of water composition, recoveries of adenoviruses are low relative to other viruses. For example, Gibbons et al. reported high recoveries of coliphages (96%) and noroviruses (100%) but very low recoveries of HAdV 41 (< 3%) when concentrating viruses from sea water using a NanoCeram filter and 3%wt beef extract as the eluent [13]. In another study, the coxsackievirus B5 recovery from tap water was 72%, whereas the recovery of HAdV 2 from the same water was only 39% [14]. Low recoveries of adenovirus may occur

because fibers associated with each penton base of the capsid facilitate the physical entrapment of virus particles in the filter matrix [13, 14]. McMinn achieved relatively high recovery of HAdV 40 with 1MDS filter (VIRADEL method) but the standard deviation was also high (49 ± 32%) [15].

Another virus concentration method, crossflow ultrafiltration (also called tangential flow filtration), relies on size exclusion, rather than adsorption, to concentrate virions during filtration and might give higher recoveries than the VIRADEL method. An ultrafiltration (UF) membrane with pores smaller than the virion allows passage of water and low molecular weight compounds while maintaining virions in the recirculating retentate stream. The crossflow should minimize membrane fouling and virion deposition onto the membrane. Yet, significant virion deposition on membranes in crossflow ultrafiltration system is still observed [16-19]. Similar to VIRADEL, elution of virions that adsorb to the UF membrane may be accomplished using reagents such as sodium polyphosphate (NaPP) and Tween 80 to disrupt electrostatic and hydrophobic interactions between virions and the membrane [18, 20, 21]. UF can concentrate a variety of viruses including bacteriophages (e.g. MS2 [20, 22], φX174 [20, 23], P22 [19]) and human pathogenic viruses (e.g. poliovirus [16, 24], echovirus [18], and norovirus [25]).

Crossflow filtration has three major advantages over VIRADEL: (1) lower cost of UF membranes compared to VIRADEL filters, (2) simultaneous concentration of multiple types of pathogens, and (3) removal of small compounds that may inhibit qPCR analysis. However, a fraction of the virions may still adsorb on the membrane to

decrease recoveries [26]. To enhance recovery, UF membranes are typically coated with proteinaceous solutions (e.g. calf serum) to block potential virion adsorption sites and reduce virion adhesion [16, 17, 20, 21]. However, long coating times and possible contamination during storage and transportation will limit the application of calf serum blocked (CS-blocked) membranes for rapid or field sampling [27]. In a previous study, to improve virion recovery during crossflow UF, we coated membranes with a polyelectrolyte multilayer (PEM) film prepared via rapid (<1 h) layer-by-layer adsorption of polycations (chitosan, CHI) and polyanions (heparin, HE). Compared with traditional CS blocking, the PEM-coated membranes showed higher recovery of bacteriophage P22 from both DI water and a membrane bioreactor effluent [19].

Despite the need for improved HAdV concentration and recovery, crossflow UF has not been comprehensively evaluated for this application. Pei et al. employed crossflow UF to recover viruses including HAdV 2 from tap water, but they coupled this process with VIRADEL. These authors reported 42.4% recovery of HAdV 2 by VIRADEL only, whereas they did not determine the recovery of HAdV 2 in crossflow UF [22]. Skraber et al. determined the recovery of MS2, φX174 and poliovirus in crossflow UF. They also processed environmental samples containing HAdV, but they did not know the initial concentration of HAdV and thus could not determine HAdV recovery [23]. Nestola et al. reported HAdV 5 recovery from pre-filtered virus stock after virus harvest [28]. Rhodes et al. examined recoveries of multiple viruses including enteroviruses, φX 174 and HAdV 41 from tap and river water by crossflow ultrafiltration; post-elution recoveries of HAdV 41 were 69.4 ± 12.4% from tap water and 55.8 ± 7.9% from river water while pre-elution

recoveries were not reported [29]. The authors concluded that in addition to size exclusion, other factors have an impact on the virus recovery process.

Characterization of adenovirus physicochemical properties is important for designing efficient methods for their concentration. Point of zero charge (PZC) values of adenoviral serotypes are available for HAdV 2 (PZC = 3.5 to 4.0 [30]) and HAdV 5 (PZC ~ 4.5 [31]) but not for the enteric HAdV 40 and HAdV 41. Moreover, no studies quantify the surface energies of HAdV 40 and HAdV 41 virions. Recently, Wong et al. computed the extended Derjaguin-Landau-Verwey-Overbeek (XDLVO) interaction energies of HAdV 2 [30], but the calculations used surface energy parameters of surrogates.

The goal of the present work is to improve HAdV recovery from water. We build on our earlier experimental and modeling study [19] to pursue two specific objectives: 1) elucidate specific physicochemical mechanisms that control HAdV 40 adhesion to a membrane surface and 2) evaluate crossflow UF for concentration and recovery of HAdV 40 from several water matrices. We employ two types of membranes to examine the effects of membrane properties on virion recovery. The approach includes comprehensive physicochemical characterization of HAdV 40, evaluation of virion-virion and virion-membrane interactions using the XDLVO, and crossflow filtration tests with feed waters spiked with HAdV 40. The premise of the study is that understanding virion interactions can guide process design for improving pre-elution and post-elution recoveries.

4.2 Materials and Methods

4.2.1 Reagents and water samples

All reagents were of ACS analytical grade or higher purity. Heparin (sodium salt), chitosan (medium molecular weight), calf serum, ethylenediaminetetraacetic acid (EDTA, 0.5 M in H_2O), diiodomethane, sodium chloride and sodium polyphosphate (NaPP) were purchased from Sigma-Aldrich (St. Louis, MO). Tween 80 was obtained from Fisher, and glycerol was purchased from J.T. Baker (Center Valley, PA). All solutions were prepared using deionized water (DI) water with a resistivity of 18.2 MΩ·cm (Barnstead NANOpure System, Dubuque, IA).

Tap water was supplied by the East Lansing-Meridian Water and Sewer Authority (East Lansing, MI) and used immediately after collection. Samples of surface water were collected from Lake Lansing at the boat ramp in Lake Lansing Park-South (Haslett, MI) in October 2013 and April 2014. Surface water samples were filtered through 0.45 μm membranes (mixed cellulose esters, Millipore, Billerica, MA) immediately after collection, stored at 4 ^{o}C and used within one week. All samples were characterized in terms of pH (Orion 3-Star Plus meter, Thermo Electron Corp., Waltham, MA), conductivity (Orion 550 conductivity meter, Thermo Electron Corp., Waltham, MA), total organic carbon (TOC) content, and concentrations of key cations. The TOC in each water sample was measured at least in triplicate (OI Analytical model 1010 analyzer, OI Analytical, College Station, TX). Concentrations of cations (Na^+, K^+, Mg^{2+}, and Ca^{2+})

were determined by inductively coupled plasma mass spectrometry (iCAP Q quadrupole ICP-MS, Thermo Scientific, Waltham, MA).

4.2.2 Human adenovirus 40: Propagation, purification and characterization

HAdV 40 (ATCC® VR-931™, Manassas, VA) was purchased from ATCC and propagated in A549 cells. The concentration of propagated virus, as measured by quantitative real-time polymerase chain reaction (qPCR), was 10^9 to 10^{10} GC/mL for all propagated batches. Virions were further purified using CsCl density-gradient centrifugation following the protocol described by Mautner [32]. The Supplemental Material (APPENDIX) file gives a detailed description of virus growth and purification procedures. *HAdV 40 is a human pathogen and should be manipulated following Biosafety Level 2 (BSL-2) criteria*.

HAdV 40 from the purified stock was used in all virion characterization tests. The hydrodynamic diameter of the virion was determined by dynamic light scattering (DLS, 90 Plus, Brookhaven Instruments Corp., Holtsville, NY), and the ζ-potential of the virion was calculated from phase analysis light scattering (ZetaPALS, Brookhaven Instruments Corp., Holtsville, NY). To study the effect of pH on the aggregation state and ζ-potential of HAdV 40 virion, the solution pH was adjusted by the addition of NaOH and HCl, and a 1 mM NaCl solution served as the background electrolyte at all pH values except 7.6. The pH of an unbuffered NaCl solution could not be stabilized at pH

7.6, so a solution of 10 mM Tris-HCl and 1 mM EDTA (the recommended buffer for the storage of purified HAdV 40 [32]) was used as the background electrolyte.

Transmission electron microscopy (TEM) was used to image HAdV 40. A few drops of purified virus stock were applied to a carbon-coated Formvar grid (Ted Pella, Redding, CA). Sample was rested on the grid for 1 min and washed away by drops of water. 1% uranyl formate was then used to stain the grid and excess stain was removed by filter paper. Grid was dried prior to TEM imaging. Images were recorded using a JEM-2200FS (JEOL, Tokyo, Japan) microscope with an in-column energy filter operated at 200 kV and equipped with a Direct Electron DE-20 camera.

The surface energy of HAdV 40 was determined using a protocol described previously [19]. Briefly, a virion lawn with ~ 7 layers of virions was prepared on a 30 kDa polyethersulfone membrane (Omega, Pall Corp., East Hills, NY) by filtering purified virion stock through the membrane. The virion-coated membrane was dried at room temperature until the water contact angle on the virion lawn plateaued, indicating formation of a monolayer of strongly bound water that resists evaporation. Contact angles of three probe liquids (DI water, glycerol and diiodomethane) on the virion lawn were then measured with a goniometer (model 250, ramé-hart, Succasunna, NJ) using the sessile drop method to determine surface energy components of HAdV 40.

4.2.3 XDLVO energy of virion-virion and virion-membrane interactions

XDLVO energy profiles were calculated (see APPENDIX, section S6, for details) using the surface properties (charge and energy) of HAdV 40 and membranes. Membranes were characterized in our previous study [19].

4.2.4. Membrane preparation

Prior to modification, polyethersulfone membranes (Omega, Pall Corp., East Hills, NY) with a molecular weight cutoff of 30 kDa were soaked in 0.1 M NaOH for 3 h and then in DI water for 24 h at 4 oC with water exchange after 12 h, as recommended by the manufacturer. To coat the membrane with a PEM, 1 mg/mL HE and 1 mg/mL CHI solutions were prepared in 0.15 M NaCl and adjusted to pH 5 using 1 M HCl and 1 M NaOH. Both polyelectrolyte solutions were stored at 4 oC until use. The surface of the polyethersulfone membrane was alternately exposed to each polyelectrolyte solution for 5 min with a 1 min DI water rinse between exposures. The deposition was initiated with the negatively charged HE. Alternating deposition of HE and CHI continued until 4.5 bilayers were obtained with HE as the outmost (terminal) layer. To block a membrane with calf serum, the membrane was placed in a crossflow filtration cell, and 500 mL of 5% (v/v) calf serum was circulated over the membrane overnight at 1.0 L/min at room temperature with no pressure applied across membrane. After blocking, the membrane was rinsed with DI water twice at the same rate for 10 min. The PEM-coated and CS-

blocked membranes were characterized in terms of charge and surface energy as described earlier 19.

4.2.5. Virus concentration and recovery tests

Virions were recovered from DI water, tap water and surface water. Prior to recovery experiments, 1 L water samples spiked with 1 mL of HAdV 40 stock (virion concentration of ~10^6 to 10^7 GC/mL in the diluted solution) were recirculated in the filtration system without a membrane and with the permeate port blocked. The virus concentration in the feed tank was quantified after 1 hour of recirculation (approximate time needed for filtration) and compared with that in the feed initially. No difference in virus concentration was observed, indicating that no loss of virion to the filtration apparatus. The APPENDIX shows the schematic of the crossflow filtration apparatus (Figure 17). The membrane was placed in the crossflow cell (CF042P, Sterlitech, Kent, WA) and compacted for 90 min at 40 psi (~ 276 kPa). A 1 L water sample was spiked with 1 mL of HAdV 40 stock (resulting in the virion concentration of ~10^6 to 10^7 GC/mL in the diluted solution) and 5 mL was collected to quantify virions in feed sample. 996 mL remaining sample was pressurized using compressed N_2 gas and delivered to the membrane cell using a peristaltic pump (model 621 CC, Watson Marlow, Wilmington, MA) at 2.0 L/min. A digital flow meter (101-7, McMillan, Georgetown, TX) monitored the crossflow rate. The transmembrane pressure was maintained at ~ 20 psi (~ 138 kPa) and continually monitored by a pressure transducer (0.5-5.5 V output, Cole Parmer, Vernon Hills, IL). The ratio of the crossflow flux to the initial permeate flux, J_{cf}/J_p,

ranged from $5 \cdot 10^3$ to $6 \cdot 10^3$. Permeate was collected into a flask placed on a digital balance (Adventurer Pro AV8101C, Ohaus, Parsippany, NJ), and the permeate mass was recorded in real time to calculate the flux. The data from the pressure transducer, digital flow meter and digital balance were transmitted to the computer via a data acquisition module (PCI-6023E/SC-2345, National Instruments, Austin, TX). Filtration was stopped when 900 mL were filtered. The remaining 100 mL of the retentate were analyzed for virus content so that pre-elution recovery could be calculated.

After filtration, virions were eluted off the membrane using eluent containing 0.01% NaPP and 0.01% Tween 80 (pH 6.5). For virion concentration and recovery from lake water, another eluent containing 0.01% NaPP, 0.01% Tween 80 and 0.01% EDTA (pH 7) was also employed. Elution was performed at a crossflow rate of 2.0 L/min with no transmembrane pressure applied. Feed, permeate, retentate and eluate were all analyzed for virion concentration. Samples were also taken during membrane compaction to ensure that virions did not contaminate the feed water prior to the experiment.

4.2.6 Virus quantification and recovery

DNA of HAdV 40 in water samples was extracted with a MagNA Pure Compact System (Roche Diagnostics USA, Indianapolis, IN) immediately after sample collection. qPCR was used to determine HAdV 40 concentration (see APPENDIX, section A.2, for a description of qPCR procedures). Possible effects of organic compounds in the feed

water on virion quantification by qPCR were evaluated by performing inhibition tests. Virion pre-elution recovery (r_{pre}), post-elution recovery (r_{post}) and log removal (LRV) were calculated using the following equations:

$$r_{pre} = \frac{C_r V_r}{C_f V_f}, \quad (4\text{-}1)$$

$$r_{post} = \frac{C_r V_r + C_e V_e}{C_f V_f}, \quad (4\text{-}2)$$

$$LRV = log_{10}\left(\frac{C_f + C_r}{2C_p}\right). \quad (4\text{-}3)$$

where C_f, C_r, C_e, and C_p represent virion concentrations in feed, retentate, eluate and permeate samples, respectively, and V_f, V_r, V_e, V_p are the volumes of these samples. In calculating the LRV (equation (4-3)), the virus concentration in feed was calculated by averaging the initial concentration of HAdV 40 in feed prior to filtration and the concentration of the virus in retentate after filtration: $\overline{C_f} = \frac{1}{2}(C_f + C_r)$. Thus, the reported virus removal (LRV) is the value averaged over the entire filtration process.

4.3 Results and Discussion

4.3.1 Characteristics of source waters

Table 10 provides water quality parameters for the DI water, tap water, and Lake Lansing water (sampled in spring and fall). The biggest differences among the waters are 1) much lower values of TOC, conductivity and cation concentrations in DI water and 2) high TOC and Ca^{2+} concentrations in the Lake Lansing water samples.

Table 10. Water quality characteristics.

Water source	pH range	Conductivity (µS/cm)	TOC (mg/L)	Cation concentration (mg/L)			
				Na^+	K^+	Mg^{2+}	Ca^{2+}
Deionized water	5.7 to 6.0	n/a[#]	n/a[#]	0.18 ± 0.00	0.02 ± 0.00	0.04 ± 0.00	0.06 ± 0.00
Tap water	7.5 to 8.0	319.5 ± 27.6	1.1 ± 0.1	22.18 ± 2.33	9.32 ± 0.32	1.86 ± 0.09	24.37 ± 1.83
Lake water (fall)	7.0 to 7.5	336.3 ± 12.7	7.5 ± 0.2	16.42 ± 2.53	10.91 ± 0.11	1.47 ± 0.03	30.33 ± 0.54
Lake water (spring)	7.5 to 7.8	369.3 ± 32.0	9.4 ± 0.1	16.46 ± 2.60	11.54 ± 0.20	1.50 ± 0.03	41.09 ± 0.72

[#] below detection limit.

4.3.2 Physicochemical properties of HAdV 40: Size, ζ-potential and surface charge density

Coliphages commonly serve as surrogates for human viruses [33]. However, studies on virus removal and adsorption show that coliphages (e.g. MS2 [34, 35], φX174 [34, 35], and PRD1 [34]) are not suitable models for HAdV. Moreover, unique properties of serotypes 40 and 41 of enteric HAdV (e.g. the presence of short and long fibers on the capsid [36, 37], fastidiousness in cell culture [38-40] (though cultivation improvement was reported with modified host cell line [41, 42]), and difficulty of isolation [40, 43]) make them different from other HAdV serotypes.

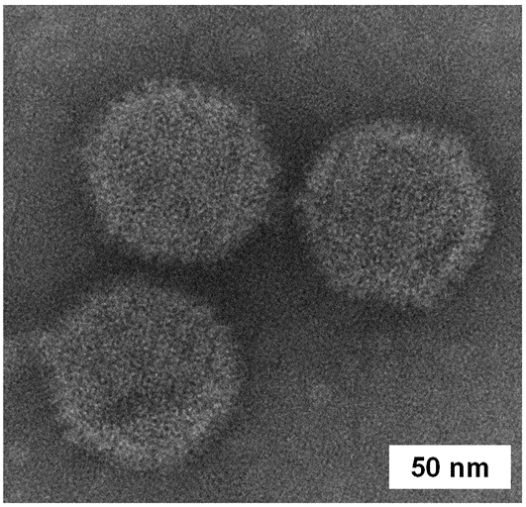

Figure 7. Transmission electron microscopy image of HAdV 40.

This uniqueness makes detailed characterization of HAdV 40 and 41 necessary. Aggregation state and ζ-potential as functions of pH were reported for HAdV serotype 2 [30], but not for HAdV 40. In this study, we measured HAdV 40 size by dynamic light

scattering and compared these data with the results of TEM imaging. We also determined the ζ-potential and surface charge density of the virion as functions of pH.

Based on TEM images (e.g. Figure 7), the diameter of HAdV 40 is ~ 80 nm. Figure 8 shows the number-based hydrodynamic diameter distribution of HAdV 40 as a function of pH, and Table 11 summarizes the hydrodynamic diameters over a wide range of pH values. At pH 5.8 (unadjusted), pH 6.7 and pH 7.6, the number-based average hydrodynamic diameters of HAdV 40, $\bar{d}^{h}_{HAdV}$, ranged from 94 ± 3 nm to 102 ± 9 nm, which agrees with typical size values reported earlier for HAdV of different serotypes [44-46]. The small increase in the hydrodynamic diameter relative to the diameter determined by TEM could stem from fibers on the HAdV 40 surface [30, 47] that we do not take into account when estimating HAdV 40 diameters from TEM images. Such fibers should, however, decrease particle diffusivity in light-scattering experiments. Additionally, shrinkage of HAdV 40 during negative staining may decrease the diameters observed in TEM images [48]. The polydispersity index of the particle diameters in the HAdV 40 suspensions at pH 5.8, 6.7, and 7.6 was 0.06 to 0.07, indicating minimal aggregation. However, between pH 4.0 and 4.7 both average size and polydispersity increased, consistent with aggregation. Aggregates up to 1 µm in size appeared at pH 4.0 and 4.3 in several measurements. In contrast to aggregation between pH 4.0 and 4.7, at pH 2.8 the virion hydrodynamic diameter is only 112 ± 20 nm, suggesting minimal aggregation. This is consistent with studies showing that the enteric adenovirus remains infective in the acidic conditions in the gut [49, 50]. A high positive ζ-potential at low pH (Figure 9) probably minimizes aggregation. At pH 9.7 the

average hydrodynamic diameter of HAdV 40 (80 ± 5 nm) was significantly lower than values measured at pH values from 5.8 to 7.6 and close to the size determined by TEM imaging. A previous study observed inactivation of adenovirus after liming [51, 52], and the reduced size at pH 9.7 may stem from virus degradation. Size reduction at pH 10 also occurred with HAdV 2 [30].

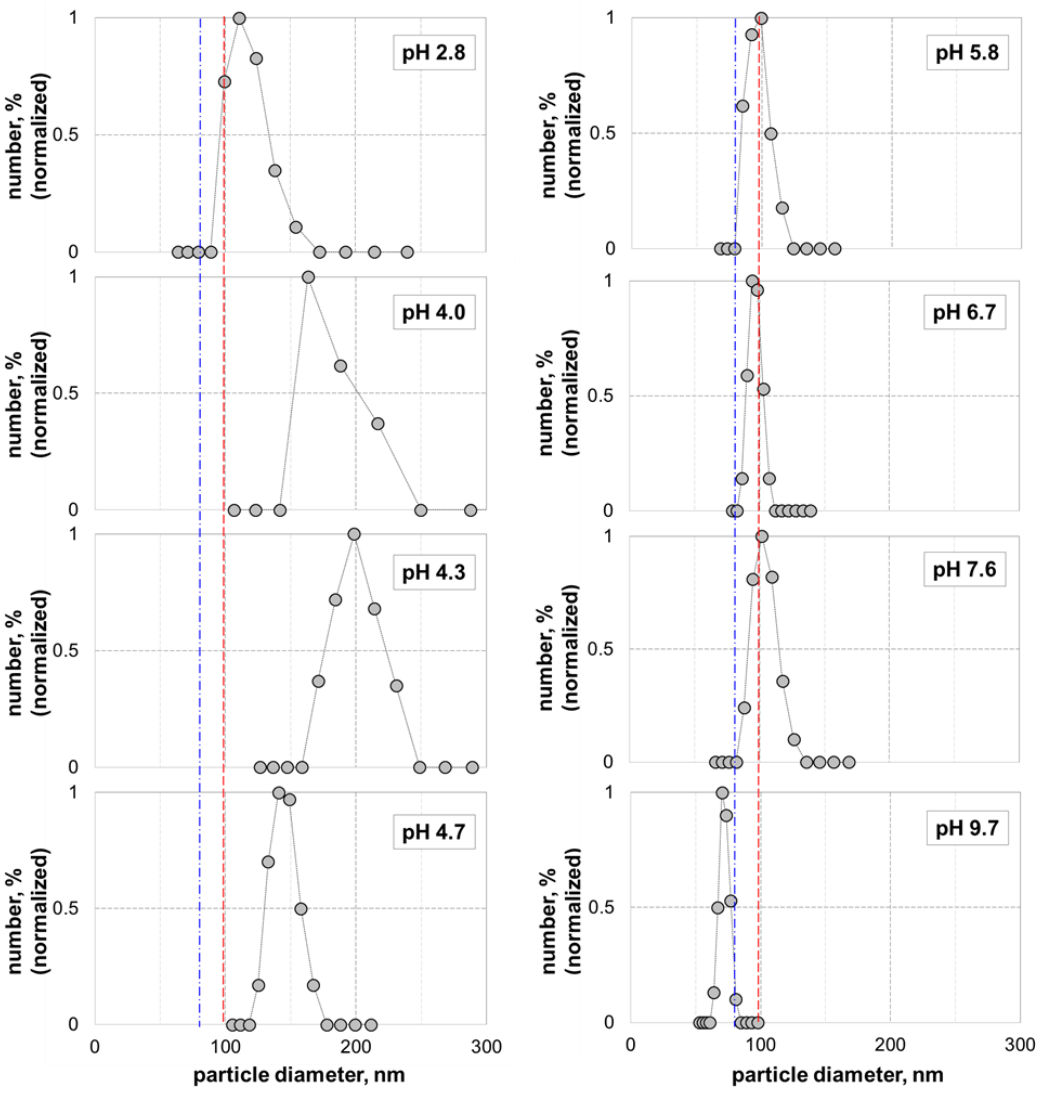

Figure 8. Normalized number-based size distribution of HAdV 40 as a function of pH. Vertical red dashed lines indicate the average modal diameter (99 nm, see APPENDIX, Table 15) in the buffer recommended for the storage of purified HAdV 40 (10 mM Tris-HCl and 1 mM EDTA, pH 7.6). Vertical blue dash-dot lines denote the average HAdV diameter (~ 80 nm) as determined by TEM. The APPENDIX shows the HAdV 40 size distribution in tap water (Figure 20).

Table 11. Parameters of HAdV 40 size distributions at different pH values [a]. Shaded (gray) areas denote pH values where significant aggregation occurs.

Water matrix	**1 mM NaCl**						**buffer [b]**	**tap water**	**1 mM NaCl**
pH	**2.8**	**4.0**	**4.3**	**4.7**	**5.8**	**6.7**	**7.6**	**7.5 to 8.0**	**9.7**
$\bar{d}^{h}_{HAdV}$ **(nm)**	112 ± 20	284 ± 99	238 ± 69	149 ± 3	94 ± 3	95 ± 3	103 ± 9	109 ± 14	80 ± 5
Polydispersity	0.22 ± 0.06	0.31 ± 0.04	0.31 ± 0.01	0.10 ± 0.01	0.06 ± 0.01	0.07 ± 0.02	0.07 ± 0.01	0.11 ± 0.01	0.12 ± 0.03

Note:
a. Additional parameters - modal diameter and half width and half maximum – are given in the APPENDIX (Table 15)
b. 10 mM Tris-HCl and 1 mM EDTA (buffer recommended for the storage of purified HAdV 40).

Figure 9 present the virion ζ-potentials determined from electrophoretic mobilities (see APPENDIX, Figure 23) using an approximate expression derived by Ohshima [53]; the expression provides an accurate (<1% error) estimate for ζ-potentials for arbitrary values of κa, where a is the radius of the virion and κ is the Debye-Hückel parameter (see APPENDIX, section A.9). Due to the large virion diameters, Smoluchowski's expression for electrophoretic mobility, applicable for $\kappa a \gg 1$, is not accurate. Thus, we used Ohshima's expression.

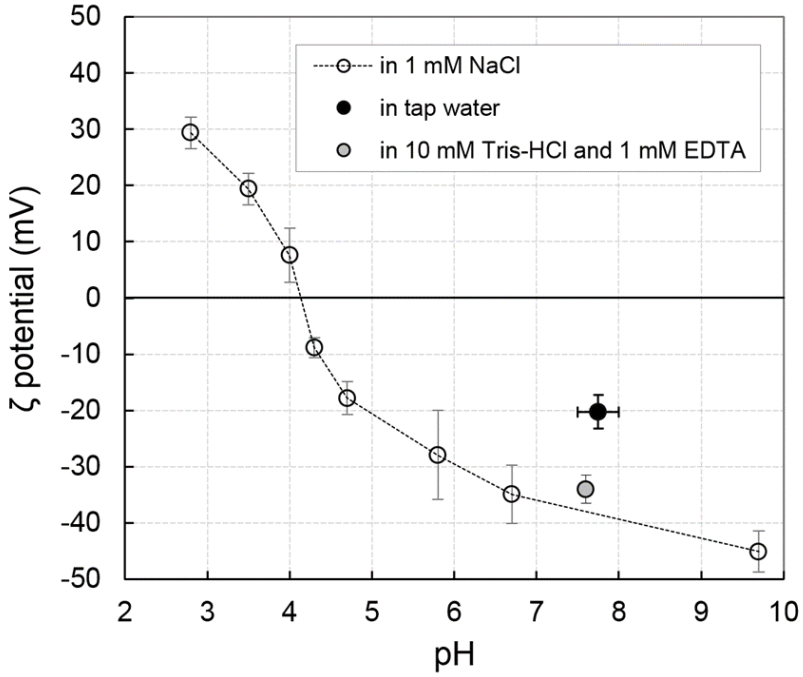

Figure 9. ζ-potential of HAdV 40 as a function of pH.

The ζ-potential increased from -22.0 mV to -30.5 mV when the pH increased from 5.8 to 7.6. The negative surface charge on the virion likely minimizes aggregation, but for several measurements in this pH range some aggregates (300 to 350 nm, 1.2 ± 0.5% of the total population) appeared, possibly as an artifact of the dialysis process [32].

Relatively small absolute values of the ζ-potential between pH 4.0 and 4.7 probably allow for the extensive aggregation described above.

As Figure 9 shows, the PZC of HAdV 40 particles is between pH 4.0 and 4.3. Favier et al. predicted the theoretical PZC of each major capsid protein of HAdV 40 using their primary sequences and showed that the PZC values of hexon, penton base, long fiber protein and short fiber protein were ~ 6.7, 5.8, 7.5 and 7.8, respectively [49]. All of these values are higher than the HAdV 40 PZC we determined, which is consistent with prior observations that the PZC of an intact virion is lower than the PZC values of its structural protein components [54]. PZC values were reported to be in the 3.5 to 4.0 range for HAdV 2 [30] and 4.5 for HAdV 5 [31], consistent with the low PZC of HAdV 40.

At pH values where virions aggregate, the measured ζ–potential is that of an aggregate of virions, and not a single virion. In this case, we calculated virion ζ–potentials using an expression developed by Makino and Ohshima [55]; the expression connects the surface charge density of a particle with its ζ–potential, diameter, and Debye length (see APPENDIX, section A.10). The calculation assumed that surface charge density is an intensive property and does not depend on the aggregation state of the virion in the same solution.

The average ζ-potential of HAdV 40 in tap water (pH 7.5 to 8.0) was -17.7 mV, which is much smaller than the ζ-potential (-30.5 mV) of HAdV 40 in a buffered solution with a

similar pH (pH 7.6). The difference could stem from specific adsorption of divalent or multivalent ions onto virions in tap water.

4.3.3 Surface energy components of HAdV 40

To determine the surface energy components of HAdV 40, we applied the procedure we developed previously for examination of P22 bacteriophage [19]. The technique includes measuring the contact angles of several liquids on a lawn of virions. As Table 12 shows, the apolar surface energy component (γ^{LW}) of HAdV 40 was 41.6 mJ/m^2, a value typical for biological materials [56]. The electron donor (γ^-) and electron acceptor (γ^+) components of surface energy were 14.7 mJ/m^2 and 0.01 mJ/m^2, respectively, making the polar component of HAdV 40 surface energy, $\gamma^{AB} = 2\sqrt{\gamma^+\gamma^-}$, equal to 0.84 mJ/m^2. Very small values of γ^+ were also reported for tobacco mosaic virus [56], bacteriophage P22 [19] and multiple proteins [56], suggesting that this is a common characteristic of proteins and non-enveloped viruses.

Based on values of γ^{LW}, γ^+ and γ^- for water and HAdV 40, the calculated polar adhesion energy between HAdV 40 and water is 79.7 mJ/m^2 which is insufficient to overcome the energy of cohesion of water (-102.0 mJ/m^2). As a result, virion-virion interactions for HAdV 40 in water have a negative interfacial free energy (ΔG_{vwv} = -30.4 mJ/m^2), so HAdV 40 is hydrophobic.

Table 12. Contact angles, calculated surface energy parameters and the enerinterfacial interaction when immersed in water for HAdV 40.

Contact angle with probe liquid (^{0})			Surface energy parameters (mJ/m^2)					Free energy of interfacial virion-virion interaction in water, ΔG_{vwv} (mJ/m^2)
H_2O	Glycerol	DIM[#]	γ^{LW}	γ^+	γ^-	γ^{AB}	γ^{TOT}	
68 ± 2	64 ± 1	36 ± 2	41.6	0.01	14.7	0.8	42.4	-30.4

4.3.4. XDLVO energy profile of virion-virion interfacial interaction in aqueous media

Several studies suggest that the classic Derjaguin-Landau-Verwey-Overbeek theory does not accurately predict the interaction between colloids and various surfaces in aqueous media because the calculations do not account for acid-base interactions that dominate at short separation distances [57, 58]. In the present study, we employ the extended DLVO model to evaluate virion-virion and virion-membrane interfacial interactions. Inputs to the model include the surface characteristics of HAdV 40 (see sections 3.2 and 3.3) and membranes [19].

Figure 10 shows XDLVO energy profiles of virion-virion interfacial interactions at different pH values. For all pH values except 7.6, the calculations were performed for HAdV in 1 mM NaCl. For pH 7.6, size and zeta potential values used in XDLVO calculations were for virions in the recommended buffer (1 mM EDTA + 10mM Tris). For pH values > 5.8, the height of the energy barrier increases with pH with the sole

exception of pH of 7.6. The deviation from the trend is due to the different background solution used (10 mM Tris and 1 mM EDTA instead of 1 mM NaCl; see section 3.2). Negligible aggregation of virions for pH ≥5.8 is due to the high energy barrier (from 24.5 kT to 52.6 kT). At pH 4.7 where the energy barrier is 8.0 kT, significant aggregation occurs. At pH 4.0 and pH 4.3, the energy barrier decreases to below 1.2 kT leading to further aggregation. Due to the high positive ζ-potential (29.4 mV) at pH 2.8, the energy barrier is 20.7 kT and the virion suspension is stable.

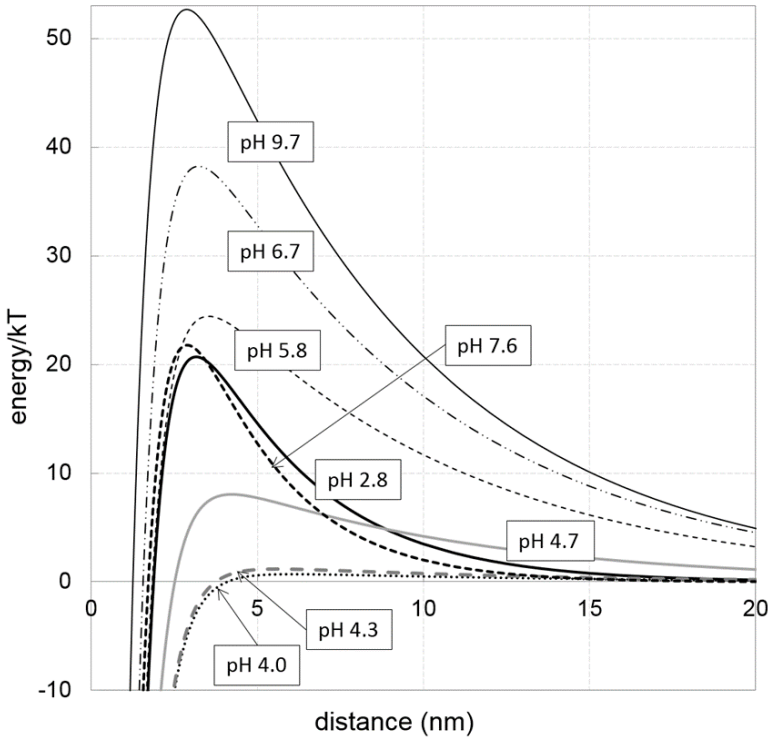

Figure 10. XDLVO energy profile of virion-virion interfacial interactions in 1 mM NaCl a for HAdV 40 at different pH values. (For pH 7.6, size and zeta potential values used in XDLVO calculations were for virions in the recommended buffer (1 mM EDTA + 10mM Tris), and not in 1 mM NaCl.)

4.3.5 XDLVO energy of virion-membrane interfacial interaction in membrane feed solutions: DI water and tap water.

XDLVO calculation of virion-membrane interactions in DI water were performed for an ionic strength of 0.2 mM; this is the approximate ionic strength determined from conductivity measurements of DI water spiked with HAdV 40 stock. However, the streaming potential of the membrane could only be measured in 1 mM NaCl electrolyte, so this value was used to approximate the membrane charge in the HAdV-spiked DI water. The approximation is reasonable because the electrophoretic mobility of virions measured in DI water (-1.65 ± 0.19 $\mu m \cdot S^{-1} \cdot V^{-1} \cdot cm$; pH 5.8) and in 1 mM NaCl solution (-1.72 ± 0.48 $\mu m \cdot S^{-1} \cdot V^{-1} \cdot cm$; pH 5.8) were not statistically different.

At separation distances > 5 nm, van der Waals or electrostatic interactions dominate the XDLVO energy of interfacial interaction between HAdV 40 and membranes in both DI and tap water (see APPENDIX, Figures 21 and 22). However, as the separation distance increases, the magnitude of each interaction decreases. The magnitude of van der Waals interaction energy, for example, decreases to less than 0.5 kT as the separation distance increases to approximately 15 nm. Over a shorter range (from the minimum equilibrium cut-off distance of ~ 0.16 nm to 0.7 nm), however, the acid-base interaction energy is significantly greater than both van der Waals and electrostatic interaction energies. In 1 mM NaCl at pH=5.8 (unadjusted), the PEM-coated membrane is negatively charged (ζ = -7.0 ± 3.0 mV [19]). Due to the hydrophilicity of the PEM as well as a repulsive electrostatic interaction between the virion and the membrane

surface, the secondary minimum in the membrane-virion interaction energy profile is shallow (-4.2 kT) (Figure 11A, solid line). The same membrane carries a positive charge (ζ = 5.6 ± 0.4 mV) in tap water. The charge reversal could stem from specific adsorption of various cations from tap water onto the membrane surface, and a similar charge reversal occurred with latex particles as the solution ionic strength increased [59, 60]. For the membrane-virion interaction energy profile in tap water, electrostatic attraction coupled with van der Waals attraction at large separation distances and a predominant repulsive acid-base interaction at small separation distances yields a -10.3 kT secondary minimum at the separation distance of 3.2 nm (Figure 11A, dashed line). This secondary minimum may lead to reversible adsorption of HAdV 40 onto the membrane surface during tap water filtration.

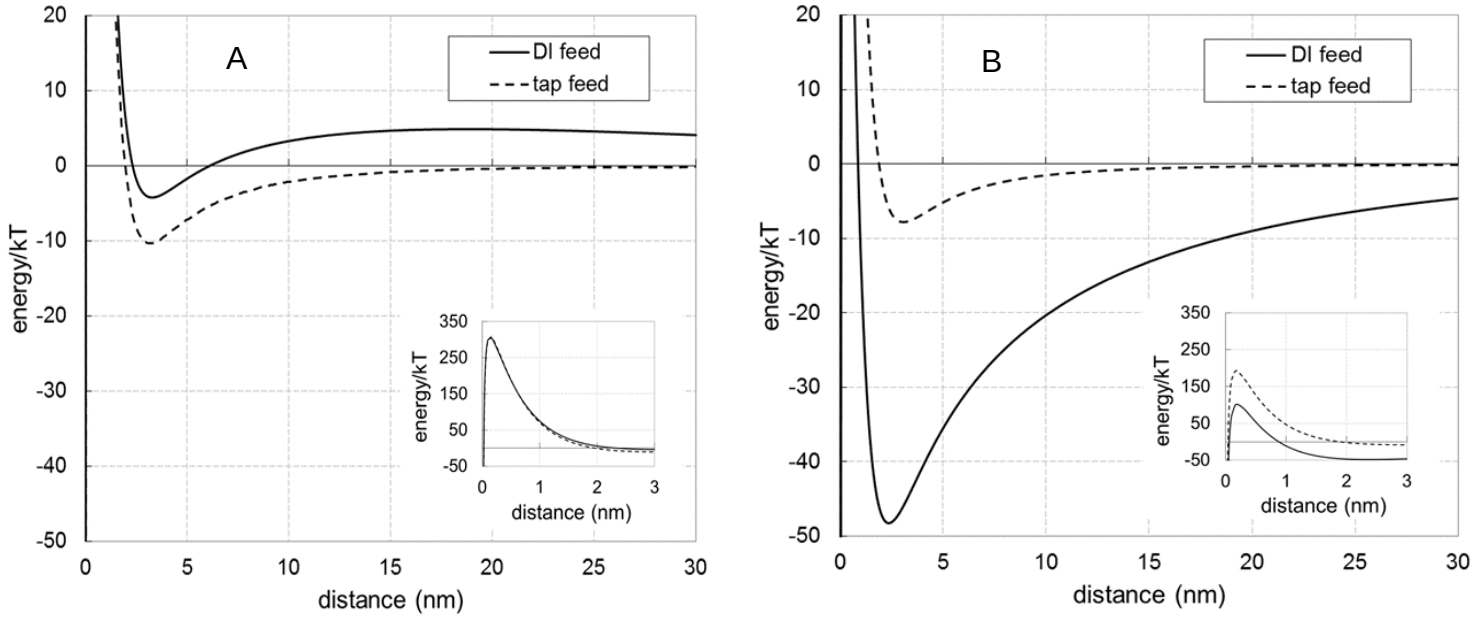

Figure 11. XDLVO energy of interfacial interaction of HAdV 40 in aqueous media with a PEM-coated membrane (A) and a CS-blocked membrane (B). The energies were calculated from surface parameters determined at pH 5.8.

Even though the PZC of bovine serum albumin, a major component of calf serum, is in the 4.7 to 5.6 range [61-63], CS-blocked membranes in 1 mM NaCl solution at pH=5.8 (unadjusted) carry a weak positive charge (ζ =3.0 ± 2.0 mV) [19]. The small positive charge on these membranes may stem from other components in calf serum such as bovine IgG (PZC range from 7.5 to 8.3 [64]). The XDLVO energy profile for the interaction of an HAdV 40 virion and a CS-blocked membrane shows a -48.2 kT secondary minimum at a separation distance of 2.4 nm (Figure 11B, solid line), which suggests deposition of a significant amount of virion.

In tap water, the ζ-potential of CS-blocked membranes was 2.8 ± 1.0 mV, similar to that in 1 mM NaCl. Compared with experiments in 1 mM NaCl, the reduced negative charge of HAdV 40 in tap water (see Figure 9) leads to lower virion-membrane electrostatic attraction, and the depth of the secondary minimum in tap water is only -7.9 kT for interactions of the virion and the CS-blocked membrane (Figure 11B, dashed line).

4.3.6 Virus recovery from DI water

Pre-elution virion recovery (see eq. (1)) after crossflow UF of DI water spiked with virions was significantly greater with a PEM-coated membrane (74.8 ± 9.7%) than with a CS- blocked membrane (54.1 ± 6.2%). The higher recovery likely stems from the negative charge and hydrophilicity of the PEM-coated membrane [19]. However, the <100% recovery indicates that some virion adsorption takes place on the PEM-modified membrane even though the secondary minimum in the XDLVO energy profile is shallow

(Figure 11A, solid line). This adsorption may stem from microscale attraction [56, 65], whereas XDLVO theory describes only macroscopic interactions. For example, in experiments on *B. cepacia* adhesion Hwang et al. reported bacterial adhesion in the absence of a secondary minimum in the XDLVO energy profile and suggested the adhesion stems from cell appendages such as pili and flagella [66]. HAdV 40 fibers, which consist of long, thin shafts terminated with globular knobs, may extend beyond the characteristic length of macroscopic repulsion (~ Debye length) to achieve microscopic attraction between a virion and a membrane. Interactions such as those between electron donor sites on the fiber knob and electron acceptor sites on the membrane may overcome the macroscopic repulsion and lead to local attraction. Debye lengths for HAdV 40 at different pH values in 1 mM NaCl (see APPENDIX, Table 14) are smaller than the length of both longer and shorter fibers (~ 30 nm and ~ 18 nm, respectively [36]) on HAdV 40. In HAdV-spiked DI water, the Debye length is ~ 23 nm (see APPENDIX, Table 14) still smaller than 30 nm HAdV fibers. Other possible explanations for the incomplete pre-elution recovery with PEM-coated membranes include local electrostatic attraction due to charge heterogeneity and the presence of non-XDLVO interactions (e.g. bridging by multivalent cations).

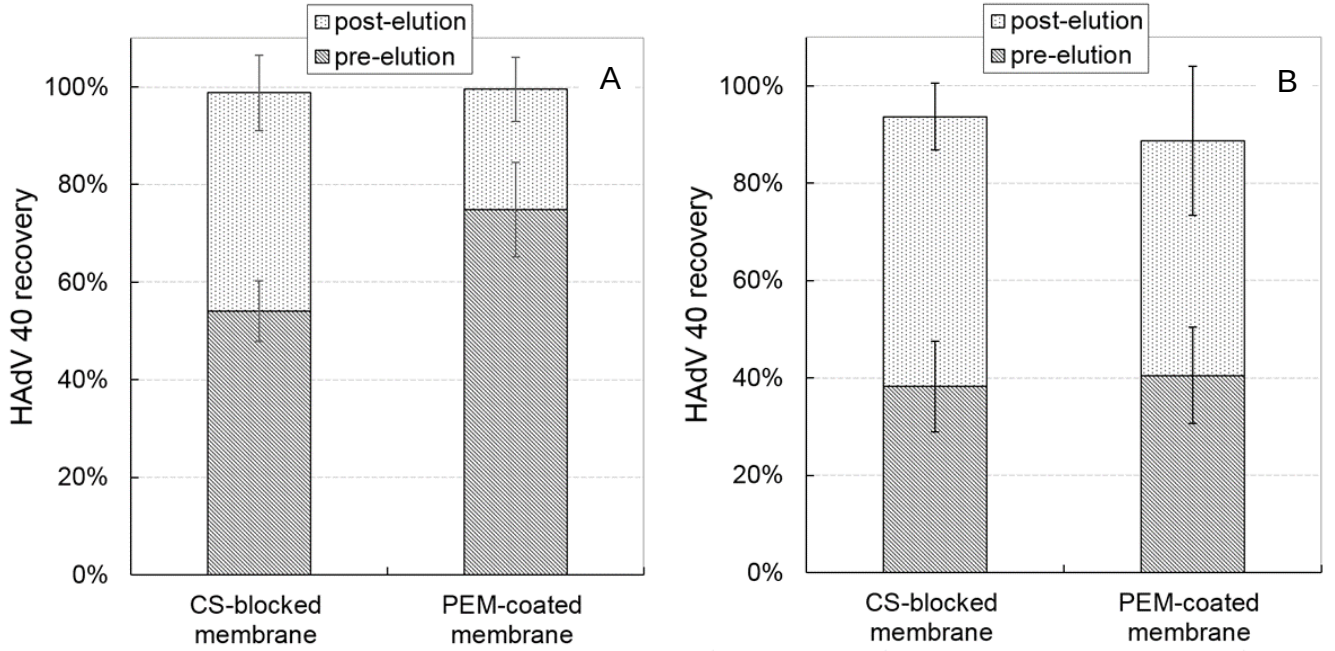

Figure 12. Recovery of HAdV 40 with CS-blocked and PEM-coated membranes from HAdV-spiked deionized water (A) and tap water (B).

The relatively low virion recovery from DI water after crossflow UF with CS-blocked membranes likely stems from the secondary minimum in the XDLVO energy profile (Figure 11B, solid line). The secondary minimum is sufficiently deep (-48.2 kT) to capture virions with an average thermal energy of ~ 0.5 kT [67]. The fact that pre-elution recovery after crossflow UF is higher with PEM-coated membranes than with CS-blocked membranes is consistent with our previous findings for crossflow filtration of bacteriophage P22 in DI water, where PEM-coated membranes gave significantly higher pre-elution recovery (80%) than CS-blocked membranes (30%) [19].

After filtration, we eluted virions to increase recovery. For both PEM-coated and CS-blocked membranes, eluents containing 0.01% NaPP and 0.01% Tween 80 give high post-elution recoveries (see eq. (2)) of 99.5 ± 6.6% for PEM-coated membranes and 98.8 ± 7.7% for CS-blocked membranes. During elution, adsorption of NaPP on the membrane likely increases the negative charge on the surface to enhance electrostatic repulsion between the negatively charged virion and the membrane. Additionally, Tween 80, a nonionic surfactant, should minimize hydrophobic interactions between the membrane surface and adsorbed virion. Thus, both NaPP and Tween 80 could help release the virion from the membrane.

The relatively high feed concentration of adenovirus (~10^6 to 10^7 GC/mL) in our study may lead to a higher recovery and a smaller variance than filtration of lower virion concentrations because at high concentrations the virion may saturate sorption sites. However, we had to use a relatively high virion concentration to accurately quantify the

low concentration of virions in the permeate (and further quantify both virion removal and the fraction of the virion adsorbed on the membrane). The HAdV 40 removal was high with both CS-blocked membrane (LRV up to 2.17) and PEM-coated membrane (LRV up to 4.64), so the permeate concentration was much lower than the feed concentration.

4.3.7 Virus recovery from tap and surface water

We also evaluated the HAdV 40 recovery from tap water and from lake water collected in two different seasons. Because organic molecules in surface waters may inhibit qPCR detection of virions, [68, 69] we initially performed inhibition tests (see APPENDIX, section A.5 for details). Briefly, DI, tap and surface water samples were spiked with HAdV 40 from the stock suspension, viral DNA was extracted, and the virion concentration in each water matrix was determined by qPCR. Consistent with minimal qPCR inhibition, we observed no differences in virion concentrations in the three water matrices.

With tap water, we saw no statistically significant difference in pre-elution virion recovery after crossflow UF with PEM-coated membranes (40.5 ± 9.9%) and with CS-blocked membranes (38.3 ± 9.3%). Based on XDLVO predictions for CS-blocked membranes (Figure 11B), the pre-elution recovery from tap water should be higher than from DI water. However, the opposite occurred – for CS-blocked membranes, the average pre-elution recovery from tap water was ~ 16% lower than from DI water

(Figure 12). The discrepancy suggests that non-XDLVO effects (e.g. steric interactions [70] or Ca^{2+} bridging [71]) should be considered. Another possible cause for the discrepancy is virion adsorption to dissolved and suspended species present in the tap water (TOC = 1.1± 0.1 mg/L) and on the membrane surface. Permeate flux declined ~ 15% to 20% during crossflow UF of tap water (see APPENDIX, Figure 18) suggesting the formation of a fouling layer on the membrane surface.

The pre-elution recovery from tap water after crossflow UF with the PEM-coated membrane was ~ 34% lower than from DI water (Figure 12). In addition to the possible effects described above for the CS-blocked membranes, charge reversal of the PEM membrane in tap water may decrease the pre-elution recovery. Pre-elution recovery from tap water has a larger variance, ranging from 30% to 50% for both types of membranes. Such variances likely stem from variations in tap water quality over several months of sample collection and tests.

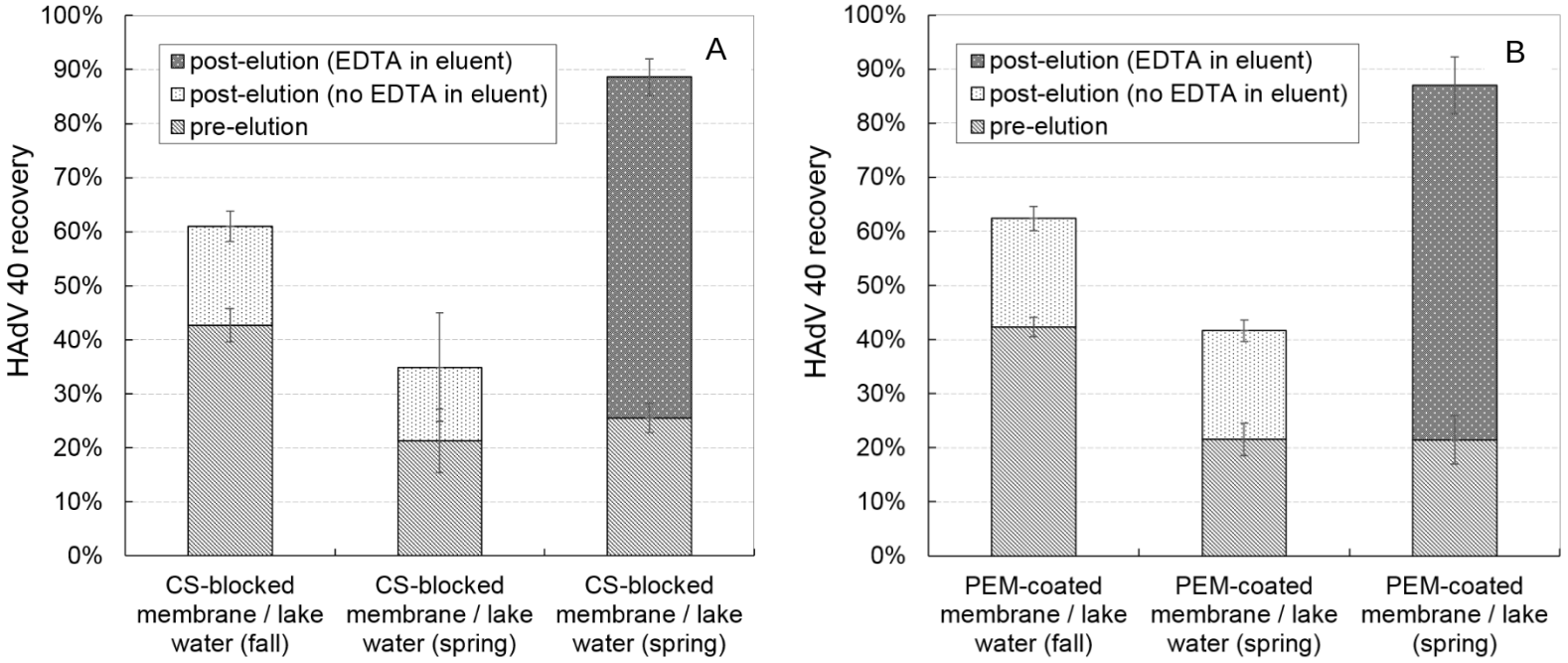

Figure 13. Recovery of HAdV 40 from surface water after crossflow UF with CS-blocked membranes (A) and PEM-coated membranes (B).

Surface water is a complex matrix containing naturally occurring organic and inorganic species, both dissolved and colloidal. Pre-elution recoveries from surface water collected in the fall were ~ 40% with both PEM- and CS-coated membranes, which is similar to recoveries from tap water, but significantly lower than recoveries from DI water. The TOC in surface water collected in the fall was 7.5 ± 0.2 mg/L. For surface water, permeate flux declined more than 50% over 90 min of crossflow UF (see APPENDIX, Figure 18) with membranes of each type. Foulants formed a cake layer and masked the anti-adhesive properties of the membrane surface leading to the deposition of virions on membranes. Virions could also be adsorbed to various components of the feed water (e.g. humic acid, clay, silica particles) and co-deposited on the membrane. Post-elution recovery was higher for tap water (Figure 12B) than for surface water suggesting that fouling also decreased the effectiveness of the elution process.

Many studies showed that divalent cations such as Ca^{2+} (30.3 ± 0.5 mg/L in fall surface water) enhance deposition of virions on natural organic matter via inner-sphere complexation with carboxyl groups on both surfaces [72, 73], and on clay and silica by screening the charge [74]. Calcium bridging could also occur between carboxyl groups on natural organic matter and on the HAdV 40 viral capsid (e.g. carboxylic groups on fiber knobs) leading to virion loss to the membrane surface. Bridging by other cations may also occur (e.g. by iron [75], copper [76], and aluminum [77]). In general, virion-foulant interactions, rather than virion-membrane interactions, likely govern recovery in UF from

complex waters. This is consistent with the result that pre-elution recovery from surface water was not statistically different for the two membrane types (Figure 13).

We also analyzed virion recovery from the surface water collected from the same lake in early spring after ice melted. Flux decline also occurred for both membranes during filtration of spring surface water (see APPENDIX, Figure 18), and pre-elution recoveries with both membranes were ~20%. Lower recovery from spring surface water compared to that from fall surface water could stem from higher concentrations of Ca^{2+} (41.1 ± 0.7 mg/L) and TOC (9.4 ± 0.1 mg/L), see Table 10.

Post-elution recovery with CS-blocked membranes was 61.0 ± 2.8% and 34.9 ± 10.1% for water samples collected in fall and spring, respectively. For PEM-coated membranes, post-elution yielded 62.4 ± 2.2% and 41.6 ± 2.0% recoveries for fall and spring samples. Thus, virions adsorbed from surface water on both membranes were not eluted as effectively (Figure 13) as those adsorbed from DI or tap water (Figure 12) when using an eluent with NaPP and Tween 80 only.

To increase the elution efficiency, we added 0.01 wt% EDTA to the eluent to complex Ca^{2+} [78]. EDTA (1 mM) is a component of the storage buffer for HAdV 40, so it should not inactivate the virus [32]. With EDTA in the eluent, the post-elution recovery from spring and fall surface water, averaged over all PEM-coated and CS-blocked membranes, increased to 84.3 ± 4.5%. The increased elution efficiency is consistent with the hypothesis that calcium binding decreases virion recovery from surface water.

In a previous study we showed that a PEM consisting of a weak polycation and a strong polyanion disassembles as low pH [79]. Because HAdV 40 tolerates acidic conditions such a PEM could enable a simple additional processing step to improve the overall recovery: disassembling the PEM after elution could release trapped virions to potentially achieve 100% recovery.

4.3.8 Virus removal

As Figure 14 shows, in tests with HAdV 40-spiked waters of all types, virion removal (see eq. (3)) by PEM-coated membranes was typically an order of magnitude higher than removal by CS-blocked membranes. However, the loss of 1% of virions to the permeate by CS-blocked membranes should not significantly decrease recoveries.

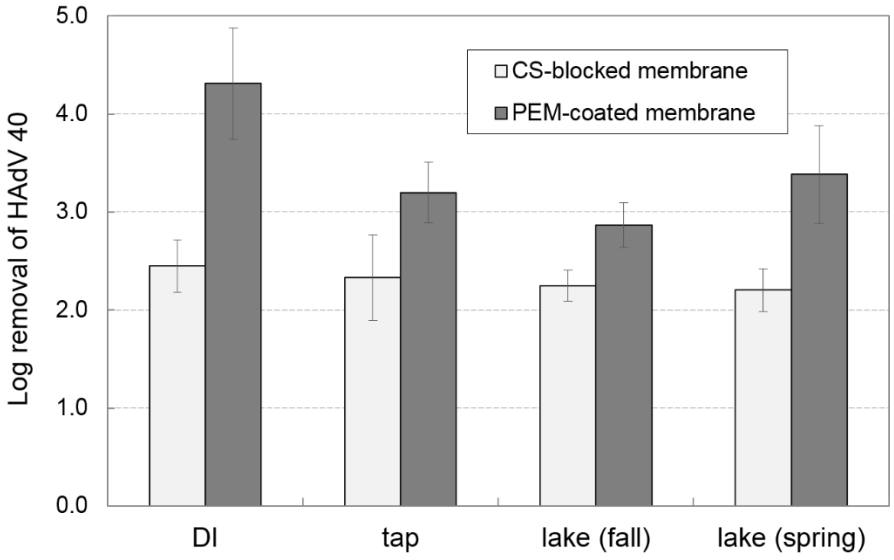

Figure 14. Removal of HAdV 40 by crossflow ultrafiltration with calf-serum blocked membranes and membranes coated by a polyelectrolyte multilayer.

The low LRV by CS-blocked membranes might result from an uneven calf serum distribution on the membrane surface and incomplete blockage. The blocking procedure involves recirculating calf serum solution over the membrane surface and may be viewed as poorly controlled membrane fouling. In contrast, coating a membrane with multiple layers of polyelectrolytes is inherently more reproducible.

There was no consistent correlation between LRV values and the extent of membrane fouling. We showed recently that HAdV 40 removal does not simply correlate with the extent of fouling alone. Pore blockage by humic acid could enhance the virion removal, whereas cake formation by silica colloids could decrease virion removal, and the opposing effects may be compensatory when both foulants are present [80]. Surface water contains colloids and organic macromolecules of a range of sizes, which may explain the similar LRV values for surface and DI water.

4.4 Conclusions

Physicochemical characterization of HAdV 40 showed that this relatively large virus (hydrodynamic diameter of 102.5 ± 8.6 at pH 7.6 in 10 mM Tris and 1 mM EDTA) is hydrophobic (ΔG_{vwv}= -30.4 mJ/m^2) with a point of zero charge between pH 4.0 and pH 4.3. Extended Derjaguin-Landau-Verwey-Overbeek theory predicted that the hydrophilic and negatively charged (ζ = -7.0 ± 3.0 mV at pH 5.8 in 1 mM NaCl) PEM-coated membranes should be advantageous for recovering HAdV from DI water in

comparison with positively charged CS-coated membranes (ζ = 3.0 ± 2.0 mV at pH 5.8 in 1 mM NaCl).

We tested the validity of the XDLVO prediction in filtration experiments. Pre-elution recovery of HAdV from DI water (ionic strength of ~0.2 mM when spiked with HAdV stock) after crossflow UF was higher with PEM-coated membranes (r_{pre}^{PEM}= 74.8 ± 9.7%) than with CS-blocked membranes (r_{pre}^{CS} = 54.1 ± 6.2%). Although pre-elution recovery was lower from tap water, for both PEM- and CS-coated membranes virion elution using an aqueous solution of sodium polyphosphate and TWEEN 80 was effective for both DI water (r_{post}^{PEM} = 99.5 ± 6.6%; r_{post}^{CS} = 98.8 ± 7.7%) and tap water (r_{post}^{PEM} = 88.8 ± 15.3% and r_{post}^{CS} = 93.7 ± 6.9%). The near 100% efficacy of elution indicates that polyanions and surfactants (e.g. sodium polyphosphate and Tween 80) in the eluent can disrupt electrostatic and hydrophobic interactions between the virion and the membrane. Pre- and post-elution recoveries from surface waters were significantly lower (r_{pre}^{CS} and r_{pre}^{PEM} as low as ~ 21%; r_{post}^{CS} and r_{post}^{PEM} < 65%) and showed no statistically significant difference between the two membrane types. However, addition of EDTA to the eluent greatly increased the elution efficacy (r_{post}^{CS} = 88.6 ± 4.3%; r_{post}^{PEM} = 87.0 ± 6.9%), possibly by eliminating cation bridging between virions and other components of the feed water matrix in suspension or in the fouling layer on the membrane surface.

Interestingly, the membrane choice is not very important for achieving high virion recoveries. In tap water, post-elution virion recovery is nearly 100% for both PEM- and CS-coated membranes despite the higher removal of virions with PEM-coated

membranes (LRV^{PEM} = 2.82 ± 0.32 and LRV^{CS} = 1.96 ± 0.53 in tap water). For more complex water matrices such as surface water, the composition of the eluent is the most important factor for achieving high virion recovery. Evidently, the recovery of HAdV depends on its interactions with other components of the feed water (in suspension or deposited on the membrane surface as a fouling layer), and not on virion-membrane interactions. An eluent that includes a polyanion (sodium polyphosphate), a non-ionic surfactant (Tween 80) and a chelating agent (EDTA) recovers HAdV effectively (~ 88%) even from high TOC (9.4 ± 0.1 mg/L) surface water.

APPENDIX

APPENDIX

A.1 HAdV 40 propagation procedures

The HAdV 40 propagation procedure was adapted from protocols by Wong et al. [30] and Mautner [32]. A549 cells, which are susceptible to a wide range of enteric viruses, were used as the HAdV 40 host. These cells were cultured in 50 mL of cell growth medium in a culture flask with a surface area of 150 cm^2 until 90% confluence was achieved. Medium in the culture flasks was decanted, and cell cultures were inoculated with 2 mL of virus stock. The flask was incubated at 37 ^oC for 60 min and rocked gently at 15 min intervals. After 60 min, 2 mL of viral inoculums was discarded and ~25 to 30 mL of cell maintenance medium was added to the flask. The tightly sealed flask was incubated at 37 ^oC and the cytopathic effect (CPE) was checked daily. As HAdV 40 is a fastidious virus, 4 days are usually needed to observe a good CPE. Viruses should be harvested when cells round up and detach from the flask surface. Harvesting too early leads to low virus production, and harvesting too late may lead to virus release to medium. To harvest viruses, the remaining cells were gently pipetted off the flask surface. Cell suspension was centrifuged at 900 g for 10 min at 4 ^oC, and supernant was then discarded. Cell pellets were resuspended in maintenance medium and then subjected to a freeze/thaw procedure (-70 ^oC / 37 ^oC) to release virions from cells. After 3 freeze/thaw cycles, cell resuspension was centrifuged at 12,000 g for 10 min at 4 ^oC. Supernatant containing viruses was collected, aliquoted, and stored at -70 ^oC for further use.

Viruses were further purified using a CsCl density step gradient (density steps from the bottom up: 1.45 g/cm^3 CsCl, 1.38 g/cm^3 CsCl, 1.32 g/cm^3 CsCl, 40% glycerol cushion). HAdV 40 stock was then added to the top and a virus band was obtained by ultracentrifugation at 80,000 g (AH-650 rotor, Sorvall, Thermo Scientific, Waltham, MA) and 4 ^{o}C for 3 h. The band was collected by side puncture of the tube with a syringe. CsCl was removed by dialysis against the desired buffer at 4 ^{o}C with gentle stirring.

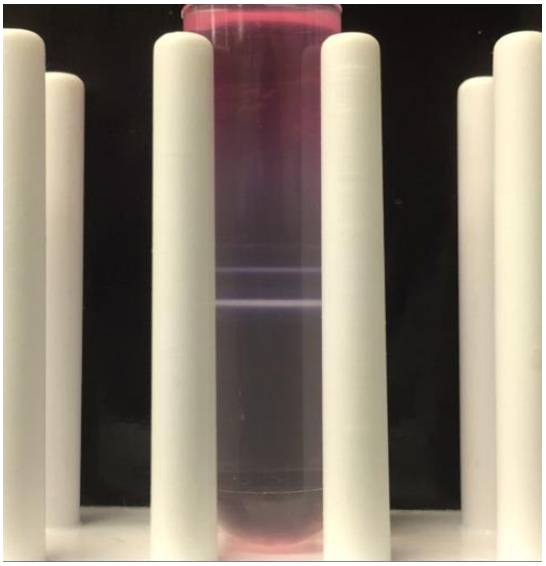

Figure 15. HAdV 40 band obtained by CsCl density gradient centrifugation.

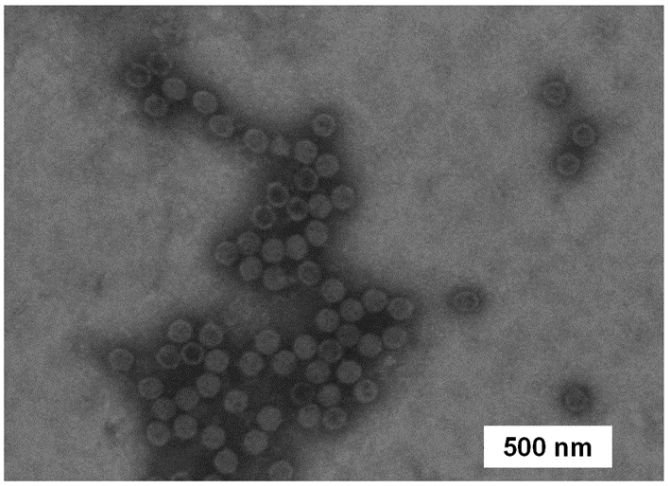

Figure 16. Transmission electron microscopy image of HAdV 40 viruses.

A.2 HAdV 40 quantification by qPCR

A MagNA Pure Compact System (Roche Diagnostics USA, Indianapolis, IN) was used to extract HAdV 40 DNA from 390 µL samples collected immediately after filtration experiments. 10 µL of carrier RNA (1 mg/mL) was added to increase DNA recovery during DNA extraction. Extracted DNA was stored in 100 µL eluates and at -20 ^{o}C prior to qPCR analysis. Each extract was quantified by qPCR in triplicate, and qPCR was performed using the LightCycler 1.5 system (Roche Diagnostics USA, Indianapolis, IN) with the primer and probe sequences described in Table 13. The volume of each PCR reaction mixture is 20 µL containing 5 µL of extracted DNA sample, 0.8 µL of forward primer (10 mM), 0.4 µL of each of two reverse primers (10 mM), 0.6 µL of Taqman Probe (10 mM), 10 µL of probe master mix (2X, Light Cycler 480 Probes, Roche) and 2.8 µL of PCR-grade water. qPCR mixtures were heated at 95°C for 15 min for DNA denaturation prior to 45 cycles of DNA amplification (95°C for 10 s, 60°C for 30 s and 72°C for 12 s). Finally, mixtures were cooled for 30 s at 40°C.

To prepare a standard curve (qPCR crossing-point (CP) values versus number of HAdV 40 DNA copies), plasmid DNA carrying cloned HAdV 40 hexon gene served as standards and was prepared following the method described earlier [9].

Table 13. Primer and probe sequences used in qPCR for HAdV 40 detection

Forward Primer (for serotype 40 and 41)	HAdV-F4041-hex157f	ACC-CAC-GAT-GTA-ACC-ACA-GAC
Reverse primer 1 (for serotype 40)	HAdV-F40-hex245r	ACT-TTG-TAA-GAG-TAG-GCG-GTT-TC
Reverse primer 2 (for serotype 41)	HAdV-F41-hex246r	CAC-TTT-GTA-AGA-ATA-AGC-GGT-GTC
Taqman probe	HAV-F4041-hex214rprobe	6-FAM-CGA-CKG-GCA-CGA-AKC-GCA-GCG-T-BHQ-1

A.3 Crossflow ultrafiltration (UF) apparatus

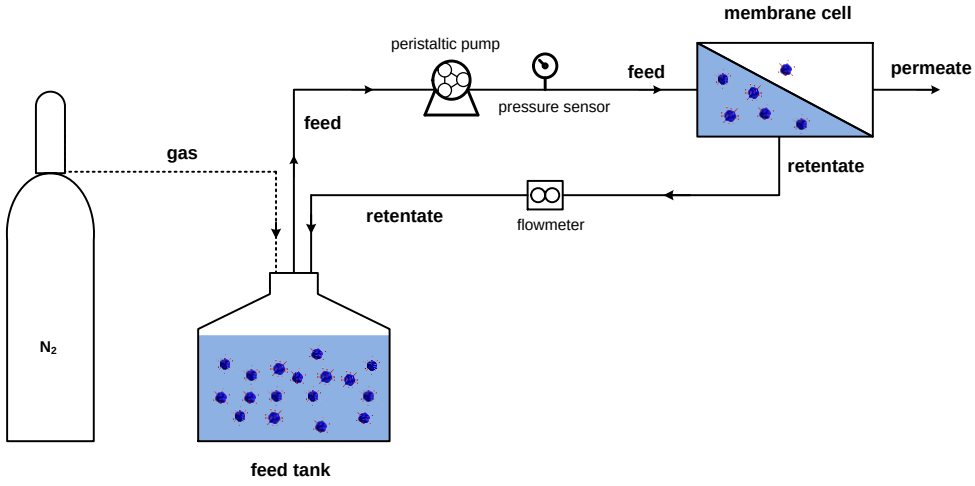

Figure 17. Crossflow filtration apparatus.

A.4 Permeate flux in HAdV 40 recovery tests.

Figure 18 shows the normalized permeate flux as a function of time during virus recovery from different water matrices. Flux values were normalized by the flux value at t = 0.

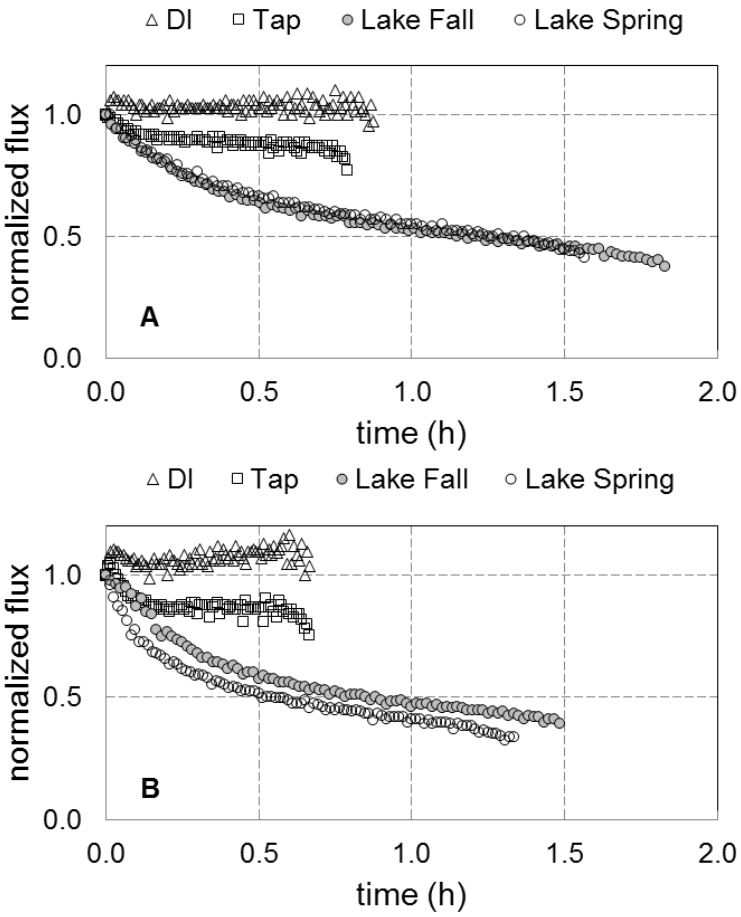

Figure 18. Normalized permeate flux as function of filtration time for CS-blocked membranes (A) and PEM-coated membranes (B).

A.5 Testing of potential inhibition of qPCR in complex water matrices.

We evaluated whether chemicals present in complex water matrices inhibit DNA extraction and qPCR detection. One liter sample of DI water, tap water and surface water were spiked with 1 mL of HAdV 40 stock. Log concentrations of DNA from complex water matrices (tap water and surface water) as well as DI water were calculated based on cross point (CP) values of DNA extracts obtained by qPCR. Similar experiments were conducted to evaluate the potential inhibition in the retentate produced by filtering tap water and surface water samples. One liter samples were filtered using the protocol for virus recovery tests, but no virus was introduced into the feed. 100 mL retentate samples were collected and spiked with 1 mL of HAdV 40 stock. The same procedure was followed for DI water samples. Log concentration of DNA from complex water matrices (tap water and surface water) as well as DI water were calculated. Our results (Figure 19) show no significant difference among the DNA concentrations determined in all of the feed and retentate matrices. This indicates there is either no inhibition or the same inhibition level for all water types in both feed and retentate.

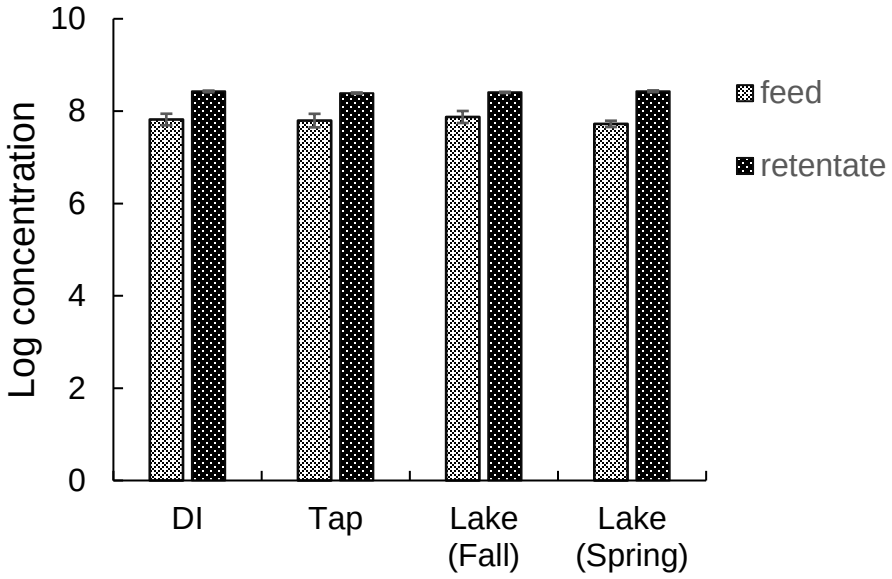

Figure 19. Log concentration of DNA detected by qPCR in feed and retentate water matrices spiked with the same concentrations of virions.

A.6 Calculation of the virus-virus interaction energy and virus-membrane interaction energy using the extended Derjaguin-Landau-Verwey-Overbeek (XDLVO) theory

The total XDLVO interfacial interaction energy, U^{XDLVO}, is given by:

$$U^{XDLVO} = U^{LW} + U^{EL} + U^{AB} \quad \text{(A-1)}$$

where U^{LW} , U^{EL}, and U^{AB} correspond to Lifshitz - van der Waals, electrical double layer, and Lewis acid-base interactions, respectively. Equations for each interaction as a function of separation distance are introduced below.

A.6.1 The case of virus-virus (sphere-sphere) interaction in water (U_{vwv})

U_{vwv} is the total interfacial interaction energy between two virions (v) immersed in water (w). As stated by eq. (A-1), U_{vwv} includes three components: U_{vwv}^{LW}, U_{vwv}^{EL}, and U_{vwv}^{AB}.

A.6.1.1 Lifshitz - van der Waals (LW) interaction energy, U_{vwv}^{LW}

$$U_{vwv}^{LW} = \frac{-A}{6}\left[\frac{2a^2}{\ell(4a+\ell)} + \frac{2a^2}{(\ell+2a)^2} + \ln\frac{\ell(4a+\ell)}{(\ell+2a)^2}\right] \quad \text{(A-2)}$$

where a is the radius of the virion, ℓ is the separation distance and A is the Hamaker constant:

$$A = 12\pi {\ell_0}^2 \Delta G_{\ell_0}^{LW} \quad \text{(A-3)}$$

where ℓ_0 is the minimum equilibrium cut-off distance, which is estimated as 0.158 nm [56-58] and $\Delta G_{\ell_0}^{LW}$ is the LW adhesion energy per unit area at ℓ_0:

$$\Delta G_{\ell_0}^{LW} = -2(\sqrt{\gamma_v^{LW}} - \sqrt{\gamma_w^{LW}})^2 \quad \text{(A-4)}$$

where γ_v^{LW} and γ_w^{LW} are LW (apolar) components of surface energy for virus and water respectively.

A.6.1.2 Electrical double layer (EL) interaction energy, U_{vwv}^{EL}

$$U_{vwv}^{EL} = 32\pi\varepsilon_r\varepsilon_0 a\left(\frac{kT}{ze}\right)^2 \gamma^2 \exp(-\kappa\ell) \quad \text{(A-5)}$$

where

$$\kappa = \sqrt{\frac{2N_A e^2 I}{\varepsilon_0 \varepsilon_r kT}} \quad \text{(A-6)}$$

where N_A is Avogadro's constant and I is ionic strength. The dimensionless γ is given by:

$$\gamma = tanh\left(\frac{ze\psi_0}{4kT}\right) \quad \text{(A-7)}$$

where ψ_0 is the surface potetntial of the virion, which can be estimated from the ζ–potential of the virion, ζ_v:

$$\psi_0 = \zeta_v \left(1 + \frac{d}{a}\right) \exp(\kappa d) \quad \text{(A-8)}$$

d is the distance from the particle's surface to the slipping plane and is usually 0.3 to 0.5 nm. We used d of 0.5 nm. The difference in $\exp(\kappa d)$ due to the choice of d = 0.3 nm rather than d = 0.5 nm, is at most 7% (seen at pH 7.6).

Eq. (A-5) is valid for $\kappa a > 5$ and $\ell < a$ [81]. In our study, $0.5\kappa\bar{d}^{h}_{HAdV} \geq 5.8$ in 1mM NaCl (Table 14) making eq. (A-5) applicable.

Equation (A-8) is valid for ζ–potential values up to ~50 mV [57]. In our study, the absolute value of $|\bar{\zeta}_{HAdV}|$ ***is*** $\leq$ 45.1 (Table 14), making eq. (A-8) applicable.

A.6.1.3 Lewis acid-base (AB) interaction energy, U^{AB}_{vwv}

$$U^{AB}_{vwv} = a\pi\lambda\Delta G^{AB}_{\ell_0} exp\left(\frac{\ell_0 - \ell}{\lambda}\right) \quad \text{(A-9)}$$

where λ is the decay length for water. The commonly used value of λ is 0.6 nm [58].

$\Delta G_{\ell_0}^{AB}$ is the AB adhesion energy per unit area at ℓ_0:

$$\Delta G_{\ell_0}^{AB} = -4\left(\sqrt{\gamma_v^+} - \sqrt{\gamma_w^+}\right)\left(\sqrt{\gamma_v^-} - \sqrt{\gamma_w^-}\right) \quad \text{(A-10)}$$

where γ_v^+ and γ_w^+ are electron-acceptor parameters of surface energy for virion and water respectively, γ_v^- and $\gamma_w^-$are electron-donor parameters of surface energy for virion and water respectively.

A.6.2 The case of virion-membrane (sphere-plate) interaction (U_{vwm})

U_{vwm} is the total interfacial interaction energy between virions (v) and membrane (m) immersed in water (w).

A.6.2.1 Lifshitz - van der Waals (LW) interaction energy, U_{vwm}^{LW}

For the sphere-plate case, Lifshitz – van der Waals (LW) interaction energy is given by [82]

$$U_{vwm}^{LW} = -\frac{A}{6}\left[\frac{a}{\ell} + \frac{a}{\ell + 2a} + \ln\frac{\ell}{\ell + 2a}\right] \quad \text{(A-11)}$$

For the virus-membrane interaction, $\Delta G_{\ell_0}^{LW}$ can be calculated as:

$$\Delta G_{\ell_0}^{LW} = 2\left(\sqrt{\gamma_w^{LW}} - \sqrt{\gamma_m^{LW}}\right)\left(\sqrt{\gamma_v^{LW}} - \sqrt{\gamma_w^{LW}}\right) \quad \text{(A-12)}$$

where γ_m^{LW} is the LW component of surface energy for the membrane.

A.6.2.2 Electrical double layer (EL) interaction energy, U_{vwm}^{EL}

$$U_{vwm}^{EL} = \pi\varepsilon_r\varepsilon_0 a\left[2\zeta_v\zeta_m \ln\left(\frac{1+e^{-\kappa\ell}}{1-e^{-\kappa\ell}}\right) + (\zeta_v^2+\zeta_m^2)\ln\left(1-e^{-2\kappa\ell}\right)\right] \quad \text{(A-13)}$$

where ζ_m is the ζ–potential of the membrane.

A.6.2.3 Lewis acid-base (AB) interaction energy, U_{vwm}^{AB}

$$U_{vwm}^{AB} = 2\pi a\lambda\Delta G_{\ell_0}^{AB}\exp\left(\frac{\ell_0-\ell}{\lambda}\right) \quad \text{(A-14)}$$

For the virus-membrane interaction, $\Delta G_{\ell_0}^{AB}$ is calculated as:

$$\Delta G_{\ell_0}^{AB} = 2\sqrt{\gamma_w^+}\left(\sqrt{\gamma_m^-}+\sqrt{\gamma_v^-}-\sqrt{\gamma_w^-}\right) + 2\sqrt{\gamma_w^-}\left(\sqrt{\gamma_m^+}+\sqrt{\gamma_v^+}-\sqrt{\gamma_w^+}\right) - 2\left(\sqrt{\gamma_m^+\gamma_v^-}+\sqrt{\gamma_m^-\gamma_v^+}\right) \quad \text{(A-15)}$$

γ_m^+ and γ_m^- are electron-acceptor and electron-donor parameters of surface energy for membrane.

To calculate each component of surface energy for the membrane and the virus, we measured contact angles of DI water, glycerol and diiodomethane on both solid surfaces (membrane surface and virus lawn) using a goniometer. We obtained the components of surface energy for the solids by substituting contact angles and surface energy components of probe liquids into eq. (A-16):

$$(1+\cos\theta)\gamma_l^{TOT} = 2\left(\sqrt{\gamma_s^{LW}\gamma_l^{LW}}+\sqrt{\gamma_s^+\gamma_l^-}+\sqrt{\gamma_s^-\gamma_l^+}\right) \quad \text{(A-16)}$$

$$\gamma^{AB} = 2\sqrt{\gamma^{+}\gamma^{-}} \quad \text{(A-17)}$$

$$\gamma^{TOT} = \gamma^{LW} + \gamma^{AB} \quad \text{(A-18)}$$

where θ is the contact angle of the probe liquid on the solid, γ^{TOT} is total surface energy, $\gamma^{LW}$is the LW component of surface energy,γ^{+} is the electron-acceptor parameter of surface energy, and γ^{-} is the electron-donor parameter of surface energy. Subscripts l and s refer to probe liquid and solid surface respectively.

The free energy of interfacial interaction between two virions when immersed in water (ΔG_{vwv}) can be determined using the following equation [83]:

$$\Delta G_{vwv} = -2\left(\sqrt{\gamma_v^{LW}} - \sqrt{\gamma_w^{LW}}\right)^2 - 4\left(\sqrt{\gamma_v^{+}\gamma_v^{-}} + \sqrt{\gamma_w^{+}\gamma_w^{-}} - \sqrt{\gamma_v^{+}\gamma_w^{-}} - \sqrt{\gamma_v^{-}\gamma_w^{+}}\right) \quad \text{(A-19)}$$

A.7 HAdV 40 size distribution in tap water.

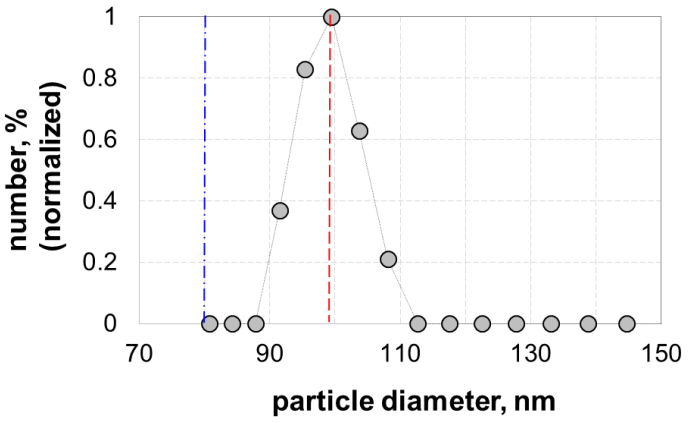

Figure 20. Normalized number-based size distribution of HAdV 40 in tap water (pH = 7.5 to 8.0). The vertical dashed red line indicates the average modal diameter (98.5 nm) in the buffer recommended for the storage of purified HAdV 40 (10 mM Tris-HCl and 1 mM EDTA, pH 7.6). The vertical dash-dot blue line denotes the average HAdV diameter (~ 80 nm) determined from TEM.

A.8 XDLVO energy of virus-membrane interfacial interaction: Relative contributions from van der Waals, electrostatic and acid-base interactions.

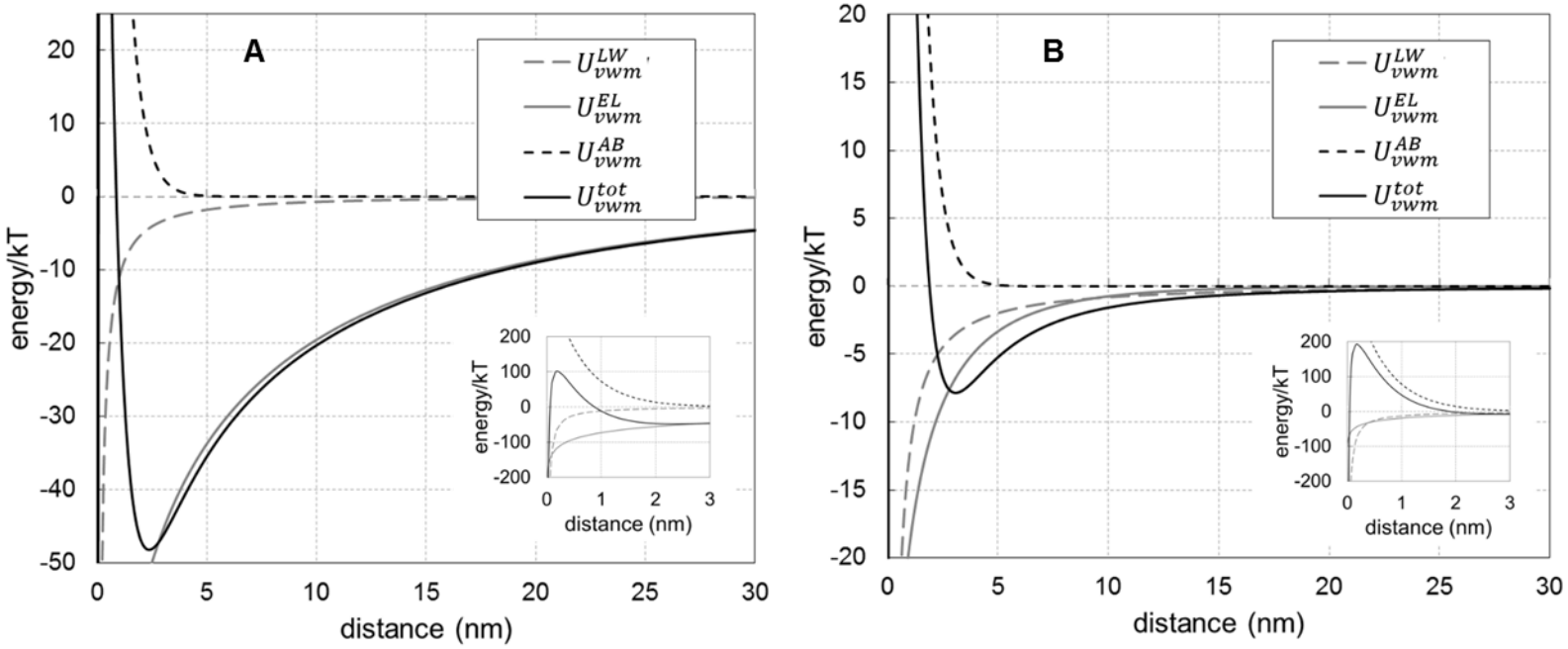

Figure 21. XDLVO energies of interfacial interaction of HAdV 40 with CS-blocked membranes in (A) DI water ($I \cong 0.2$ mM after spiking with HAdV 40) and (B) tap water.

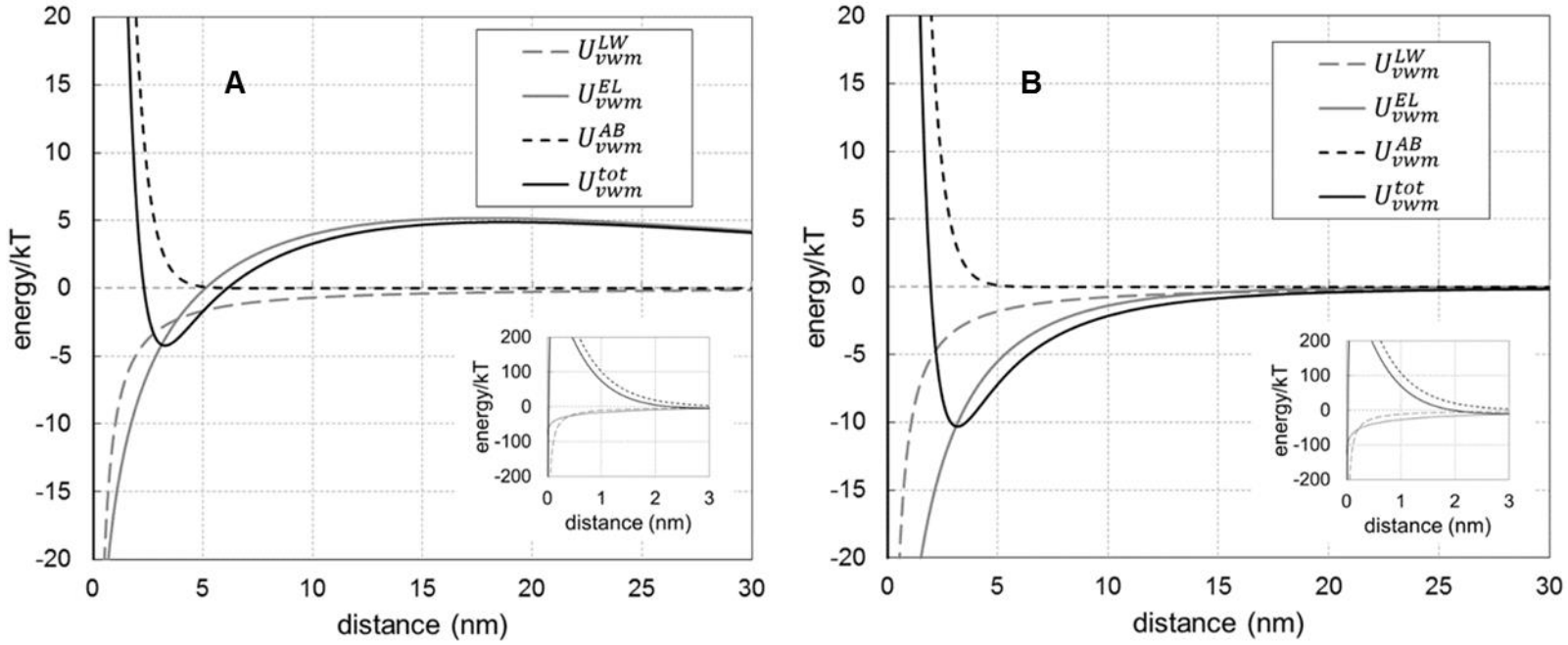

Figure 22. XDLVO energies of interfacial interaction of HAdV 40 with PEM-coated membranes in (A) DI water ($I \cong 0.2$ mM after spiking with HAdV 40) and (B) tap water.

A.9 On the determination of ζ–potential based on measured electrophoretic mobility

Figure 23 present the results of electrophoretic mobility measurements.

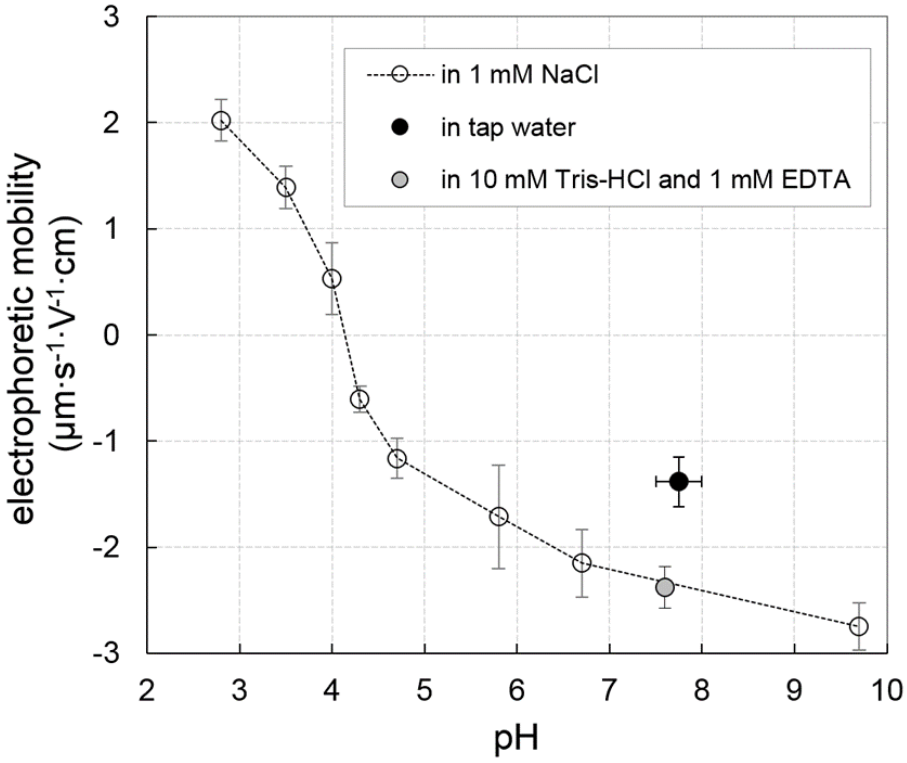

Figure 23. Electrophoretic mobility of HAdV 40 as a function of pH.

To convert measured mobilities into ζ–potential values, we used an expression derived by Ohshima [53]:

$$\mu = \frac{2}{3}\frac{\varepsilon_r \varepsilon_0}{\eta}\zeta\left[1 + \frac{1}{2\left[1 + \frac{2.5}{\kappa a[1 + 2e^{-\kappa a}]}\right]^3}\right] \quad \text{(A-20)}$$

where κ (nm^{-1}) is the Hückel parameter (κ^{-1} (nm) is the Debye length), η is the viscosity of the electrolyte, in which particles are suspended, and a is the radius of the particle. Eq. (A-20) provides an accurate (<1% error) estimate of ζ–potential for any value of κa. This is in contrast to Smoluchowski's (eq. (A-21)) and Hückel's (eq. (A-22)) expressions for electrophoretic mobility, which are applicable for $\kappa a \gg 1$ and $\kappa a \ll 1$, respectively.

$$\mu = \frac{\varepsilon_r \varepsilon_0}{\eta} \zeta \tag{A-21}$$

$$\mu = \frac{3}{2} \frac{\varepsilon_r \varepsilon_0}{\eta} \zeta \tag{A-22}$$

A.10 On the determination of ζ–potential of virus aggregates.

At pH values where virions aggregate, the ζ–potential measured is that of an aggregate of virions, and not a single virion. We calculated the ζ–potential of individual (non-aggregated) virions using eq. (A-23), which connects the surface charge density of a particle (σ) with its ζ –potential, diameter (d_p) and Debye length (κ^{-1}) [55]:

$$\sigma = \frac{2\varepsilon_r \varepsilon_0 \kappa k T}{ze} sinh\left(\frac{ze\zeta}{2kT}\right) \sqrt{1 + \frac{1}{\kappa \frac{d_p}{2}} \frac{2}{cosh^2\left(\frac{ze\zeta}{4kT}\right)} + \frac{1}{\left(\kappa \frac{d_p}{2}\right)^2} \frac{8\, ln\left[cosh\left(\frac{ze\zeta}{4kT}\right)\right]}{sinh^2\left(\frac{ze\zeta}{2kT}\right)}} \tag{A-23}$$

This calculation assumes that σ is an intensive property and does not depend on the aggregation state of the virion. To determine the ζ–potential of an individual virion from the ζ–potential measured for virion aggregates, we first used eq. (A-23) to calculate σ based on the measured ζ–potential and average size of virus aggregates. With this

value of σ, we then used eq. (A-23) again with the hydrodynamic diameter of an individual virion to calculate the ζ–potential of an individual virus (Table 14). Because ζ–potential measurements involved adding acid or base to adjust pH, the ionic strength was different at different pH values. To account for these differences we estimated the ionic strength at each pH from measured values of conductivity.

At pH values where virus aggregation occurred, the difference between ζ-potentials of aggregated virions (*measured* ζ-potential) and that of an individual virion (*calculated* ζ-potential) was relatively minor (Table 14).

Table 14. Charge characteristics of HAdV 40 at different pH values. Shaded (gray) areas denote pH values where significant aggregation occurs and $\zeta_{HAdV}^{agg} \neq \zeta_{HAdV}$.

Water matrix	**1 mM NaCl**						**buffer [a]**	**tap water**	**1 mM NaCl**	**DI water [e]**
pH	**2.8**	**4.0**	**4.3**	**4.7**	**5.8**	**6.7**	**7.6**	**7.5 to 8.0**	**9.7**	**5.8**
Ionic strength (mM) [b]	7.5	1.8	1.7	1.6	1.5	1.6	12.1	5.1	1.9	0.2
$\boldsymbol{\sigma_{HAdV}}$ **(mC/m^2)**	6.49	0.77	-0.89	-1.84	-3.02	-3.97	-9.63	-4.06	-5.88	n/a[f]
$\boldsymbol{\bar{\zeta}_{HAdV}^{agg}}$ **(mV) [c]**	n/a[d]	6.8	-7.8	-14.9	n/a[d]	n/a[d]	n/a[d]	n/a[d]	n/a[d]	n/a[f]
$\boldsymbol{\bar{\zeta}_{HAdV}}$ **(mV)**	29.4	7.5	-8.8	-17.8	-28.0	-34.9	-34.0	-20.3	-45.1	n/a[f]
Debye length, $\boldsymbol{\kappa^{-1}}$ (nm)	3.5	7.2	7.4	7.5	7.8	7.5	2.8	3.8	6.9	23.3
Hückel parameter, $\boldsymbol{\kappa}$ (nm^{-1})	0.285	0.139	0.136	0.133	0.128	0.133	0.361	0.263	0.145	0.043
$\boldsymbol{0.5\kappa\bar{d}_{HAdV}^{h}}$	16.0	19.8	16.1	9.9	6.0	6.3	18.6	14.3	5.8	2.2

Note:
[a] 10 mM Tris-HCl and 1 mM EDTA (buffer recommended for the storage of purified HAdV 40).
[b] Ionic strength at each pH is estimated based on electrical conductance measurements.
[c] Values of ζ_{HAdV}^{agg} are also reported in Figure 9. The values are included here for the ease of comparison with ζ_{HAdV}.
[d] There is no detectable aggregation of HAdV 40 at this pH.
[e] After spiking DI water with HAdV 40 stock
[f] Not measured

Table 15. Additional parameters of HAdV 40 size distribution at different pH values. Shaded (gray) areas denote pH values where significant aggregation occurs.

Water	**1 mM NaCl**						**buffer** [a]	**tap water**	**1 mM NaCl**
pH	**2.8**	**4.0**	**4.3**	**4.7**	**5.8**	**6.7**	**7.6**	**7.5 to 8.0**	**9.7**
HWHM	11.8 ± 5.7	31.3 ± 17.3	22.0 ± 1.4	18.8 ± 7.5	13.3 ± 2.4	7.6 ± 0.7	15.0 ± 3.1	6.9 ± 2.0	5.8 ± 1.8
d_{HAdV}^{mod}	101.7 ± 7.9	203.4 ±	233.2 ±	149.8 ± 8.1	94.7 ± 4.0	91.5 ± 2.7	98.5 ± 8.7	101.3 ± 5.0	76.4 ± 5.7

Note:
[a] 10 mM Tris-HCl and 1 mM EDTA (buffer recommended for the storage of purified HAdV 40).
[b] Half width at half maximum.

REFERENCES

REFERENCES

1. http://www.who.int/water_sanitation_health/diseases/burden/en/).

2. K. D. Crabtree, C. P. Gerba, J. B. Rose and C. N. Haas, *Water Sci. Technol.*, 1997, **35**, 1-6.

3. K. Mena and C. Gerba, in *Rev. Environ. Contam. Toxicol.*, ed. D. Whitacre, Springer New York, 2009, vol. 198, ch. 4, pp. 133-167.

4. G. Fongaro, M. A. do Nascimento, C. Rigotto, G. Ritterbusch, A. D. da Silva, P. A. Esteves and C. R. M. Barardi, *Virol. J.*, 2013, **10**.

5. S. C. Jiang, *Environ. Sci. Technol.*, 2006, **40**, 7132-7140.

6. C. E. Enriquez, C. J. Hurst and C. P. Gerba, *Water Res.*, 1995, **29**, 2548-2553.

7. J. A. Thurston-Enriquez, C. N. Haas, J. Jacangelo, K. Riley and C. P. Gerba, *Appl. Environ. Microbiol.*, 2003, **69**, 577-582.

8. S. Choi and S. C. Jiang, *Appl. Environ. Microbiol.*, 2005, **71**, 7426-7433.

9. I. Xagoraraki, D. H. W. Kuo, K. Wong, M. Wong and J. B. Rose, *Appl. Environ. Microbiol.*, 2007, **73**, 7874-7881.

10. N. Albinana-Gimenez, M. P. Miagostovich, B. Calqua, J. M. Huguet, L. Matia and R. Girones, *Water Res.*, 2009, **43**, 2011-2019.

11. T. T. Fong, M. S. Phanikumar, I. Xagoraraki and J. B. Rose, *Appl. Environ. Microbiol.*, 2010, **76**, 715-723.

12. O. Olayinka and O. Anthony, *Virol. J.*, 2015, **12**, 98.

13. C. D. Gibbons, R. A. Rodriguez, L. Tallon and M. D. Sobsey, *J. Appl. Microbiol.*, 2010, **109**, 635-641.

14. L. A. Ikner, M. Soto-Beltran and K. R. Bright, *Appl. Environ. Microbiol.*, 2011, **77**, 3500-3506.

15. B. R. McMinn, *J. Virol. Methods*, 2013, **193**, 284-290.

16. D. Berman, M. E. Rohr and R. S. Safferman, *Appl. Environ. Microbiol.*, 1980, **40**, 426-428.

17. H. A. Morales-Morales, G. Vidal, J. Olszewski, C. M. Rock, D. Dasgupta, K. H. Oshima and G. B. Smith, *Appl. Environ. Microbiol.*, 2003, **69**, 4098-4102.

18. A. L. Polaczyk, J. Narayanan, T. L. Cromeans, D. Hahn, J. M. Roberts, J. E. Amburgey and V. R. Hill, *J. Microbiol. Methods*, 2008, **73**, 92-99.

19. E. V. Pasco, H. Shi, I. Xagoraraki, S. A. Hashsham, K. N. Parent, M. L. Bruening and V. V. Tarabara, *J. Membr. Sci.*, 2014, **469**, 140-150.

20. V. R. Hill, A. M. Kahler, N. Jothikumar, T. B. Johnson, D. Hahn and T. L. Cromeans, *Appl. Environ. Microbiol.*, 2007, **73**, 4218-4225.

21. P. B. Liu, V. R. Hill, D. Hahn, T. B. Johnson, Y. Pan, N. Jothikumar and C. L. Moe, *J. Microbiol. Methods*, 2012, **88**, 155-161.

22. L. Pei, M. Rieger, S. Lengger, S. Ott, C. Zawadsky, N. M. Hartmann, H. C. Selinka, A. Tiehm, R. Niessner and M. Seidel, *Environ. Sci. Technol.*, 2012, **46**, 10073-10080.

23. S. Skraber, C. Gantzer, K. Helmi, L. Hoffmann and H. M. Cauchie, *Food Environ. Virol.*, 2009, **1**, 66-76.

24. G. Belfort, Y. Rotem and E. Katzenelson, *Water Res.*, 1975, **9**, 79-85.

25. D. S. Francy, E. A. Stelzer, A. M. Brady, C. Huitger, R. N. Bushon, H. S. Ip, M. W. Ware, E. N. Villegas, V. Gallardo and H. D. Lindquist, *Appl. Environ. Microbiol.*, 2013, **79**, 1342-1352.

26. L. A. Ikner, C. P. Gerba and K. R. Bright, *Food Environ. Virol.*, 2012, **4**, 41-67.

27. V. R. Hill, A. L. Polaczyk, D. Hahn, J. Narayanan, T. L. Cromeans, J. M. Roberts and J. E. Amburgey, *Appl. Environ. Microbiol.*, 2005, **71**, 6878-6884.

28. P. Nestola, D. L. Martins, C. Peixoto, S. Roederstein, T. Schleuss, P. M. Alves, J. P. B. Mota and M. J. T. Carrondo, *Plos One*, 2014, **9**.

29. E. R. Rhodes, E. M. Huff, D. W. Hamilton and J. L. Jones, *J. Virol. Methods*, 2016, **228**, 31-38.

30. K. Wong, B. Mukherjee, A. M. Kahler, R. Zepp and M. Molina, *Environ. Sci. Technol.*, 2012, **46**, 11145-11153.

31. E. I. Trilisky and A. M. Lenhoff, *J. Chromatogr. A*, 2007, **1142**, 2-12.

32. V. Mautner, in *Adenovirus Methods and Protocols*, eds. W. M. Wold and A. Tollefson, Humana Press, 2007, vol. 130, ch. 11, pp. 145-156.

33. M. M. F. Mesquita and M. B. Emelko, in *Bacteriophages*, ed. I. Kurtboke, Intech, 2014.

34. M. Abbaszadegan, B. K. Mayer, H. Ryu and N. Nwachuku, *Environ. Sci. Technol.*, 2007, **41**, 971-977.

35. M. I. Bellou, V. I. Syngouna, M. A. Tselepi, P. A. Kokldnos, S. C. Paparrodopoulos, A. Vantarakis and C. V. Chrysikopoulos, *Sci. Total Environ.*, 2015, **517**, 86-95.

36. A. H. Kidd, J. Chroboczek, S. Cusack and R. W. H. Ruigrok, *Virology*, 1993, **192**, 73-84.

37. J. D. Song, X. L. Liu, D. L. Chen, X. H. Zou, M. Wang, J. G. Qu, Z. Z. Lu and T. Hung, *Virology*, 2012, **432**, 336-342.

38. G. W. Gary, Jr., J. C. Hierholzer and R. E. Black, *J. Clin. Microbiol.*, 1979, **10**, 96-103.

39. J. C. De Jong, J. G. Kapsenberg, C. J. Muzerie, A. G. Wermenbol, A. H. Kidd, G. Wadell, R. G. Firtzlaff and R. Wigand, *J. Med. Virol.*, 1983, **11**, 215-231.

40. J. C. Dejong, K. Bijlsma, A. G. Wermenbol, M. W. Verweijuijterwaal, H. Vanderavoort, D. J. Wood, A. S. Bailey and A. Osterhaus, *J. Clin. Microbiol.*, 1993, **31**, 1562-1569.

41. V. Sherwood, H.-G. Burgert, Y.-H. Chen, S. Sanghera, S. Katafigiotis, R. E. Randall, I. Connerton and K. H. Mellits, *J. Gen. Virol.*, 2007, **88**, 71-76.

42. M. Kim, M. Y. Lim and G. Ko, *Appl Environ Microbiol.*, 2010, **76**, 2509-2516.

43. C. T. Tiemessen and A. H. Kidd, *J. Gen. Virol.*, 1995, **76**, 481-497.

44. I. Wilhelmi, E. Roman and A. Sanchez-Fauquier, *Clin. Microbiol. Infect.*, 2003, **9**, 247-262.

45. M. A. Kennedy and R. J. Parks, *Mol. Ther.*, 2009, **17**, 1664-1666.

46. G. R. Nemerow, P. L. Stewart and V. S. Reddy, *Curr. Opin. Virol.*, 2012, **2**, 115-121.

47. L. Gutierrez, S. E. Mylon, B. Nash and T. H. Nguyen, *Environ. Sci. Technol.*, 2010, **44**, 4552-4557.

48. J. L. Putaux, A. Buleon, R. Borsali and H. Chanzy, *Int. J. Biol. Macromol.*, 1999, **26**, 145-150.

49. A. L. Favier, W. P. Burmeister and J. Chroboczek, *Virology*, 2004, **322**, 93-104.

50. Z.-Z. Lu, X.-H. Zou, L.-X. Dongi, J.-G. Qu, J.-D. Song, M. Wang, L. Guo and T. Hung, *J. Gene Med.*, 2009, **11**, 128-138.

51. J. J. Hansen, P. S. Warden and A. B. Margolin, *Int. J. Environ. Res. Public Health*, 2007, **4**, 61-67.

52. C. L. Bean, J. J. Hansen, A. B. Margolin, H. Balkin, G. Batzer and G. Widmer, *Int. J. Environ. Res. Public Health*, 2007, **4**, 53-60.

53. H. Ohshima, *J. Colloid Interface Sci.*, 1994, **168**, 269-271.

54. E. Norrby, in *Curr. Top. Microbiol. Immunol.*, eds. W. Arber, W. Braun, F. Cramer, R. Haas, W. Henle, P. H. Hofschneider, N. K. Jerne, W. Kikuth, P. Koldowsky, H. Koprowski, O. Maaløe, R. Rott, H. G. Schweiger, M. Sela, L. Syruček, P. K. Vogt and E. Wecker, Springer Berlin Heidelberg, 1968, vol. 43, ch. 1, pp. 1-43.

55. K. Makino and H. Ohshima, *Langmuir*, 2010, **26**, 18016-18019.

56. C. J. Van Oss, *Interfacial forces in aqueous media - second edition*, Taylor & Francis Group, 2006.

57. C. J. van Oss, *J. Mol. Recognit.*, 2003, **16**, 177-190.

58. J. A. Brant and A. E. Childress, *J. Membr. Sci.*, 2002, **203**, 257-273.

59. A. Martin-Molina, J. A. Maroto-Centeno, R. Hidalgo-Alvarez and M. Quesada-Perez, *Colloids Surf., A*, 2008, **319**, 103-108.

60. C. Schneider, M. Hanisch, B. Wedel, A. Jusufi and M. Ballauff, *J. Colloid Interface Sci.*, 2011, **358**, 62-67.

61. K. M. Kanal, G. D. Fullerton and I. L. Cameron, *Biophys. J.*, 1994, **66**, 153-160.

62. S. R. Ge, K. Kojio, A. Takahara and T. Kajiyama, *J. Biomater. Sci. Pol.*, 1998, **9**, 131-150.

63. L. R. S. Barbosa, M. G. Ortore, F. Spinozzi, P. Mariani, S. Bernstorff and R. Itri, *Biophys. J.*, 2010, **98**, 147-157.

64. R. V. Josephson, E. M. Mikolajick and D. P. Sinha, *J. Dairy Sci.*, 1972, **55**, 1508-1510.

65. K. Hori and S. Matsumoto, *Biochem. Eng. J.*, 2010, **48**, 424-434.

66. G. Hwang, S. Kang, M. Gamal El-Din and Y. Liu, *Colloid Surface B*, 2012, **91**, 181-188.

67. M. W. Hahn and C. R. O'Melia, *Environ. Sci. Technol.*, 2004, **38**, 210-220.

68. D. Sutlovic, M. D. Gojanovic, S. Andelinovic, D. Gugic and D. Primorac, *Croat. Med. J.*, 2005, **46**, 556-562.

69. C. N. Albers, A. Jensen, J. Baelum and C. S. Jacobsen, *Geomicrobiol. J.*, 2013, **30**, 675-681.

70. B. L. Yuan, M. Pham and T. H. Nguyen, *Environ. Sci. Technol.*, 2008, **42**, 7628-7633.

71. J. Kim, W. Q. Shan, S. H. R. Davies, M. J. Baumann, S. J. Masten and V. V. Tarabara, *Environ. Sci. Technol.*, 2009, **43**, 5488-5494.

72. M. Pham, E. A. Mintz and T. H. Nguyen, *J. Colloid Interface Sci.*, 2009, **338**, 1-9.

73. L. Gutierrez and T. H. Nguyen, *Environ. Sci. Technol.*, 2012, **46**, 8705-8713.

74. M. P. Tong, Y. Shen, H. Y. Yang and H. Kim, *Colloids Surf., B*, 2012, **92**, 340-347.

75. A. L. Rose and T. D. Waite, *Marine Chem.*, 2003, **84**, 85-103.

76. T. Karlsson, P. Persson and U. Skyllberg, *Environ. Sci. Technol.*, 2006, **40**, 2623-2628.

77. X.-H. Guan, C. Shang and G.-H. Chen, *Chemosphere*, 2006, **65**, 2074-2081.

78. Q. L. Li and M. Elimelech, *Environ. Sci. Technol.*, 2004, **38**, 4683-4693.

79. P. Ahmadiannamini, M. L. Bruening and V. V. Tarabara, *J. Membr. Sci.*, 2015, **491**, 149-158.

80. Z. Yin, V. V. Tarabara and I. Xagoraraki, *J. Membr. Sci.*, 2015, **482**, 120-127.

81. M. Elimelech, X. Jia, J. Gregory and R. Williams, *Particle Deposition and Aggregation: Measurement, Modelling and Simulation*, Elsevier Science, 1998.

82. J. Gregory, *J. Colloid Interface Sci.*, 1981, **83**, 138-145.

83. C. J. van Oss, *Interfacial forces in aqeuous media - second edition*, Taylor & Francis Group, 2006.

CHAPTER FIVE

Conclusions

Conclusions on individual projects described in the dissertation are provided at the end of corresponding Chapters. This Chapter lists several overarching conclusions drawn based on the entirety of the work:

The optimal choice of a sample purification method depends on the intended application and is most often a matter of tradeoff. One needs to consider the relevance of "endpoints" (e.g. desired virus purity, efficiency of recovery, effects on virus infectivity) for the application to choose an appropriate method. Practical considerations such as time and cost often factor into the decision.

Understanding virus interactions with dissolved species in the sample at the molecular level is important for increasing virus recovery from complex matrices such as crude stock or natural water. Relatively little is known definitively about such interactions now. Virus fate during sample concentration is governed by physicochemical interactions between the virus and the filter. Primary concentration methods, currently the bottleneck in the overall concentration process, need to be designed to harness these interactions to achieve higher and more reproducible recoveries.

Interlaboratory and interstudy comparisons of virus recovery data must be drawn with extreme caution due to the variability of various parameters used in different studies.

The effects of concentration process parameters are complex and, in many cases, appear to be interrelated. Understanding the virus-filter interactions and the effects - individual and combined - of various parameters is important for the design of an effective membrane-based concentration process. Systematic study to identify general trends surrogate microorganisms and water matrices would be an improvement over the trial and error approach used now.

Due to the challenge in virus recovery from environmental waters, public health protection could not rely on detection alone; instead it should be accompanied by regulatory measures to control the public access to potentially contaminated water sources. To protect public health most effectively, the continued development of the detection technology should be accompanied by regulatory work and environmental policy decision making.